

**Investigating metabolic alterations in various systems relating to
the gut microbiome using mass spectrometry-based
metabolomics**

**A Dissertation Presented for the
Doctor of Philosophy
Degree
The University of Tennessee, Knoxville**

**Courtney Jayde Christopher
December 2022**

Copyright © 2022 by Courtney J. Christopher
All rights reserved.

DEDICATION

This dissertation is dedicated to my family – I would not have made it here without your continuous love, support, and encouragement as I pursue my dream.

ACKNOWLEDGEMENTS

Throughout my graduate career, I have been fortunate to have the support and encouragement of those surrounding me. First, I would like to thank my advisor, Dr. Shawn R. Campagna, as he helped cultivate my passion for science and provided me with ample opportunity to explore my scientific interest. Shawn has pushed me beyond what I believed I was capable of accomplishing and has encouraged me to pursue my dreams. I have appreciated his mentorship and look forward to collaborating with him in the future. I would also like to thank Drs. Bhavya Sharma, Michael Best, and Alison Buchan for dedicating their time to serve on my committee and providing valuable feedback.

I also want to acknowledge a few educators from Pigeon Forge High School who helped prepare me for success: Mr. Keith Henegar, Dr. Tanya Morgan, and Mrs. Sandra Jessel. From Lincoln Memorial University, I would like to thank Dr. Ashleigh Thomas, Dr. Giancarlo Cuadra, Dr. Kevin Cooper, Dr. Josh Boone, Dr. Gavin Kirton, Dr. Julie Hall, and Dr. Steve Everly for being great mentors and inspiring and encouraging me to attend grad school. My goal in graduate school was to use analytical chemistry techniques to answer biological questions and study complex biological interactions, and I was given the opportunity to work with many collaborators on answering a variety of biological questions. I would specifically like to thank Dr. Alison Buchan for giving me the opportunity to learn about bacteriophages, Dr. Laurie Byerley collaborating on my first gut microbiome project, and Dr. Daria Ilatovskaya for allowing me to study physiological changes in sexual dimorphisms. These collaborations have inspired my future scientific endeavors.

Over the last four years, I've had the pleasure of working with the most supportive colleagues: Dr. Amanda May, Dr. Hector Castro, Dr. Eric Tague, Dr. Brandon Kennedy, Dr. Caleb Gibson, Dr. Alex Fisch, Dr. Josh Powers, Haley Fielland, Dr. Katarina Jones, Dr. Katha Höland, and Dr. Ashley Starck, Brittni Woodall, Lindsay Brown, Zane Vickery, Wesley Seaton, Alex Walls, Maliha Tabassum, Qudus Sarumi, Blessing Abiodun, Joshua Moses, Opeyemi Tade, and Hank Marshall. I could never thank Dr. Amanda May, Dr. Hector Castro, and Dr. Katarina Jones enough for their support, encouragement, friendship, and, at times, brutal honesty. Thank you all for reading and providing edits for all of my documents.

Finally, I would like to thank my family for supporting me throughout graduate school. To my husband, Ryan, who has made so many sacrifices for me to pursue this journey, and has always encouraged me when I needed it most. Thank you for supporting me and reminding me to have fun along the way. To my parents, John and Angie, thank you for teaching me the importance of having a strong work ethic and dedication. My parents have been my biggest cheerleaders. I also want to thank my mom for being the best role model as I watched her receive her bachelor's and master's degrees while working a full-time job, and this has been a constant source of my motivation. I would also like to thank my sister, Macy,

and grandparents, Herman and Sharon for their love, support, and encouragement throughout this journey. I truly could not have asked for a better support system!

ABSTRACT

The study of small molecules, or metabolites, is a vital tool when studying biological systems, such as the gut microbiome. The collection of small molecules within a system, known as the metabolome, provides information about the physiological status and is directly related to phenotype. The metabolome is highly sensitive to environmental factors and is more dynamic than the proteome, transcriptome, or genome. Like the metabolome, the gut microbiome is easily impacted by environmental factors, such as diet and stress, which leads to changes in composition and/or function of the microbes. In turn, these alterations in the gut microbiome heavily impact metabolome, demonstrating the intrinsic link between the gut microbiome and metabolism. The first chapter demonstrates how dietary supplements can alter the human gut microbiome and metabolome. The second study investigates how heat stress, an environmental factor, systemically impacts poultry metabolism. The final chapter of this dissertation uses a culture-based technique to identify potential nutrient requirements for a gut parasite infecting poultry. Together, this dissertation highlights the applicability of using mass spectrometry-based metabolomics to investigate various systems relating to the gut microbiome.

While it is well known that diet impacts the gut microbiome composition and function, there is little known about the impact of protein consumption on the microbiome in young physically active adults. This study used a multi-omics approach to analyze the fecal metabolome and microbiome of participants who reported using protein supplements and those who did not. This study determined that unique metabolic profiles are not related to traits, energy and fatigue, and protein supplementation led to alterations in nitrogen metabolism. Specifically, purine degradation was favored in the participants who reported using protein supplements.

Heat stress is known to alter the gut microbiome causing gut injury altering intestinal permeability in poultry. However, the underlying mechanism is not fully defined. Therefore, this study explored the systemic impact of heat stress on poultry and revealed that heat stress impacts the broiler chick metabolome in the small intestines, intestinal digesta, and plasma in a duration dependent manner. Energy metabolism was altered in all regions analyzed, specifically, with alterations in purine metabolism.

The final chapter focuses on understanding the nutrient requirements of the gut parasite, *Histomonas meleagridis*, that infects poultry. As a result of this study, it was proposed the riboflavin, which contributed most to the differences in metabolic profiles between the cells grown with and without rice starch, may be a necessary nutrient requirement for *Histomonas meleagridis*.

TABLE OF CONTENTS

INTRODUCTION.....	1
Gut microbiome and metabolism	1
Metabolomics overview	2
Outline of dissertation	3
CHAPTER 1 AN EXPLORATORY STUDY: GUT MICROBIOME ALTERATIONS IN YOUNG PHYSICALLY ACTIVE ADULTS WITH AND WITHOUT SELF- REPORTED PROTEIN SUPPLEMENTATION AND THE RELATIONSHIP TO TRAITS ENERGY AND FATIGUE	4
1.1 Abstract	5
1.2 Introduction.....	6
1.3 Results.....	8
1.4 Discussion	24
1.5 Methods.....	28
1.5.1 Experimental Approach.....	28
1.5.2 Sample Collection	29
1.5.3 Dietary Assessment	30
1.5.4 Physical Activity Assessment.....	30
1.5.5 Microbial Community Analysis	30
1.5.6 Prediction of Metabolic Profile.....	31
1.5.7 Metabolomics	31
1.5.8 Statistical Analysis	32
1.6 Conclusions	32
APPENDIX	34
CHAPTER 2 HEAT STRESS INDUCES UNIQUE METABOLIC ALTERATIONS IN THE SMALL INTESTINES, INTESTINAL DIGESTA, AND PLASMA OF BROILER CHICKS	35
2.1 Abstract	36
2.2 Introduction.....	37
2.3 Results.....	38
2.3.1 Significant differences between small intestine, intestinal digesta, and plasma	38
2.3.2 Heat stress induces a significant impact on the metabolic profile of broiler chicks	41
2.3.3 The impact of heat stress on the metabolome is duration dependent	71
2.4 Discussion	77
2.4.1 Heat stress impacts energy metabolism.....	78
2.4.2 Heat stress induces considerable changes in the small intestines.....	79
2.4.3 Intestinal digesta and plasma metabolomes are affected by heat stress	81
2.5 Methods.....	82
2.5.1 Ethics Statement.....	82
2.5.2 Birds, Diets, and Heat Stress Challenge	82

2.5.3 Sample Collection and Preparation.....	83
2.5.4 Ultra-High Performance Liquid Chromatography—High Resolution Mass Spectrometry (UHPLC–HRMS) Metabolomics Analysis.....	83
2.5.6 Data Processing and Statistical Analysis	84
2.6 Conclusions	84
APPENDIX	85
CHAPTER 3 METABOLIC PROFILE OF HISTOMONAS MELEAGRIDIS AND UNDEFINED BACTERIAL POPULATION IN DWYER’S MEDIA WITH AND WITHOUT RICE STARCH IDENTIFIES RIBOFLAVIN AS A POSSIBLE REQUIREMENT FOR AXENIC CULTURES.....	92
3.1 Abstract	94
3.2 Introduction.....	94
3.3 Results.....	96
3.3.1 Histomonas meleagridis growth	96
3.3.2 Growth of undefined bacteria	96
3.3.3 Metabolic profile of Histomonas meleagridis and undefined bacterial populations in Dwyer’s media with and without rice	96
3.4 Discussion	101
3.5 Methods.....	107
3.5.1 Histomonas meleagridis strain preparation	107
3.5.2 Sample collection and preparation	107
3.5.2 Data analysis.....	108
3.6 Conclusion.....	108
CONCLUSION	110
VITA	129

LIST OF TABLES

Table 1.1 Subject Characteristics.....	10
Table 1.2 Dietary Intake	11
Table 1.3 Relative abundance of bacterial species that were significantly different	15
Table 1.4 Bacteria taxa significantly correlated with specific traits. Same colored bacteria names correlate with more than one trait.	23
Table 2.1 Overview of metabolites significantly altered by heat stress. Metabolites were considered to be significantly altered if $p < 0.05$ and had a fold change of ≥ 1.5 . Pre-heat stress (PHS), TN-control (TN-control), pair-fed (PF), acute heat stress (AHS), cyclic heat stress (CHS), heat stress (HS) .	44
Table 2.2 Metabolites significantly increased or decreased by acute heat stress (AHS) or cyclic heat stress (CHS) in the jejunum.....	46

LIST OF FIGURES

Figure 1.1 Flowchart showing participant recruitment.	9
Figure 1.2 Jaccard plot of beta diversity. Each orange dot corresponds to a participant (No PS) who reported not using protein supplements. The orange circle highlights the range of values. Each green dot represents one participant who reported using protein supplements (PS). The green circle shows the variation. Although the groups overlap, the differences were significant ($p = 0.035$), demonstrating community separation by this method.	14
Figure 1.3 Predicted functional pathways. Pathways that were significantly different between the two groups are shown along with the Bonferroni-corrected p-value. Orange bars are the No PS group, while the green bars are the PS group.	20
Figure 1.4 Metabolomics analysis showing PS induces metabolic alterations. (A) 3D PLS-DA plot showing separation of the PS and NPS groups, indicating unique metabolic profiles. (B) This plot shows the top 15 metabolites with the highest VIP scores contributing most to the observed separation of groups. Allantoin contributes most to the separation of the PS and NPS groups in the PLS-DA plot. (C) Metabolites with a VIP score > 1 were used for pathway analysis. The pathways impacted most by PS include pyrimidine metabolism, glycolysis and gluconeogenesis, cysteine and methionine metabolism, purine metabolism, and the TCA cycle.	21
Figure 1.5 Nitrogen metabolism pathways. Assembling the metabolome and microbiome data suggested nitrogen metabolism was altered in the gut environment of participants who reported consuming a protein supplement compared to those who did not. Blue boxes represent information derived from the participant’s dietary recall. The orange and green arrows in each box show which group had higher or lower intake. Evidence derived from predicted functional pathways is highlighted in pink, while the purple boxes are metabolites or pathways identified by metabolomics.	22
Figure 1.6 A principal component analysis (PCA) for the 20 survey subjects. (A) clearly shows two distinct clusters: left blue and right red. (B) shows the average \pm SD for each trait. MF, ME, PF, and PE were not significantly different between the two clusters.	25
Figure 1.7 Heatmap showing the \log_2 fold change and p-values for all identified metabolites in fecal samples. Metabolite relative abundances were altered by PS.	34
Figure 2.1 Experimental design representation and heat stress challenge. Temperature was gradually reduced from 32 °C to approximately 23 °C on d 21. At d 29, the experiment followed a completely randomized design with three treatments (8 replicate pens/treatment, 28 birds/pen): a control group (TN) where the birds were raised under thermoneutral condition (23 °C) from d 29–42, a chronic cyclic heat-stressed group (CHS) where the birds were	

exposed to high ambient temperature (35 °C) for 8 h/d (9:30 am to 5:30 pm) from d 29–42, and a pair-fed group (PF) where the birds were raised like the control group (similar environmental conditions, 23 °C) and fed the same amount of feed as the CHS group. Two additional groups were also used: an acute heat-stressed group (AHS) where some TN birds were exposed to 35 °C for 2 h before sampling on d 42, and a preheat-stressed group (PHS) where CHS birds were sampled before starting the heat stress on d 42.

AHS, acute heat stress; CHS, chronic cyclic heat stress; HS, heat stress; PHS, preheat stress; PF, pair fed..... 39

Figure 2. 2 Venn diagram comparing the detected metabolites in each region. There were 17 metabolites unique to the tissue (duodenum, jejunum, and ileum), 15 metabolites unique to the digesta (ileal and cecal), and metabolites unique to the plasma..... 40

Figure 2. 3 *3D partial least-squares discriminant analysis (PLS-DA) displays that biological location, rather than HS, has the greatest impact on the metabolic profiles as four distinct clusters are present (small intestines, ileal digesta, cecal digesta, and plasma) when all samples are plotted with treatment and biological location information used for grouping. Within each cluster, there is no apparent distinction for heat stress.*..... 42

Figure 2.4 *Partial least-squares discriminant analysis (PLS-DA) plots for each treatment. Within each treatment, samples were grouped by biological location (duodenum, jejunum, ileum, ileal digesta, cecal digesta, and plasma). Each plot shows 4 distinct clusters that correspond to the small intestines, cecal digesta, ileal digesta, and plasma. Pre-heat stress (PHS), TN-control (TN-control), pair-fed (PF), acute heat stress (AHS), cyclic heat stress (CHS), cecal digesta (CD), ileal digesta (ID), plasma (P), jejunum (J), ileum (I), duodenum (D).* 43

Figure 2.5 *Partial least-squares discriminant analysis (PLS-DA) plots for each region of the small intestines (duodenum, jejunum, and ileum). Within each treatment, samples were grouped by treatment Pre-heat stress (PHS), TN-control (TN-control), pair-fed (PF), acute heat stress (AHS), cyclic heat stress (CHS). The heat stress samples were most clearly separated from the other treatment groups in the jejunum.*..... 52

Figure 2.6 2D (top) *Partial least-squares discriminant analysis (PLS-DA) plots for pairwise comparisons of each treatment to the TN-control in the duodenum. CHS has the most separation from the control. The treatment groups show more separation from the TN-control in 3D (bottom) PLS-DA plots. Pre-heat stress (PHS), TN-control (TN-control), pair-fed (PF), acute heat stress (AHS), cyclic heat stress (CHS), cecal digesta (CD), ileal digesta (ID), plasma (P), jejunum (J), ileum (I), duodenum (D)* 53

Figure 2.7 2D (top) *Partial least-squares discriminant analysis (PLS-DA) plots for pairwise comparisons of each treatment to the TN-control in the jejunum. CHS and AHS had the most separation from the control. The treatment groups show more separation from the TN-control in 3D (bottom) PLS-DA*

plots. Pre-heat stress (PHS), TN-control (TN-control), pair-fed (PF), acute heat stress (AHS), cyclic heat stress (CHS), cecal digesta (CD), ileal digesta (ID), plasma (P), jejunum (J), ileum (I), duodenum (D)	55
Figure 2.8 2D (top) <i>Partial least-squares discriminant analysis</i> (PLS-DA) plots for pairwise comparisons of each treatment to the TN-control in the ileum. CHS and AHS had the most separation from the control. The treatment groups show more separation from the TN-control in 3D (bottom) PLS-DA plots. Pre-heat stress (PHS), TN-control (TN-control), pair-fed (PF), acute heat stress (AHS), cyclic heat stress (CHS), cecal digesta (CD), ileal digesta (ID), plasma (P), jejunum (J), ileum (I), duodenum (D)	57
Figure 2.9 Metabolites with a variable importance in projection (VIP) score >1 in each pairwise comparison within the small intestine regions was used to generate a Venn diagram to determine metabolites that significantly contributed to the differences between the acute heat stress (AHS) and TN-control (TN-control) metabolic profiles in all three regions.	59
Figure 2.10 Metabolites with a variable importance in projection (VIP) score >1 in each pairwise comparison within the small intestine regions was used to generate a Venn diagram to determine metabolites that significantly contributed to the differences between the cyclic heat stress (CHS) and TN-control (TN-control) metabolic profiles in all three regions.	61
Figure 2.11 2D (left) <i>Partial least-squares discriminant analysis</i> (PLS-DA) plots for the ileal digesta. 3D (right) PLS-DA plots for the ileal digesta. C) 2D PLS-DA plots for the cecal digesta. D) 3D PLS-DA plots for the cecal digesta (right plot shows the rotated side view for better separation). Pre-heat stress (PHS), TN-control (TN-control), pair-fed (PF), acute heat stress (AHS), cyclic heat stress (CHS).....	62
Figure 2.12 2D (top) <i>Partial least-squares discriminant analysis</i> (PLS-DA) plots for pairwise comparisons of each treatment to the TN-control in the ileal digesta. The treatment groups show more separation from the TN-control in 3D (bottom) PLS-DA plots. Pre-heat stress (PHS), TN-control (TN-control), pair-fed (PF), acute heat stress (AHS), cyclic heat stress (CHS), cecal digesta (CD), ileal digesta (ID), plasma (P), jejunum (J), ileum (I), duodenum (D).....	65
Figure 2.13 2D (top) <i>Partial least-squares discriminant analysis</i> (PLS-DA) plots for pairwise comparisons of each treatment to the TN-control in the cecal digesta. CHS and AHS had the most separation from the control. The treatment groups show more separation from the TN-control in 3D (bottom) PLS-DA plots. Pre-heat stress (PHS), TN-control (TN-control), pair-fed (PF), acute heat stress (AHS), cyclic heat stress (CHS), cecal digesta (CD), ileal digesta (ID), plasma (P), jejunum (J), ileum (I), duodenum (D).....	67
Figure 2.14 Metabolites with a variable importance in projection (VIP) score >1 in each pairwise comparison within the intestinal digesta was used to generate a Venn diagram to determine metabolites that significantly contributed to the	

differences between the acute heat stress (AHS) and TN-control (TN-control) metabolic profiles in the digesta.	69
Figure 2.15 Metabolites with a variable importance in projection (VIP) score >1 in each pairwise comparison within the intestinal digesta was used to generate a Venn diagram to determine metabolites that significantly contributed to the differences between the cyclic heat stress (CHS) and TN-control (TN-control) metabolic profiles in the digesta.	70
Figure 2.16 2D and 3D <i>Partial least-squares discriminant analysis</i> (PLS-DA) plots for the plasma. The side view of the the 3D PLS-DA (right) shows separation of the heat stress groups from the control. Pre-heat stress (PHS), TN-control (TN-control), pair-fed (PF), acute heat stress (AHS), cyclic heat stress (CHS).	72
Figure 2.17 2D (top) <i>Partial least-squares discriminant analysis</i> (PLS-DA) plots for pairwise comparisons of each treatment to the TN-control in the plasma. CHS and AHS had the most separation from the control. The treatment groups show more separation from the TN-control in 3D (bottom) PLS-DA plots. Pre-heat stress (PHS), TN-control (TN-control), pair-fed (PF), acute heat stress (AHS), cyclic heat stress (CHS), cecal digesta (CD), ileal digesta (ID), plasma (P), jejunum (J), ileum (I), duodenum (D)	73
Figure 2.18 3D <i>Partial least-squares discriminant analysis</i> (PLS-DA) plots for each biological region. Within each region, samples were grouped by treatment Pre-heat stress (PHS), TN-control (TN-control), pair-fed (PF), acute heat stress (AHS), cyclic heat stress (CHS). This analysis shows the I the jejunum there was clear separation of the heat stress groups from all other groups.	75
Figure 2.19 Heatmap displaying log ₂ fold change for all identified metabolites in the duodenum. Pre-heat stress (PHS), TN-control (TN-control), pair-fed (PF), acute heat stress (AHS), cyclic heat stress (CHS)	85
Figure 2.20 Heatmap displaying log ₂ fold change for all identified metabolites in the jejunum. Pre-heat stress (PHS), TN-control (TN-control), pair-fed (PF), acute heat stress (AHS), cyclic heat stress (CHS)	86
Figure 2.21 Heatmap displaying log ₂ fold change for all identified metabolites in the ileum. Pre-heat stress (PHS), TN-control (TN-control), pair-fed (PF), acute heat stress (AHS), cyclic heat stress (CHS)	87
Figure 2.22 Heatmap displaying log ₂ fold change for all identified metabolites in the ileal digesta. Pre-heat stress (PHS), TN-control (TN-control), pair-fed (PF), acute heat stress (AHS), cyclic heat stress (CHS)	88
Figure 2.23 Heatmap displaying log ₂ fold change for all identified metabolites in the cecal digesta. Pre-heat stress (PHS), TN-control (TN-control), pair-fed (PF), acute heat stress (AHS), cyclic heat stress (CHS)	89
Figure 2.24 Heatmap displaying log ₂ fold change for all identified metabolites in the plasma. Pre-heat stress (PHS), TN-control (TN-control), pair-fed (PF), acute heat stress (AHS), cyclic heat stress (CHS)	90

Figure 2.25 The sum of the moralized relative abundance of all identified metabolites for each region and treatment was compared. Pre-heat stress (PHS), TN-control (TN-control), pair-fed (PF), acute heat stress (AHS), cyclic heat stress (CHS), cecal digesta (CD), ileal digesta (ID), plasma (P), jejunum (J), ileum (I), duodenum (D)	91
Figure 3. 1 Growth curve of <i>Histomonas meleagridis</i> grown in Dwyer's media with (SDM) and without (NR) rice starch. The mean of the log values is represented on the vertical axis and the hours post inoculation (HPI) on the horizontal axis.	97
Figure 3.2 Growth curve of undefined bacteria in <i>H. meleagridis</i> cultures using Dwyer's media with (SDM) and without (NR) rice starch. The mean of the log values is represented on the vertical axis and the hours post inoculation (HPI) on the horizontal axis. CFU is colony forming unit.	98
Figure 3.3 Heatmap of intracellular metabolites of <i>Histomonas meleagridis</i> and undefined bacteria in Dwyer's media with (SD) and without (NR) rice starch showing the change in relative abundance of metabolites between the two media at various timepoints. Fold change equals \log_2 (average relative abundance for NR / average relative abundance for SD). Orange indicates metabolite has higher relative abundance in NR treatment, while blue indicates the metabolite has lower abundance in NR treatment, and black represents metabolite that do not change in relative abundance between the two treatments. The brightness represents the magnitude of change. P-values indicate if the change in relative metabolite abundance is significantly different between media conditions as follows, * ≤ 0.1 , ** ≤ 0.05 , *** ≤ 0.01 . NR is no rice media, SD is standard Dwyer's media, AA is amino acids and TCA is tricarboxylic acid cycle.....	99
Figure 3.4 Partial least squares discriminant analysis (PLS-DA) of metabolites in Dwyer's media with (SD) and without (NR) rice inoculated with <i>H. meleagridis</i> and undefined bacterial population at blank and 0 HPI (t0). Ellipse represents 95% confidence interval.....	102
Figure 3.5 Variable importance in projection (VIP) scores for the top 15 metabolites contributing most to the differences in the metabolic profile between Dwyer's media with and without rice inoculated with <i>H. meleagridis</i> and undefined bacteria in the media blank and 0 HPI. Metabolites with a VIP score over 1 are driving the separation in the PLS-DA plot. Riboflavin has the highest VIP score in all 5 components (5.3907-1.1438).....	103
Figure 3.6 Average peak intensity vs time for riboflavin in Dwyer's media with (SD) and without (NR) rice before (media) and after inoculation with <i>H. meleagridis</i> and undefined bacteria showing an increase in SDM from t0-t166 hours.	106

INTRODUCTION

Gut microbiome and metabolism

The gut microbiome is one of the most complex ecosystems as it harbors roughly 100 trillion microbial cells, including bacteria, viruses, fungi, archaea, and eukaryotic microbes.¹ These microbes are responsible for maintaining many functions crucial for the health of the host (human and animal). Some of these crucial functions include aiding in digestion and metabolism, energy production, protection against pathogens, regulation of host immunity, and strengthening the integrity of the gut.² Collectively, the gut microbiota contains many more genes than the host and, therefore, is capable of performing numerous metabolic functions that the host does not have the ability to do.³ These microbes have even been referred to as the hidden metabolic “organ” because of their advanced metabolic capacity and vital impact on the wellbeing of the host.¹

For example, the gut microbiome has the ability to synthesize various vitamins (riboflavin, biotin, and thiamine), biotransform bile, and metabolize carbohydrates that the host is unable to digest.⁴ This demonstrates the intrinsic link between the gut microbiome and host metabolism as the host depends on microbial-derived metabolites since it lacks the necessary enzymes for digestion.⁵⁶ This highlights the host dependency on the microbes to provide essential nutrients. These microbial-derived metabolites can be absorbed in the intestinal tissue and eventually enter circulation, highlighting how the gut microbiota directly influences host health and metabolism.²

However, the gut microbiome is very sensitive to environmental factors which leads to alterations in microbial composition as the gut microbiota coevolves with the host. Even minute changes in microbial composition can have an impact, either beneficial or harmful, to the host.¹ A disruption in the gut microbiota, which is known as dysbiosis, has recently been implicated in pathogenesis of many diseases, such as metabolic syndrome, inflammatory bowel disease, cardiovascular disease, and obesity to name a few.⁷ This demonstrates the necessity to better understand how environmental factors impact the gut microbiome in order to maintain normal physiology and host health.

Furthermore, many research efforts have recently focused on the impacts of diet on gut microbiome alterations.⁸⁻¹¹ Animal studies have shown that changes in diet can shift the composition of the gut microbiota within a day.¹²⁻¹⁴ However, one aspect of diet that has not been well studied with regards to the impact on the microbiota is the use of protein supplements that are frequently taken in an attempt to build muscle by young physically active adults.¹⁵ While the impact of protein supplements on the gut microbiome of elite athletes has been studied, the impact on young physically active adults is not well understood. Therefore, this dissertation will bridge the knowledge gap on the impact of protein supplementation in young physically active adults, as elite athletes represent a unique subset of consumers.¹⁶ In addition, exposure to heat stress has been shown to alter and damage the gut in broiler chicks, though the underlying

mechanisms leading to gut injury are still unknown.^{17, 18} Together, this exhibits the need to expand the current knowledge of how both protein supplementation and heat stress impacts the functionality and composition of the gut microbiota. Also, as the gut provides essential nutrients to the host, parasites can take advantage of this and parasitic invasion can detrimentally impact the host.¹⁹ Since these parasites are reliant on the gut microbiota for nutrients, determining the specific nutrients required for parasitic growth could aid in combating parasitic infection.

Investigating the gut microbiota can be very difficult due to the complexity of the gut. However, recent advances in culture-independent metagenomics techniques and mass spectrometry-based metabolomics has allowed for the advances in understanding the gut microbiota. With the crucial role of the gut microbiota on host health, it is imperative to understand how extrinsic factors alter the gut microbiota and the consequential impact of these factors on the host health.

Metabolomics overview

Metabolomics is the study of small, biologically relevant molecules and is the newest addition to the omics cascade. Metabolomics has emerged as a very useful tool in systems biology as it provides a unique perspective relative to other omics techniques.²⁰ Metabolomics is also very powerful in investigating an array of applications: environmental, agricultural, human health, and microbiology. One of the key distinctions about metabolomics is that it provides information on what actually *is* happening whereas genomics and proteomics offer information about what *might* happen.²⁰ Thus, metabolomics is directly linked to biological function and cellular phenotypes. The metabolome, or collection of small molecules, is highly sensitive to intrinsic and extrinsic factors.²¹ When trying to study complex biological systems, such as the gut microbiome, it is beneficial to combine metabolomics with other omics techniques, such as metagenomics, to allow for a more holistic understanding of the system.

Though metabolomics is a very useful technique, it is quite a challenging analytical technique. Metabolites have vast structural heterogeneity, which poses a challenge when analyzing complex biological samples. However, recent advances in mass spectrometry-based metabolomics have allowed for highly robust, reproducible, selective and sensitive qualitative or quantitative analysis of endogenous metabolites.²² Specifically, this has been made possible with ultra high-performance liquid chromatography high resolution mass spectrometry (UHPLC-HRMS) with the introduction of the orbitrap mass analyzer.²³ UHPLC-HRMS based metabolomics has recently become one of the most commonly used analytical techniques to study complex biological systems as untargeted metabolomics analysis allows for full scan analysis.

However, another challenge arises with full scan analysis in that there is an enormous amount of data produced with features detected from a single scan, though software packages have been produced to aid with data processing.^{20, 24,}²⁵ This also highlights another interesting challenge for metabolomics studies; in a single analysis, there are thousands of features detected but only a small portion

of these metabolites have been annotated because the current understanding of the metabolome has only begun to scrape the surface of all of the metabolites estimated to comprise a complete metabolome.²⁶ This is an exciting challenge for metabolomics as overcoming this challenge would vastly improve the current understanding biology and could help identify previously unknown metabolic pathways.

Outline of dissertation

As the gut microbiome is intrinsically linked to metabolism, this dissertation will highlight the application of metabolomics in investigating three unique systems related to the gut. These studies will contribute to expanding the current knowledge on the relationship between the gut and metabolism using an untargeted mass spectrometry-based metabolomics approach. The first study will combine metagenomics and metabolomics to determine the impact protein supplementation has on the human gut microbiome and metabolome in young physically active adults. To accomplish this, fecal samples were collected from young physically active adults who did and did not report using protein supplements. The second chapter will investigate the systemic impact of heat stress exposure on broiler chicks. Samples were collected from the small intestines (duodenum, jejunum, and ileum), intestinal digesta (ileal and cecal), and plasma of birds under different conditions: pre-heat stress, thermoneutral-control, pair fed, acute heat stress, and cyclic heat stress. The final chapter will focus on determining the nutrient requirements for the gut parasite, *Histomonas meleagridis*. Here, the metabolome of *H. meleagridis* and undefined gut microbes were compared when grown in Dwyer's media with and without rice starch supplementation to potentially identify essential nutrient requirements for *H. meleagridis* growth.

**CHAPTER 1 AN EXPLORATORY STUDY: GUT MICROBIOME
ALTERATIONS IN YOUNG PHYSICALLY ACTIVE ADULTS
WITH AND WITHOUT SELF-REPORTED PROTEIN
SUPPLEMENTATION AND THE RELATIONSHIP TO TRAITS
ENERGY AND FATIGUE**

A version of this manuscript was Byerley O. L., *et al* and Boolani A., *et al*:

Lauri O. Byerley, Karyn M. Gallivan, Courtney J. Christopher, Christopher M. Taylor, Meng Luo, Scot E. Dowd, Gregory Davis, Hector F. Castro, Shawn R. Campana, Kristin S. Ondrak; Gut Microbiome Variations in Self-Identified Muscle Builders With and Without Self-Reported Protein Supplementation; *Nutrients* 2022, 14, 533.

Author's Contributions: LOB, SRC, CJC, KSO, and KMG designed the study and LOB, KSO, and KMG recruited participants. GD helped recruit participants. LOB collected and processed the fecal samples, questionnaires, and dietary data. CMT and ML provided the fecal microbiome data with the diversity and taxa data analysis. SED provided the functional pathway analysis. CJC performed metabolomics extraction, mass spectral analysis, data processing and interpretation, and related metabolomics results to microbiome results along with HFC and SRC. LOB, KSO, KMG, CJC, HFC, and SRC analyzed and interpreted the data and conceptualized the results. LOB, KSO, KMG, CJC, HFC, SRC, and CMT wrote the manuscript. All authors approved the manuscript.

Boolani, A.; Gallivan, K.M.; Ondrak, K.S.; Christopher, C.J.; Castro, H.F.; Campagna, S.R.; Taylor, C.M.; Luo, M.; Dowd, S.E.; Smith, M.L.; Byerley, L.O. Trait Energy and Fatigue May Be Connected to Gut Bacteria among Young Physically Active Adults: An Exploratory Study. *Nutrients* 2022, 14, 466.

Author's Contributions: Conceptualization, L.O.B., K.M.G., K.S.O., and A.B.; methodology, L.O.B., A.B., C.J.C., H.F.C., and S.R.C.; formal analysis, L.O.B., A.B., C.M.T., M.L., S.E.D., C.J.C., H.F.C., M.L.S., and S.R.C.; re-sources, L.O.B. and A.B.; data curation, L.O.B., C.J.C., and A.B.; writing—original draft preparation, L.O.B., A.B., and C.J.C.; writing—review and editing, L.O.B., K.S.O., K.M.G., C.M.T., M.L., S.E.D., C.J.C., H.F.C., S.R.C., M.L.S., and A.B.; funding acquisition, L.O.B., K.M.G. and K.S.O. All authors have read and agreed to the published version of the manuscript.

1.1 Abstract

The gut microbiome is highly sensitive and easily altered by environmental factors such as diet. Muscle builders frequently alter their dietary intake by consuming protein supplements, however, there is little information regarding how consumption of protein supplements alters the gut microbiome and metabolome. The goal of this study was to analyze the gut microbiome and metabolome of self-identified muscle builders who did or did not report consuming protein supplements. There were 22 total participants (14 males and 8 females) who reported consuming a protein supplement (PS), and 17

participants (12 males and 5 females) who did not report using a protein supplement (No PS). Of these 39 participants, 20 (14 males and 6 females) participants completed a survey about traits energy and fatigue. This traits survey was used for an exploratory investigation into the correlation between traits mental energy (ME), mental fatigue (MF), physical energy (PE), physical fatigue (PF), and the gut microbiome. All participants provided a fecal sample and completed a 24-hour food recall (ASA24). Fecal metabolome and microbiome were analyzed using untargeted metabolomics and 16S rRNA gene sequencing, respectively. The untargeted metabolomics analysis showed that the PS cohort had a unique metabolic profile that was distinct from the No PS cohort using partial least-squares discriminant analysis (PLS-DA). The differences in the metabolic profiles were driven by allantoin (VIP score = 2.85, PS 2.3-fold higher), a catabolic product of uric acid. High protein diets contain large quantities of purines, which gut microbes degrade to uric acid then allantoin, and the PS group consumed significantly more protein (118 ± 12 g No PS vs. 169 ± 18 g PS, $p=0.02$). Concurrently, the order *Lactobacillales*, which facilitates purine absorption and uric acid decomposition, was higher in the PS group (22.6 ± 49 No PS vs. 136.5 ± 38.1 , PS ($p=0.007$)). Both fecal metagenomic and metabolomic analysis revealed the PS group's higher protein intake impacted nitrogen metabolism, specifically altering nucleotide degradation. In addition, the results from the traits study cohort indicated that though distinct metabolic profiles were observed, traits energy and fatigue did not correlate to these differences. However, the order *Anaerostipes* was positively correlated with ME (0.048, $p = 0.032$) and negatively correlated with MF (-0.532 , $p = 0.016$) and PF (-0.448 , $p = 0.048$) demonstrating that energy and fatigue are unique traits that could be defined by distinct bacterial communities though more robust studies are needed to confirm these exploratory findings. Overall, this study used fecal samples collected from young physically active adults to determine the impact of protein supplementation on the gut microbiome and metabolome as well as determine if traits ME, MF, PF, and PF have unique microbiome and metabolome profiles in the gut.

1.2 Introduction

The gut microbiome is one of the most complex biological ecosystems as it contains roughly 100 trillion microorganisms and encodes 100 times more genes than the human genome.^{27, 28} The microbes in the gut play many roles critical to human health such as maintaining normal gut physiology, aiding in digestion and metabolism, and producing energy.² Even minor alterations in the relative abundance of microbes in the gut can impact, either beneficial or harmful, human health. It is well known that environmental factors play a impactful role in shaping the composition and metabolic activity of the human gut microbiota.²⁹ Diet is one of the leading environmental factors impacting the composition and function of the

gut microbiome, which in turn impacts overall health. Studies have shown that alterations in diet can induce large metabolic shifts within just 24 hours.^{28, 30}

In order to study highly complex systems, such as the gut microbiome, biological processes should be studied holistically using an integrative multi-omics approach. Over the last decade, recent advances in metagenomics sequencing technology and mass spectrometry have paved the way for multi-omics approaches studying the gut microbiome. Utilizing a multi-omics approach is beneficial because it not only provides information on the microbes present, it also provides insight into the physiological state of the cells, which relates to microbial function.³¹ This holistic view of the gut microbiome allows for a better understanding of how environmental factors, such as diet, induce alterations in the gut impacting human health.

It is common for individuals wanting to build muscle to combine exercise with increased protein intake. This increased protein intake can either come from a dietary source or in the form of supplements. A recent review article reported that 40-100% of athletes used some type of supplement, including protein, intending to improve athletic performance.³² Most of the protein supplement products on the market are whey, casein, or soy-based, and research has shown that whey, casein, and/or soy protein promote similar amounts of protein synthesis and strength gains.³³ Using a multi-omics approach to investigate the microbiome of participants who consumed whey protein for 8 weeks combined with resistance training, Cronin *et al.*³⁴ showed alteration in the diversity of their gut virome were apparent. They also noted that subtle compositional and functional changes were evident in the microbiome participants who underwent 8 weeks of combined aerobic and resistance training but were otherwise sedentary.

Physical activity has been shown to alter the gut microbiome as elite athletes generally have a higher gut microbial diversity with an increase in bacterial species involved in carbohydrate metabolism, fiber metabolism, and amino acid biosynthesis.³⁵ While researchers have studied the impact of protein supplementation on the gut microbiome in elite athletes, elite athletes represent a unique subset of the population.³⁶ Currently, the fastest growing market for protein supplement consumption are recreational and lifestyle users.¹⁶ Despite this, there has been limited research efforts to investigate the impact of protein supplementation in young physically active adults. Therefore, this goal of this study was to address this knowledge gap and understand how protein supplementation influences the gut microbiome and metabolome in young physically active adults.

Similarly, there is evidence to support that diet is associated with traits energy and fatigue as it is hypothesized that consuming polyphenol-rich diets may be associated with increased feelings of mental energy.^{37, 38} Mediterranean diets have also been reported to reduce fatigue, however no distinction on mental and physical fatigue was made.³⁹ Based on these studies, it is hypothesized that diets associated with energy or fatigue could be associated with changes in the gut microbiome function or composition. This exploratory study will aim to identify specific alterations in the gut microbiome associated with traits mental energy

(ME), mental fatigue (MF), physical energy (PE), and physical fatigue (PF). Due to the sparsity of available literature on the impacts of protein supplementation on the gut microbiome and how the gut microbiome relates to traits ME, MF, PE, and PF, this exploratory work used a multi-omics approach in hopes of identifying alterations in the bacteria and metabolites present in the fecal matter. A schematic for recruiting participants is shown in Figure 1.1.

1.3 Results

Participant characteristics are shown in Table 1.1. There were no significant differences in age, weight, height, or BMI between the PS and No PS groups. Seventy-one percent of the No PS group were male, while 64% of the PS group were male. The participants self-identified as muscle builders. As part of the selection criteria, each potential participant provided the maximum weight they could lift for the squat, bench press or deadlift. On average both groups could lift 1.9 ± 0.2 lift weight (lbs)/body weight (lbs); (range of 1.0 to 3.6 lbs/lbs). Seventeen participants reported how long they had been lifting, which averaged 11 ± 2 yrs. The data collected from the training worksheet confirmed that our participants participated in activities designed to maintain or increase their current muscle mass specifically. Also, this information was compiled and reported as upper and lower body resistance exercise volume (Table 1.1).

The participant's physical activity was assessed using the IPAQ. There was no significant difference in the amount of time the participants spent sitting daily, although the PS group tended to sit less (No PS: 324 ± 250 ; PS: 267 ± 124 minutes/day). As for physical activity, total walking (No PS: 1893 ± 432 ; PS: 2318 ± 544 METS-minutes/week) and moderate activity (No PS: 2613 ± 645 ; PS: 3432 ± 733 METS-minutes/week) did not differ significantly between the two groups. Both groups' total physical activity level was consistent with a high level of physical activity (vigorous activity >1500 MET minutes per week). Still, total physical activity was significantly higher for the PS group because they spent significantly more time doing vigorous activity.

Twenty-four participants (65%) reported using a supplement (not protein), and 41 different supplements were reported. The most commonly used supplement was creatine (13.8%), and the supplements that four or more participants used were: AminoX branch chain amino acids by BSN (7.5%), a multivitamin pill (6.3%), beta-alanine (5%), fish oil (5%), and glutamine (5%).

Dietary intake is reported in Table 1.2. There were no significant group differences in energy intake, but the macronutrient distribution of the calories from protein and fat was significantly different. The No PS group consumed significantly more fat than the PS group (Table 1.1). Because the percent of calories derived from carbohydrates was similar between the groups (Table 1.1), the difference was made up with protein. The PS group derived more calories from protein ($28 \pm 2\%$), while the No PS derived $20 \pm 2\%$ of their calories from protein ($p < 0.0027$). This marked difference in protein intake reflected a difference of more than 0.5 g/kg of

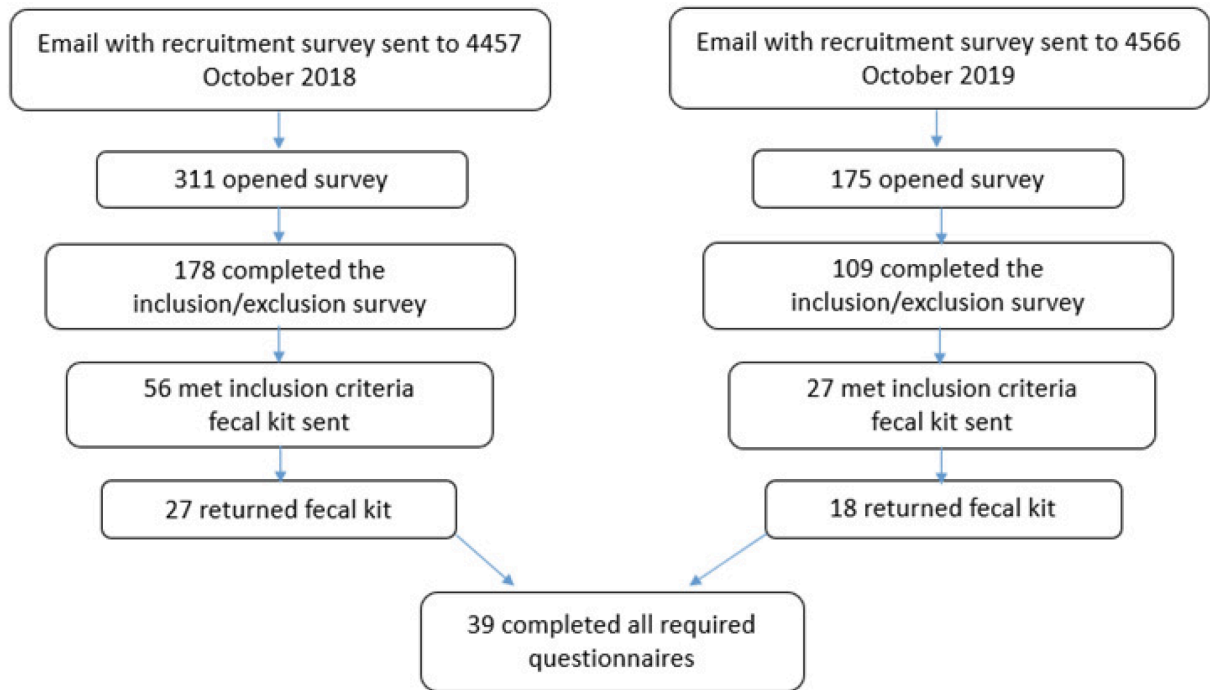


Figure 1.1 Flowchart showing participant recruitment.

Table 1.1 Subject Characteristics

	NPS (No protein supplement) (n=17)	PS (Protein supplement) (n=22)	P-value
Age	33 ± 2 ¹	32 ± 1	0.84
Weight (lbs)	176 ± 8	173 ± 7	0.79
Height (inches)	67 ± 1	67 ± 1	0.72
BMI	27 ± 1	27 ± 1	0.99
Males	12	14	
Females	5	8	
Total Physical Activity (MET- minutes per week)	7040 ± 1282	12081 ± 1870	0.03
Total Vigorous Activity (MET- minutes/week)	2535 ± 830	6331 ± 1284	0.02
Upper Body Resistance Exercise Volume (kg/week)	15,743 ± 13,103	31,067 ± 49,323	0.15
Lower Body Resistance Exercise Volume (kg/week)	16,694 ± 19,430	56,464 ± 127,594	0.16
Bristol Scale	3.8 ± 0.4	3.3 ± 0.2	0.25
Number of Supplements (count)	0.9 ± 1.5	1.4 ± 2.4	0.45

¹ mean ± SEM

Table 1.2 Dietary Intake

	NPS (n=17)	PS (n=22)	P-value
Number of Foods	19 ± 2 ¹	21 ± 2	0.26
Energy (kcal)	2551 ± 429	2452 ± 199	0.84
Protein (g)	117.6 ± 11.8	169.3 ± 17.6	0.02
Protein (g/kg body weight)	1.49 ± 0.14	2.15 ± 0.19	0.009
Calories from protein (%)	20.1 ± 1.5	27.5 ± 1.7	0.003
Carbohydrate (g)	228.3 ± 37.9	239.3 ± 25.9	0.81
Calories from carbohydrates (%)	36.5 ± 2.9	39.3 ± 2.6	0.48
Fiber (g)	18.9 ± 2.1	27.3 ± 3.1	0.03
Total Sugar (g)	93.3 ± 20.7	88.1 ± 13.4	0.84
Kcal from sugar (%)	13.7 ± 1.7	14.1 ± 1.50	0.84
Ratio of protein to carbohydrate (g:g)	0.67 ± 0.11	0.89 ± 0.16	0.26
Fat (g)	109.0 ± 13.7	92.9 ± 9.0	0.33
Total saturated fatty acids	34.1 ± 6.0	29.3 ± 3.2	0.49
Total polyunsaturated fatty acids	24.8 ± 2.7	19.6 ± 2.1	0.14
Total monounsaturated fatty acids	40.6 ± 5.1	35.6 ± 4.2	0.46
Calories from fat (%)	40.8 ± 2.7	33.9 ± 1.9	0.05
Iron (mg)	14.7 ± 1.5	19.5 ± 1.8	0.05
Magnesium (mg)	369 ± 30	533 ± 77	0.03
Potassium (mg)	3064 ± 303	3996 ± 395	0.07
Vitamin C (mg)	120 ± 22	217 ± 49	0.08
Folate, food (mcg)	263 ± 30	375 ± 56	0.09
Intact fruits (whole or cut) of citrus, melons, and berries (cup eq.)	0.065 ± 0.04	0.443 ± 0.15	0.02

Table 1.2 continued

Beans and Peas (legumes) computed as protein foods (oz.eq.)	0.132 ± 0.12	0.97 ± 0.4	0.045
Beans and Peas (legumes) computed as vegetables (cup eq.)	0.032 ± 0.03	0.24 ± 0.10	0.045
Healthy Eating Index (HEI)	54.0 ± 13.3	61.8 ± 15.1	0.088
Water (g)	3914 ± 304	4266 ± 441	0.51
Alcohol (g) (14 g = 1 standard drink)	31.4 ± 25.8	1.92 ± 1.1	0.27
Caffeine (mg)	180.3 ± 42.3	156.1 ± 28.5	0.64

¹mean ± SEM

protein intake for the PS group. This protein was primarily derived from food sources as only 4 of the 22 participants consumed a protein supplement (25.3 ± 3.8 g, 13% of their total protein intake) on the day of the recall. Most of the difference in protein intake between the PS and No PS was derived from beans and peas. The PS group was asked to report the protein supplement they typically consumed. Twenty-one different supplements were reported, and 17 (81%) contained whey protein.

Despite a similar carbohydrate intake, the PS group consumed about 1.5 times more fiber than the No PS group. Total sugar consumption was not significantly different between the groups but the No PS group tended to consume more sugar. Finally, alcohol and caffeine intake tended to be higher in the No PS group, although not significant.

The 2010-2015 HEI index, a value that determines how closely one's diet adheres to the US Dietary Guidelines, is 59 for the American diet (<https://www.fns.usda.gov/healthy-eating-index-hei>). A score of 100 indicates one is adhering to the guidelines. The average score for both the No PS and PS groups was close to 59 (Table 1.2); the No PS group having a lower HEI score than the PS group, although not significant.

Bacterial diversity was measured within a sample (alpha) and between samples (beta). We used Chao, Shannon, Faith PD, and Simpson to measure alpha diversity. These indexes consider the number of unique operational taxonomic units (OTUs), richness, the relative abundance of OTUs, and evenness. All four measures found that the No PS and PS groups had similar alpha diversity. Bray-Curtis, Jaccard, and UniFrac were used to measure beta diversity. Only Jaccard similarity (ANOSIM) was significantly different ($p=0.035$). As shown in Figure 1.2, the two groups overlapped with a modest difference in community separation between the two groups.

Table 1.3 shows the bacterial species that were significantly different between the No PS and PS groups. In all cases, a greater relative abundance of the taxa was observed in the PS group. As expected, the changes occurred in the more predominant bacteria phyla, Bacteroidetes, Firmicutes, and Actinobacteria, which made up 46%, 43%, and 2.5% of the bacteria present in the gut, respectively. The most changes in taxa were observed in the Firmicutes phylum (74%). The significantly different changes observed in Actinobacteria derived from the Coriobacterilia class with *Adlercreutzia* at the genus level. For the Bacteroidetes phylum, the changes were seen in the *Bacteroidales* order at the family or genus level. Five different families within the Firmicutes were affected. The most striking difference was with the bacteria *Ruminococcaceae* family, 34 times greater in the PS group than the No PS group.

The bacteria identified as significantly different were correlated with dietary protein, fiber, and fat. These associations are shown in Table 1.3, and the bacteria species belonged to the Actinobacteria, Bacteroidetes, and Firmicutes phyla. All correlations were positive, with more bacteria associating with dietary

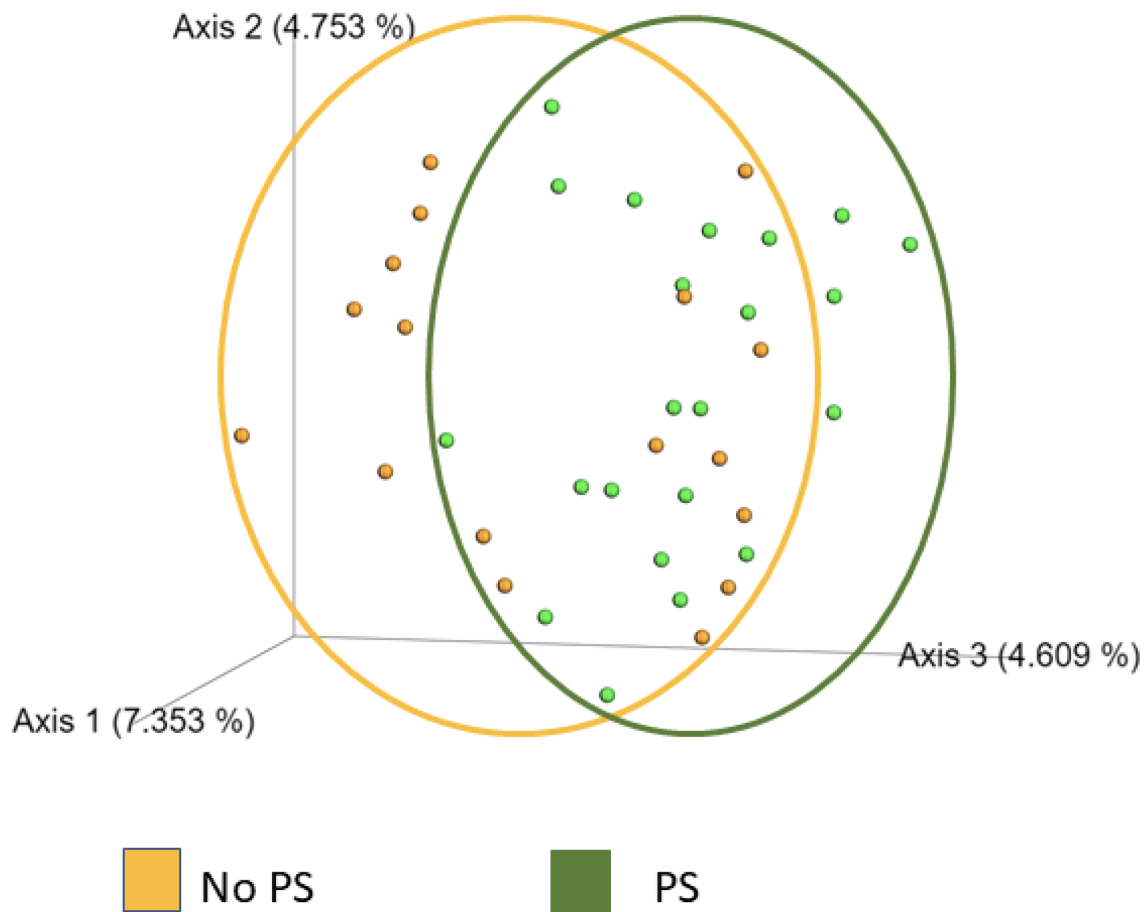


Figure 1.2 Jaccard plot of beta diversity. Each orange dot corresponds to a participant (No PS) who reported not using protein supplements. The orange circle highlights the range of values. Each green dot represents one participant who reported using protein supplements (PS). The green circle shows the variation. Although the groups overlap, the differences were significant ($p = 0.035$), demonstrating community separation by this method.

Table 1.3 Relative abundance of bacterial species that were significantly different

Bacteria	NPS	PS	P-value	Association with Dietary Protein		Association with Dietary Fat	
				Correlation Coefficient	P-value	Correlation Coefficient	P-value
p__Actinobacteria;c__Coriobacteriia	94.9 ± 33.6 ¹	565.5 ± 158.0	0.008	.332	0.039	.513	0.0008
p__Actinobacteria;c__Coriobacteriia;o__Coriobacteriales	94.9 ± 33.6	565.5 ± 158.0	0.008	.332	0.039	.513	0.0008
p__Actinobacteria;c__Coriobacteriia;o__Coriobacteriales;f__Coriobacteriaceae	94.9 ± 33.6	565.5 ± 158.0	0.008	.332	0.039	.513	0.0008
p__Actinobacteria;c__Coriobacteriia;o__Coriobacteriales;f__Coriobacteriaceae;g__Adlercreutzia	4.3 ± 2.1	54.3 ± 14.1	0.002				
p__Bacteroidetes;c__Bacteroidia	8923.1 ± 1941.1	16425.5 ± 1362.1	0.004	.333	0.038	.393	0.013
p__Bacteroidetes;c__Bacteroidia;o__Bacteroidales	8923.1 ± 1941.1	16425.5 ± 1362.1	0.004	.333	0.038	.393	0.013
p__Bacteroidetes;c__Bacteroidia;o__Bacteroidales;f__Bacteroidaceae;g__Bacteroides;__	181.6 ± 45.4	438.4 ± 81.4	0.0096				
p__Bacteroidetes;c__Bacteroidia;o__Bacteroidales;f__Rikenellaceae	857.8 ± 269.3	2083.7 ± 265.7	0.003				

Table 1.3 continued

p__Bacteroidetes;c__Bacteroidia;o__Bacteroidales;f__Rikenellaceae;g__	850.2 ± 267.7	2068.4 ± 263.4	0.0026					
p__Firmicutes;c__Bacilli	30.5 ± 6.8	195.3 ± 42.3	0.0009					
p__Firmicutes;c__Bacilli;o__Lactobacillales	22.6 ± 4.9	136.5 ± 38.1	0.007					
p__Firmicutes;c__Bacilli;o__Turicibacterales	7.1 ± 4.5	58.5 ± 17.6	0.009					
p__Firmicutes;c__Bacilli;o__Turicibacterales;f__Turicibacteraceae	7.1 ± 4.5	58.5 ± 17.6	0.009					
p__Firmicutes;c__Bacilli;o__Turicibacterales;f__Turicibacteraceae;g__Turicibacter	7.1 ± 4.5	58.5 ± 17.6	0.0094					
p__Firmicutes;c__Clostridia	6433.2 ± 1303.2	16415.6 ± 1526.5	0.0000	2		.413	0.009	
p__Firmicutes;c__Clostridia;o__Clostridiales	6431.3 ± 1303.0	16403.7 ± 1522.5	0.0000	2		.414	0.009	
p__Firmicutes;c__Clostridia;o__Clostridiales;f__	242.7 ± 74.3	739.8 ± 153.0	0.007		.322	0.046	.462	0.003
p__Firmicutes;c__Clostridia;o__Clostridiales;f__g__	242.7 ± 74.3	739.8 ± 153.0	0.0066		.322	0.046	.462	0.003
p__Firmicutes;c__Clostridia;o__Clostridiales;f__Clostridiaceae	97.8 ± 23.3	250.4 ± 47.2	0.007					

Table 1.3 continued

p__Firmicutes;c__Clostridia;o__Clostridiales;f__Lachnospiraceae	2960.9 ± 639.1	7179.0 ± 686.7	0.0001	.382	0.016
p__Firmicutes;c__Clostridia;o__Clostridiales;f__Lachnospiraceae;g__	665.6 ± 147.1	1401.9 ± 118.5	0.0004	.344	0.032
p__Firmicutes;c__Clostridia;o__Clostridiales;f__Lachnospiraceae;g__[Ruminococcus]	190.7 ± 42.5	539.7 ± 80.0	0.0005	.380	0.017
p__Firmicutes;c__Clostridia;o__Clostridiales;f__Lachnospiraceae;g__[Ruminococcus];s__torques	13.7 ± 6.4	110 ± 32.7	0.008		
p__Firmicutes;c__Clostridia;o__Clostridiales;f__Lachnospiraceae;g__Anaerostipes	17.2 ± 4.9	56.4 ± 12.4	0.0066		
p__Firmicutes;c__Clostridia;o__Clostridiales;f__Lachnospiraceae;g__Coproccoccus	371 ± 123	1238.5 ± 191.7	0.0006		
p__Firmicutes;c__Clostridia;o__Clostridiales;f__Ruminococcaceae	2328.5 ± 565.8	6663.8 ± 732.5	0.00004	.373	0.019
p__Firmicutes;c__Clostridia;o__Clostridiales;f__Ruminococcaceae;__	55.9 ± 10.8	373.2 ± 75.4	0.0004		

Table 1.3 continued

p__Firmicutes;c__Clostridi a;o__Clostridiales;f__Rum inococcaceae;g__	259.7 ± 74.4	798.3 ± 178.9	0.0097			.443	0.005
p__Firmicutes;c__Clostridi a;o__Clostridiales;f__Rum inococcaceae;g__Faecalib acterium	1372.5 ± 450.4	3488.4 ± 257.8	0.0004				
p__Firmicutes;c__Clostridi a;o__Clostridiales;f__Rum inococcaceae;g__Oscillos pira	318.6 ± 73.6	822.5 ± 111.8	0.0006			.445	0.005
p__Firmicutes;c__Clostridi a;o__Clostridiales;f__Rum inococcaceae;g__Rumino coccus	314 ± 84	1167.9 ± 275.1	0.0065				
p__Firmicutes;c__Clostridi a;o__Clostridiales;f__Veill onellaceae	569.2 ± 122.6	1127.6 ± 147.1	0.0060 0	.345	0.031	.362	0.024
p__Firmicutes;c__Clostridi a;o__Clostridiales;f__Veill onellaceae;g__Phascolar cibacterium	171.1 ± 78.3	746.2 ± 151.8	0.0021			.518	0.0007
p__Firmicutes;c__Clostridi a;o__Clostridiales;f__Veill onellaceae;g__Phascolar cibacterium;s	205.5 ± 79.7	719.7 ± 155.8	0.0062			.518	0.0007

¹ mean ± SEM

fat than protein or fiber. Although dietary fat was not significantly different between the groups, 41% of the No PS dietary calorie intake came from fat, while 34% of the PS dietary calories were derived from fat. Only two bacterial species correlated with dietary fiber (not shown in table): p__Firmicutes;c__Clostridia;o__Clostridiales;f__Lachnospiraceae;g__Coprococcus ($p < 0.032$) and p__Firmicutes;c__Clostridia;o__Clostridiales;f__Ruminococcaceae;g__Oscillospira ($p < 0.032$).

The predicted functional pathways that were significantly different are shown in Figure 1.3. Ten pathways emerged as significantly different between the No PS and PS groups. Eight of the ten pathways (arginine and proline metabolism; biosynthesis of unsaturated fatty acids; caffeine metabolism; circadian rhythm-plant; fatty acid elongation in mitochondria; non-homologous end-joining; steroid biosynthesis; and systemic lupus erythematosus) were more highly expressed in the PS group. Nucleotide metabolism and RIG-1-like receptor signaling pathway were more highly expressed in the No PS samples.

Alterations in the fecal metabolome are shown in Figure 1.7. Heatmaps serve as a visualization tool for changes in the relative abundance of metabolites (Fig 1.7). A few metabolites were significantly different in relative abundance between the two groups (Figure 4A): allantoin ($p < 0.01$), dipicolinate ($p < 0.05$), tricarballylic acid ($p < 0.01$), octulose 8/1 phosphate ($p < 0.05$), xanthosine ($p < 0.01$), dATP ($p < 0.01$), abscisate ($p < 0.01$), pimelic acid ($p < 0.01$), methyl glutaric acid ($p < 0.05$), lactate ($p < 0.01$), sucralose ($p < 0.01$), S-ribosyl-L-homocysteine ($p < 0.05$), homocysteine ($p < 0.01$), quinolinate ($p < 0.05$), sulfolactate ($p < 0.01$), and homocarnosine ($p < 0.01$). Despite few significant changes, the 3D PLS-DA showed separation of the PS group and the No PS group, indicating different metabolic profiles between the groups (Figure 1.4A). Metabolites with a variable importance in projection (VIP) score > 1 drove the separation in the PLS-DA plot, contributing most to the differences observed between groups (Figure 1.4B). Using metabolites with a VIP score > 1 for pathway analysis, it was evident that purine and pyrimidine metabolism were altered in response to protein supplementation. Additionally, glycolysis, cysteine and methionine metabolism, and the TCA cycle were also perturbed (Figure 1.4C). All of the altered pathways are interconnected with nitrogen metabolism (Figure 1.5).

The bacteria correlated with each trait are shown in Table 1.4. Traits ME and PF were correlated with more than one phylum, respectively. Only trait mental energy was correlated with members of the Actinobacteria and Verrucomicrobia, while members of Proteobacteria and Bacteroidetes were only associated with trait PF. Interestingly, at least one member of the Firmicutes phyla was correlated with every trait, but only one Firmicute member, c__Clostridia;o__Clostridiales;f__Lachnospiraceae;g__Anaerostipes;s__, was correlated with more than one trait (i.e., ME, MF, PF).

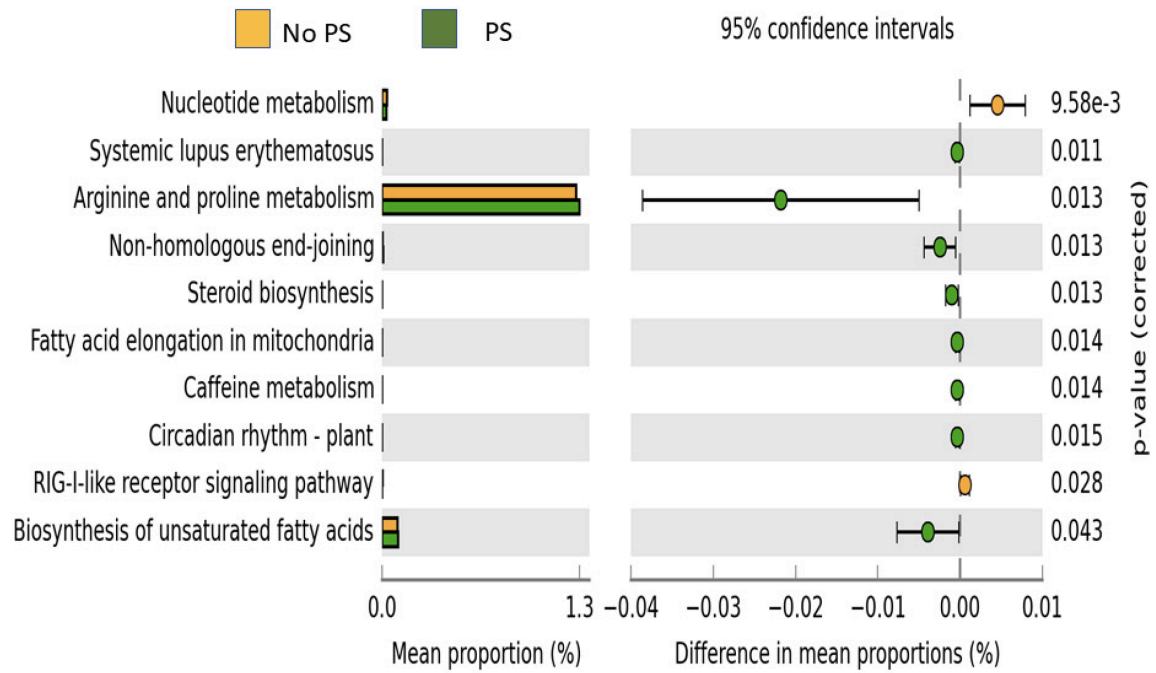


Figure 1.3 Predicted functional pathways. Pathways that were significantly different between the two groups are shown along with the Bonferroni-corrected p-value. Orange bars are the No PS group, while the green bars are the PS group.

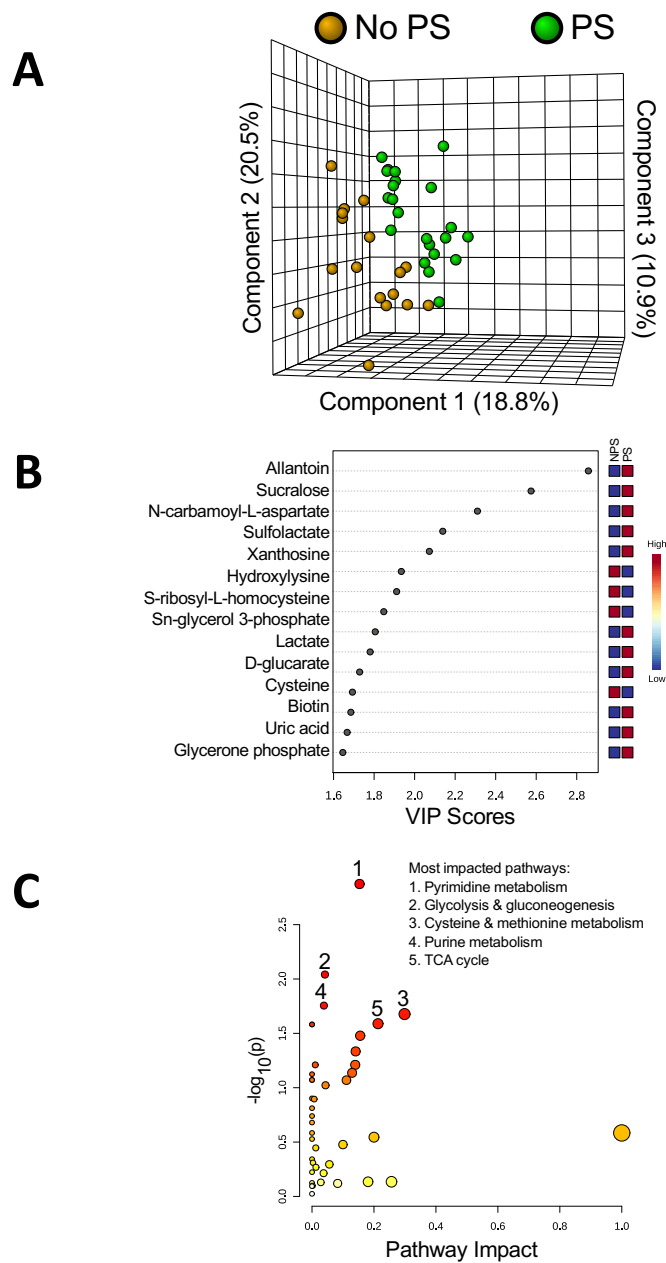


Figure 1.4 Metabolomics analysis showing PS induces metabolic alterations. (A) 3D PLS-DA plot showing separation of the PS and NPS groups, indicating unique metabolic profiles. (B) This plot shows the top 15 metabolites with the highest VIP scores contributing most to the observed separation of groups. Allantoin contributes most to the separation of the PS and NPS groups in the PLS-DA plot. (C) Metabolites with a VIP score > 1 were used for pathway analysis. The pathways impacted most by PS include pyrimidine metabolism, glycolysis and gluconeogenesis, cysteine and methionine metabolism, purine metabolism, and the TCA cycle.

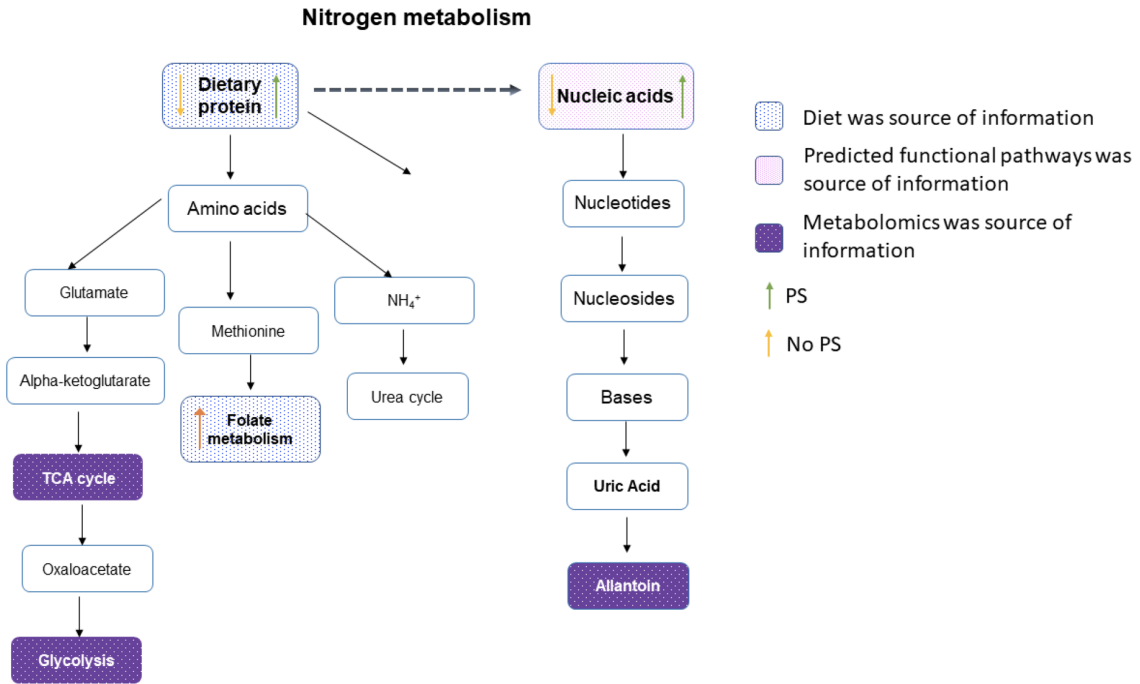


Figure 1.5 Nitrogen metabolism pathways. Assembling the metabolome and microbiome data suggested nitrogen metabolism was altered in the gut environment of participants who reported consuming a protein supplement compared to those who did not. Blue boxes represent information derived from the participant’s dietary recall. The orange and green arrows in each box show which group had higher or lower intake. Evidence derived from predicted functional pathways is highlighted in pink, while the purple boxes are metabolites or pathways identified by metabolomics.

Table 1.4 Bacteria taxa significantly correlated with specific traits. Same colored bacteria names correlate with more than one trait.

	Correlation Coefficient	Significance
Trait Mental Energy		
p__Actinobacteria	0.469	0.037
p__Firmicutes	0.520	0.019
p__Firmicutes;c__Bacilli;o__Turicibacterales	0.470	0.037
p__Firmicutes;c__Bacilli;o__Turicibacterales;f__Turicibacteraceae	0.470	0.037
p__Firmicutes;c__Bacilli;o__Turicibacterales;f__Turicibacteraceae;g__Turicibacter	0.470	0.037
p__Firmicutes;c__Clostridia;o__Clostridiales;f__Lachnospiraceae;g__s__	0.461	0.041
p__Firmicutes;c__Clostridia;o__Clostridiales;f__Lachnospiraceae;g__[Ruminococcus];s__gnavus	0.478	0.033
p__Firmicutes;c__Clostridia;o__Clostridiales;f__Lachnospiraceae;g__Anaerostipes;s__*	0.480	0.032
p__Firmicutes;c__Clostridia;o__Clostridiales;f__Ruminococcaceae;g__s__	0.454	0.044
p__Firmicutes;c__Clostridia;o__Clostridiales;f__Lachnospiraceae;g__Coprococcus;s__catus	0.479	0.032
p__Firmicutes;c__Clostridia;o__Clostridiales;f__Lachnospiraceae;g__Roseburia;s__faecis	0.558	0.011
p__Verrucomicrobia;c__Verrucomicrobiae	0.475	0.034
p__Verrucomicrobia;c__Verrucomicrobiae;o__Verrucomicrobiales	0.475	0.034
p__Verrucomicrobia;c__Verrucomicrobiae;o__Verrucomicrobiales;f__Verrucomicrobiaceae	0.475	0.034
p__Verrucomicrobia;c__Verrucomicrobiae;o__Verrucomicrobiales;f__Verrucomicrobiaceae;g__Akkermansia	0.475	0.034
Trait Mental Fatigue		
p__Firmicutes;c__Erysipelotrichi	0.451	0.046
p__Firmicutes;c__Erysipelotrichi;o__Erysipelotrichales	0.451	0.046
p__Firmicutes;c__Erysipelotrichi;o__Erysipelotrichales;f__Erysipelotrichaceae	0.451	0.046
p__Firmicutes;c__Clostridia;o__Clostridiales;f__Lachnospiraceae;g__Anaerostipes;s__	-0.532	0.016
Trait Physical Energy		
p__Firmicutes;c__Erysipelotrichi;o__Erysipelotrichales;f__Erysipelotrichaceae;g__Holdemania	-0.533	0.015
p__Firmicutes;c__Clostridia;o__Clostridiales;f__Lachnospiraceae;g__Dorea;s__	-0.463	0.040
p__Firmicutes;c__Clostridia;o__Clostridiales;f__Peptostreptococcaceae;g__s__	-0.461	0.041
Trait Physical Fatigue		
p__Firmicutes;c__Clostridia;o__Clostridiales;f__Christensenellaceae;g__s__	-0.630	0.003
p__Firmicutes;c__Clostridia;o__Clostridiales;f__Lachnospiraceae;g__Anaerostipes;s__	-0.448	0.048
p__Proteobacteria;c__Gammaproteobacteria;o__Pasteurellales	0.445	0.049
p__Proteobacteria;c__Gammaproteobacteria;o__Pasteurellales;f__Pasteurellaceae	0.445	0.049
p__Proteobacteria;c__Gammaproteobacteria;o__Pasteurellales;f__Pasteurellaceae;g__Haemophilus	0.512	0.021
p__Bacteroidetes;c__Bacteroidia;o__Bacteroidales;f__Bacteroidaceae;g__Bacteroides;s__	-0.451	0.046

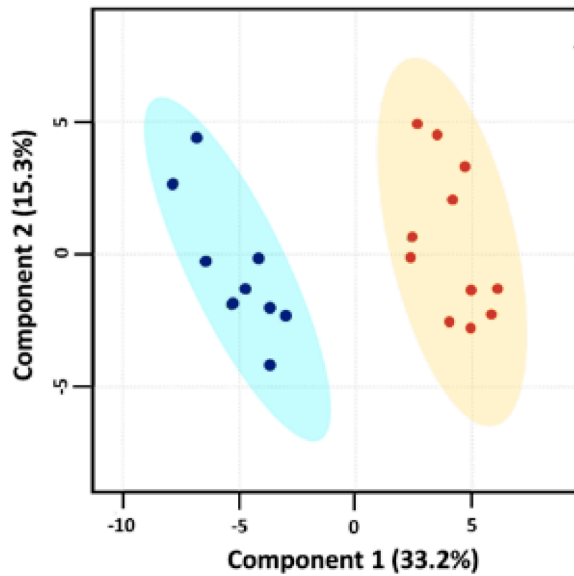
PCA analysis revealed that the subjects naturally separated into two distinct clusters (left or right, Figure 1.6A). Of the identified metabolites, 100 metabolites had a significantly higher relative abundance in the left group (presented in blue), including but not limited to biotin, serine, and shikimate. The right group (presented in red) had only six metabolites with a higher relative abundance, including propionyl-CoA, acetyl-CoA, and NAD⁺. There were no statistically significant differences in PF, PE, MF, or ME when comparing the subjects on the left to those on the right (Figure 1.6B). Therefore, the separation of the clusters observed on the PCA plot cannot be attributed to traits, so distinct metabolic profiles based on MF, ME, PF, and PE were not observed in the study.

1.4 Discussion

To our knowledge, this is the first study to investigate the gut microbiome of young physically active adults who self-identified as muscle builders taking a protein supplementation. Often a high protein, low dietary fiber diet is associated with bodybuilding. Scientific studies have shown that fiber and protein can influence the abundance of microbial communities present in the gut, although protein's effects are less understood than fiber. The recommended fiber intake for men and women under 50 years of age is 38 g/day and 25 g/day, respectively.⁴⁰ However, research has shown that many individuals fall short of these guidelines. For example, in a study comparing the gut microbiota of 15 distance runners and 15 bodybuilders, Jang *et al.*⁴¹ reported that dietary fiber intake was similar between the two groups: 17 g/day (distance runners) and 19 g/day (bodybuilders). However, the average protein intake was 103 g for the distance runners and 236 g for the bodybuilders. Interestingly, there were differences in the gut microbiome between these groups. At the genus and species levels, *Faecalibacterium*, *Clostridium*, *Haemophilus*, and *Eisenbergiella* were the highest ($p < 0.05$) in bodybuilders while *Bifidobacterium* and *Parasutterella* were the lowest ($p < 0.05$) in bodybuilders. In our study, fiber intake for our groups was similar to Jang *et al.*'s⁴¹ study, but unexpectedly, the PS group consumed 8 gms more fiber than the No PS group. However, neither group met the recommended amount of fiber daily. Our participant's average protein intake was less than Jang *et al.*⁴¹ bodybuilder's protein intake. *Faecalibacterium* was the only bacteria for which we observed changes that Jang *et al.*⁴¹ also reported.

The Recommended Dietary Intake for protein is 0.8 g/kg body weight⁴² based on net nitrogen balance, translating to a mean dietary need of 63 g/day for our athletes. However, protein is needed to build and repair muscle, so 1.2 to 2.0 g protein/kg body weight/day is recommended for strength-training athletes.⁴³ Our participants consumed 1.5 to 2.2 g protein/kg body weight; the No PS group at the lower end and the PS group at the upper end of the recommendation. On a moderately high protein diet in which protein makes up 15% of total energy intake, 17 g dietary protein/day goes undigested in the small intestine and enters the colon for putrefaction.⁴⁴ In our study, protein intake was 20-27% of calories. Based on

A.



B.

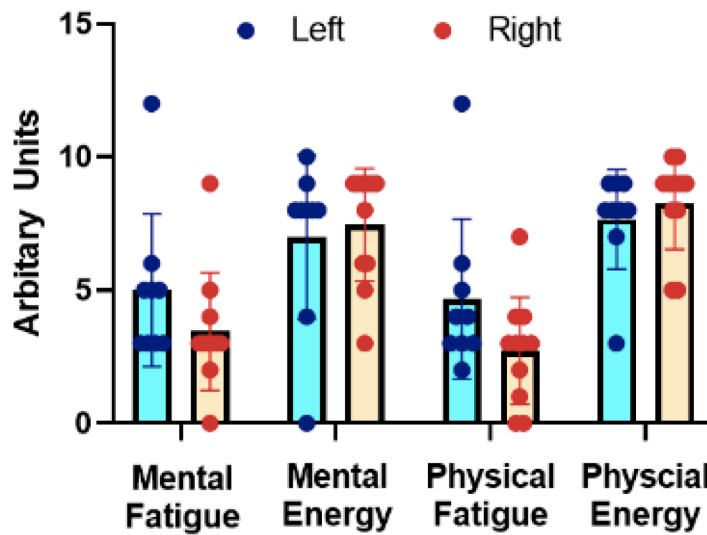


Figure 1.6 A principal component analysis (PCA) for the 20 survey subjects. (A) clearly shows two distinct clusters: left blue and right red. (B) shows the average \pm SD for each trait. MF, ME, PF, and PE were not significantly different between the two clusters.

Gibson et al.'s⁴⁴ findings, we deduct more than 17 g of protein reached the colon for putrefaction.

A high protein, low carbohydrate diet favors a pathogenic, pro-inflammatory colonic microbiota. Jang *et al.*⁴¹ concluded from their study of sedentary individuals, bodybuilders and distance runners that a high protein diet might negatively impact gut microdiversity and decrease short chain fatty acid-producing commensal bacteria. Increased protein fermentation can be attenuated by the addition of dietary fiber.⁴⁵ While our PS group had a higher protein intake, their fiber intake was less than the dietary recommended amount and therefore may not have been sufficient to provide this benefit. We did note an increase in several butyrate producing species in the gut microbiota of the PS group.

In addition to protein intake, diet quality affects gut microbiome diversity⁴⁶. HEI is a measure of dietary quality, and both groups score demonstrated that they did not meet the US Dietary Guidelines. Thus, only one diversity measure was significantly different between the two groups, so despite the significant difference in protein and fiber intake, these differences were not enough to alter gut microbiota diversity. Other studies have reported no change in gut microbial diversity following resistance exercise.^{41, 47, 48}

In healthy individuals, the phyla *Firmicutes*, *Bacteroidetes*, *Actinobacteria*, and *Proteobacteria* make up 98% of the bacteria present in the human GI tract.⁴⁹⁵⁰ Our study observed changes in the relative abundance of species within three of these phyla, Firmicutes, Bacteroidetes, and Actinobacteria. More changes were seen in the Firmicutes phyla, and many taxa in this phyla are butyrate-producing.⁵¹ Lactobacillales abundance was significantly greater in the PS group and this family of bacteria functions in purine absorption⁵² and uric acid decomposition.⁵³

Host health is affected by the structure and diversity of the gut microbiota. At the genus level, we observed higher levels of *Adlercreutzia*, *Bacteroides*, *Turicibacter*, *Anaerostipes*, *Coprococcus*, *Faecalibacterium*, *Oscillospira*, *Roseburia*, *Blautia*, *Ruminococcus*, and *Phascolarctobacterium* in the protein supplemented group. *Oscillospira* is a common gut bacterial genus, and several recent gut microbiota investigations have demonstrated its underlying significance for host health in several chronic diseases like obesity.⁵⁴ Chen *et al.*⁵⁴ found it inversely correlated with Bristol stool type and that it may play a role in decreased bowel movements and aggravate constipation. Constipation can be a problem with bodybuilders who consume large amounts of protein. However, none of our participants reported constipation, we excluded participants taking laxatives, and the Bristol score was similar between both groups (~3). This score characterizes stool as sausage-like with cracks on the surface. As well, *Oscillospira* has also been positively associated with leanness.⁵⁵ *Phascolarctobacterium* is a substantial acetate/propionate producer (short-chain fatty acids) and is associated with the metabolic state and positive mood.⁵⁶ Jang *et al.*⁴¹ found *Faecalibacterium* significantly higher in bodybuilders compared to distance runners and sedentary

individuals. Also, they reported *Blautia*, a short-chain fatty acid producer, to be the lowest in the bodybuilders compared to controls.

Only a few studies have looked at the effect of protein supplementation, usually whey, on the gut microbiomes of athletes. For example, Moreno-Perez et al. supplemented cross-country runners with 10g whey isolate and 10 g beef hydrolysate in 200 ml orange drink for 10 weeks. They found increased abundance of the Bacteroidetes phylum and decreased *Roseburia*, *Blautia*, and *Bifidobacterium longum*. While our participants did not supplement daily, we also found an increased relative abundance of *Roseburia* and *Blautia* in our PS group.

Nitrogen metabolism can be altered by protein consumption. A high-protein diet contains a large quantity of purine, a nucleotide. Purines play a vital role in energy metabolism and are used as building blocks for DNA synthesis.⁵⁷ Uric acid is produced when purines are enzymatically degraded.⁵⁸ Uric acid is then further degraded to allantoin, the metabolite with the highest VIP score. The PS group had a significantly higher allantoin relative abundance in their feces compared to the No PS group. Since allantoin and uric acid, along with other metabolites involved in purine metabolism, are driving the separation between the PS and No PS groups, it can be concluded that higher levels of dietary protein favor purine degradation. This evidence is further supported by a greater relative abundance of f. Lactobacillales in the PS group ($p = 0.007$), a bacteria family that functions in purine absorption and uric acid decomposition.⁵⁹ Additionally, genes encoding for nucleotide metabolism were significantly more abundant in the No PS group. This observation could be expected because the No PS group had a lower protein intake, which leads to fewer purines, creating a greater need for genes involved in purine metabolism. It has been documented that purine-rich diet can activate the purine degradation pathway which results in the production of uric acid and allantoin.⁶⁰ It is not surprising that protein supplementation results in increased purine degradation.

Interestingly, *Anaerostipes* was correlated with trait ME, MF, and PF in the anticipated direction. Higher levels of *Anaerostipes* are associated with activation of fatty acid oxidation, synthesis, and lipolysis inhibition, which in turn decreases circulating lipid plasma levels and body weight.⁶¹ It also suppresses colon inflammation and can downregulate insulin signal transduction in adipose tissue. Although this study did not differentiate which function the bacteria serve in each trait, based on previous findings⁶² and the other bacteria associated with the traits, the authors hypothesize that *Anaerostipes*' anti-inflammatory function may be associated with MF and PF. In contrast, the metabolic function of the *Anaerostipes* bacteria may be correlated with trait ME.

This study is not without its limitations. First, the participants were recruited online, and although we emailed many potential candidates, we demonstrated that participants could be recruited in this manner. Second, once lockdowns from the

COVID pandemic started, we could no longer recruit participants which reduced our sample size. Third, we had to rely on the participants self-reporting their resistance training because they were recruited and participated in the study online. Self-reporting has inherent errors, but we used several measures, self-reported workout form, and IPAQ, to verify their training claims. These were used to determine if the participants were physically active and had consistent resistance training. Fourth, the two groups were divided based on the participant's reported protein supplement use. All PS group participants reported using a protein supplement, while the No PS group reported not using a protein supplement to promote muscle gains. We also verified this with the ASA24 24-hour recall. The ASA24 reports supplement usage, and only the participants in the protein supplemented group reported using a protein supplement 24 hours before they collected their fecal sample.

1.5 Methods

This multi-omics study aimed to identify the bacteria present in the fecal matter of young physically active adults using resistance exercise who reported taking or not taking a protein supplement. Participants were recruited from Sports and Health Science majors at the online university, American Public University System (APUS). This study was approved by the Institutional Review Board at APUS (protocol # 2018-097) and the Louisiana State University Health Sciences Center (LSUHSC) (protocol # 10217).

1.5.1 Experimental Approach

A schematic for recruiting participants is shown in Figure 1.1. Participants were excluded if they met at least one of the following criteria: 1) took an antibiotic in the last three months, 2) consumed an anti-diarrhea medicine in the last week, 3) took a laxative in the last week, 4) consumed prebiotics in the last week, 5) consumed probiotics in the last week, 6) been diagnosed with cancer, 7) have Crohn's disease, 8) taking prescription drugs other than oral contraceptives, 9) cutting for an upcoming competition or tournament, 10) under 25 years of age, or 11) lived outside the contiguous United States. We asked potential participants to share their maximum squat, bench press or deadlift and then calculated a weight lifted to body mass ratio. Those who could not lift at least half of their body weight were excluded. Each participant was asked if they consumed a protein supplement so they could be assigned to one of two groups: protein supplement (PS) and no protein supplement (No PS). The participants that met the criteria were sent an email welcoming them to the study and requested verification that they were willing to participate. If their response was positive, they were sent a fecal collection kit. After collecting their fecal sample, the participant completed a supplement questionnaire, a workout questionnaire, an online version of the International Physical Activity Questions (IPAQ), and a 24-hour food recall using the ASA24. Each participant completed the study at their physical location anywhere in the contiguous United States. Participants were recruited in two cohorts one year

apart at the same time of year (October/November/December). For successful participation in the study, the participant had to complete: 1) written informed consent, 2) signed HIPAA consent, 3) acknowledgement that they were training to build muscle, 4) completed the required questionnaires, and 5) returned fecal sample. Thirty-nine participants provided a fecal sample and completed all the required forms.

Of the 39 individuals who participated in the study, 20 of the subjects consented and completed the survey regarding traits energy and fatigue. All study procedures were approved by the Institutional Review Board at the American Public University System (2021–045–OL, 14 April 2021). The survey was conducted online using Qualtrics (Qualtrics, XM, Provo, UT). The mental and physical state and trait energy and fatigue scales [18] were used to discriminate between mental and physical energy and fatigue. The reliability and temporal stability of these scales has been previously demonstrated [21–23,43–47]. For the current study, reliability was tested using Cronbach’s Alpha test in SPSS (IBM Corp. Released 2020. IBM SPSS Statistics for Windows, Version 27.0. Armonk, NY, USA: IBM Corp). The scores were PE, 0.767, PF, 0.899, ME, 0.890, and MF, 0.893.

1.5.2 Sample Collection

A fecal sample was collected using an at-home, self-collection kit (The Biocollective, Denver, CO) sent to them via Fed Ex overnight along with a freezer brick, Styrofoam shipping container, and cardboard box to fit over the Styrofoam shipping container. The kit contained a specially designed biocollector that was placed over the toilet for fecal collection. Once the fecal sample (without urine) was collected, the biocollector was inserted into a special zip locking barrier bag that was inserted into a ziplock specimen bag. Then the specimen bag was placed in a Styrofoam shipping container, and a frozen freezer brick was placed on top. The Styrofoam container was placed into the cardboard box, sealed, and shipped overnight. To prevent receiving samples on a Saturday or Sunday, the participant was instructed to ship the sample on the same day of collection and collect it on a Monday-Thursday, no holidays. If the sample was not returned within 24 hours of collection, the sample was discarded, and the participant was excluded from the study. Upon receipt in the lab at LSUHSC, the sample was mixed in the sample bag in a biosafety level 2 hood and small portions aliquoted into sterile microcentrifuge tubes designed for cold storage. The tubes were placed in liquid nitrogen for quick freezing and stored in a -80° C freezer. At the same time, a sample of approximately 250 mg was processed for DNA isolation using the QIAamp PowerFecal DNA Kit (Qiagen, Germantown, MD, USA), which included bead-beating. The isolated DNA was stored at -80° C until microbial community analysis.

1.5.3 Dietary Assessment

Participants were asked to recall the foods they ate 24 hours prior to their fecal sample collection. They used the freely available, automated, web-based, self-administered 24-hour dietary assessment (ASA24) (<https://epi.grants.cancer.gov/asa24/>)⁶³, which is available on the web and mobile devices and is funded and maintained by the National Cancer Institute. Each participant was sent a unique user ID and password. Although the ASA24 program collects information on supplement use, we also asked participants to provide information about their supplement on a separate form. The 2010-2015 Healthy Eating Index (HEI) was calculated from the food group data provided by ASA24 using the SAS program code available for free online by the National Cancer Institute (<https://epi.grants.cancer.gov/he/calculating-hei-scores.html>).

1.5.4 Physical Activity Assessment

Physical activity was assessed using the International Physical Activity Questionnaire (IPAQ) long-form converted to an online format. Also, each participant was asked to provide their muscle-building workout routine on a separate form since the IPAQ does not ask specifically about resistance training. In this form, participants reported the exercise name, workouts per week, sets per workout, reps per set, weight lifted, and 1-RM. Volume loads (weight lifted in kg x reps x sets x workouts per week) for upper body or lower body exercises were calculated similarly to the methods of Haff.⁶⁴

1.5.5 Microbial Community Analysis

A Thermo Scientific™ NanoDrop™ spectrophotometer (ThermoFisher Scientific, Waltham, MA) was used to determine the quantity and purity of the isolated fecal DNA. Two amplification steps using the AccuPrime Taq high fidelity DNA polymerase system (Invitrogen, Carlsbad, CA) were performed to prepare a sequencing library. Also, a negative control with the control from DNA extraction and a positive control of Microbial Mock Community HM-276D (BEI Resources, Manassas, VA) were set during amplicon library preparation. Genomic DNA and the gene-specific primers with Illumina adaptors were used to amplify the 16S ribosomal DNA hypervariable region V4: Forward 5'TCGTCGGCAGCGTCAGATGTGTATAAGAGACAG GTGCCAGCMGCCGCGGTAA3'; Reverse 5' GTCTCGTGGGCTCGGAGATGTGTATAAGAGACAG GGACTACHVGGGTWTCTAAT 3'. AMPure XP beads were used to purify the indexed amplicon libraries, quantified using Quant-I PCR products. The purified amplicon DNA was amplified using the primers with different molecular barcodes: forward 5' AATGATACGGCGACCACCGAGATCTACAC [i5] TCGTCGGCAGCGTC 3'; reverse 5' CAAGCAGAAGACGGCATACGAGAT [i7] GTCTCGTGGGCTCGG 3'. The indexed amplicon libraries were purified using AMPure XP beads, quantified using Quant-iT PicoGreen (Invitrogen), then normalized and pooled. The KAPA Library Quantification Kit (Kapa Biosystems)

was used to quantify the pooled library, which was diluted and denatured according to Illumina's sequencing library preparation guidelines. As an internal control and to increase 16S RNA amplicon library diversity, 10% PhiX was added to the sequencing library. The paired-end sequencing was performed on an Illumina MiSeq (Illumina, San Diego, CA) using the 2×250bp V2 sequencing kit.

QIIME2 (Quantitative Insights Into Microbial Ecology) with the DADA2 plugin⁶⁵ was used to process raw fastq files. Forward and reverse reads were truncated to a uniform length of 240 bp, and 20 bp were trimmed off the front of each read to remove the primer. DADA2 identified amplicon sequence variants (ASVs) were merged, and any that fell out of the expected 250bp – 255bp length were discarded. Any ASVs that appeared in only one sample were removed using contingency-based filtering, and chimeric ASVs were removed using the consensus method. ASVs were aligned using mafft and fasttree⁶⁶, and a phylogenetic tree for diversity analysis was built. Greengenes v13.8 was used for taxonomic classification.⁶⁷ After primary data analysis, the remaining reads were analyzed using QIIME2.⁶⁸

The QIIME analysis included 39 samples and read counts ranging from 6,729 to 99,983, with an average read count per sample of 44812. Alpha rarefaction was performed at a level of 6,729 reads to include all samples.

1.5.6 Prediction of Metabolic Profile

The 16S sequencing data was used to identify potential microbial functions. The raw data were formatted and imported into QIIME2. Closed-reference clustering against the Greengenes 13_5 97% OTUs reference database was used to develop a dereplicated feature table and representative sequences. The closed-reference OTU table was used as input into the PICRUSt⁶⁹ pipeline, and the resulting PICRUSt metagenome data were further analyzed using STAMP (Statistical Analysis of Metagenomic Profiles).⁷⁰ Pathways were labeled at Level 2 since several pathways were not classified at Level 1, which causes an error in STAMP. From this, KEGG (Kyoto Encyclopedia of Genes and Genomes) pathways were compared between protein supplemented (PS) and nonprotein supplemented (No PS) participants.

1.5.7 Metabolomics

Samples were processed at the Biological and Small Molecule Mass Spectrometry Core (BSMMS) at the University of Tennessee, Knoxville, TN (RRID: SCR_021368). The fecal sample from each participant was divided into aliquots (roughly 50-100 mg) and extracted in biological triplicate. Polar metabolites were extracted from fecal samples using an acidic acetonitrile extraction procedure, using 40:40:20 HPLC grade ACN/MeOH/H₂O with 0.1 M formic acid.⁷¹ Global metabolic profiling, using ultra high-performance liquid chromatography high resolution mass spectrometry (UHPLC-HRMS), was used to analyze the fecal microbiome. A 25-minute reverse-phase chromatographic

separation was performed using a Synergi 2.6 μm Hydro RP column (100 mm x 2.1 mm, 100 \AA ; Phenomenex, Torrance, CA) and an UltiMate 3000 pump (Dionex). After chromatographic separation, analytes were ionized using negative mode electrospray ionization. A Thermo Scientific Exactive Plus Orbitrap (San Jose, CA) was utilized for mass analysis operating in full-scan mode.^{23, 72} A package from ProteoWizard, msConvert was used to convert raw spectral files to .mzML format.⁷³ Metabolomics analysis and visualization engine (MAVEN) was used to identify metabolites based on exact mass (± 5 ppm) and retention time using an in-house library.^{24, 74} A total of 170 metabolites were identified from the untargeted metabolomics analysis.

1.5.8 Statistical Analysis

A power calculation determined 24 participants were needed per group (PS and No PS). Thirty-nine participants completed the study prior to beginning of the COVID19 pandemic. It was decided to stop participant recruitment at the start of the pandemic since the time length was unknown, and we did not want to risk exposure to the virus from fecal samples.

Data were expressed as mean \pm SEM (standard error of the mean), and the tables presented the actual p -value. A value of $p < 0.05$ was considered statistically significant and was determined a priori. SPSS (IBM Corp. Released 2020. IBM SPSS Statistics for Windows, Version 27.0. Armonk, NY: IBM Corp) was used for statistical comparisons. Differences in alpha and beta diversity were determined using QIIME 1.9.0, and figures were drawn using GraphPad Prism 9 (GraphPad Software, San Diego, CA). Significant differences in bacterial species between the No PS and PS groups were determined using Mann Whitney U. Only p -values < 0.01 are reported for the bacterial species identified as significantly different. STAMP was used to determine statistical differences in functional pathways between the groups and to generate post hoc (Tukey-Kramer) plots for each KEGG pathway that was significantly different between No PS and PS.

Metabolite peak intensities were normalized by weight of each fecal sample aliquot. MetaboAnalyst 5.0 was used to generate partial least-squares discriminant analysis (PLS-DA) plots, variable importance in projection (VIP) scores, and pathway analysis using the normalized metabolomics data. In MetaboAnalyst, the normalized data were filtered by interquartile range, log-transformed, and Pareto scaled.²⁵ Heatmaps were generated using R (version 1.0.153), which display \log_2 fold changes and p -values calculated by a Student's T-test.

1.6 Conclusions

This exploratory study showed that the gut metabolome and microbiome is impacted by protein supplementation and/or diet. While the alterations were minimal, protein supplementation did induce changes in the function and composition of the gut microbiota. There was a clear impact on nitrogen metabolism in response to protein supplementation. The PS group had a distinct

metabolic profile from the No PS group, and allantoin was the metabolite contributing most to these differences. This revealed that the PS group was favoring the degradation of purines, as uric acid was also increased in the PS group. Opposite to this, the participants from the No PS group seemed to favor nucleotide biosynthesis and metabolism as they had more genes associated with nucleotide metabolism suggesting the greater need of the gut microbiota to synthesize nucleic acids due to not being supplied an excess exogenous nitrogen source. The health consequences to the host are unknown but several metabolites, for example, uric acid, the precursor of allantoin, are associated with inflammatory processes.⁷⁵ Additional studies are warranted to determine the health consequences to the host. This study also showed that traits ME, MF, PE, and PF did not display unique metabolic profiles but could be defined by distinct bacterial communities, though more robust studies are needed to validate the findings from this exploratory study.

APPENDIX

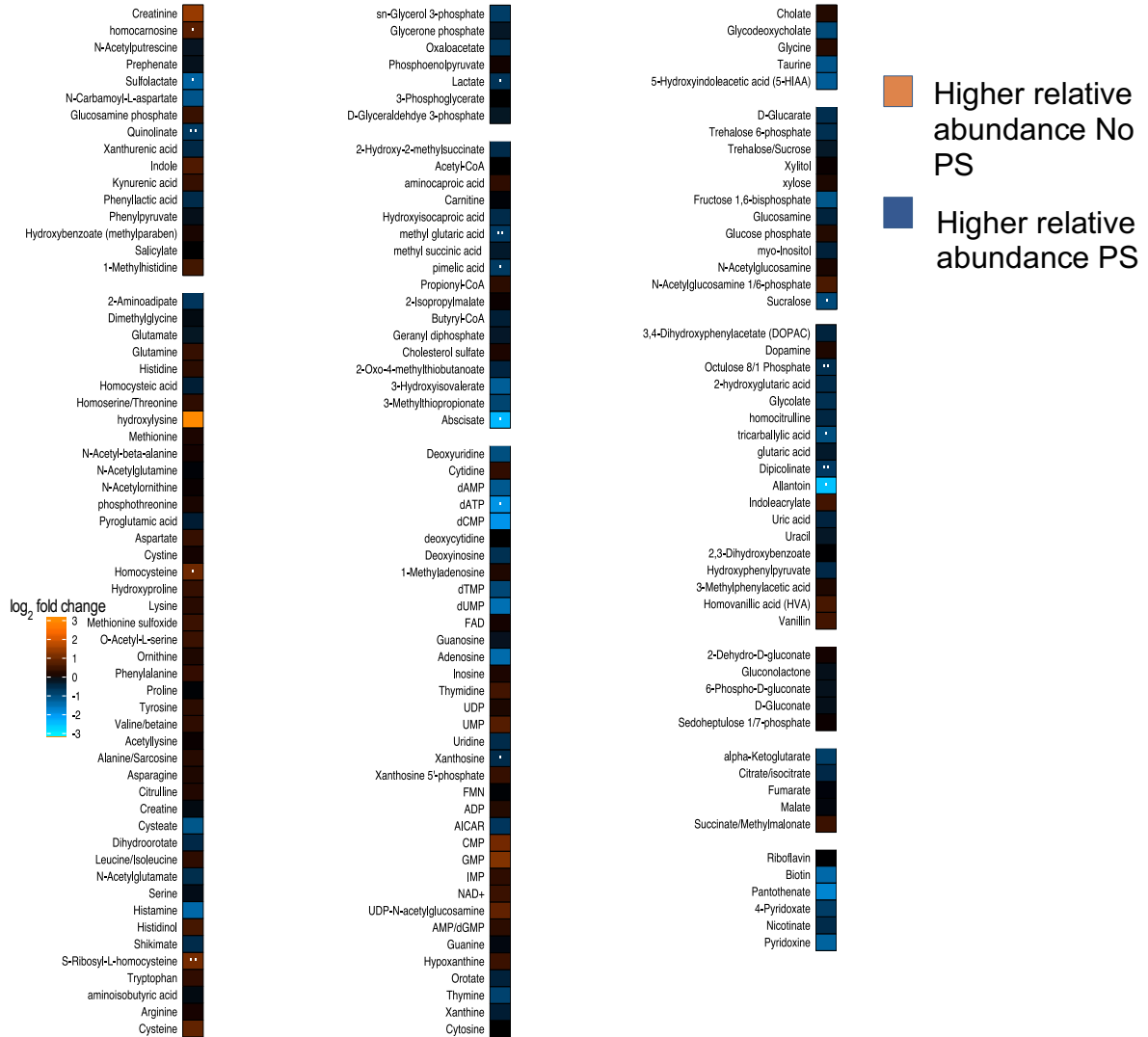


Figure 1.7 Heatmap showing the log₂ fold change and p-values for all identified metabolites in fecal samples. Metabolite relative abundances were altered by PS.

**CHAPTER 2 HEAT STRESS INDUCES UNIQUE METABOLIC
ALTERATIONS IN THE SMALL INTESTINES, INTESTINAL
DIGESTA, AND PLASMA OF BROILER CHICKS**

A version of this chapter was originally published by Dridi J. S., et al.:

Jalila S. Dridi, Elizabeth S. Greene, Craig W. Maynard, Giorgio Brugaletta, Alison Ramser, Courtney J. Christopher, Shawn R. Campagna, Hector Castro, Sami Dridi; Duodenal metabolic profile changes in heat-stressed broilers; *Animals* 2022, 12, 1337.

SD, SRC, and CJC designed the experiment and purchased the reagents. ESG and SD conducted the trial and processed the animals at the end of the trial. CJC, HFC and SRC performed the metabolomics analysis. CJC interpreted, processed, and analyzed metabolomics data. JSD, CJC, and S.D. wrote the manuscript with input from all authors.

A version of this chapter will be a part of a future publication titled:
Heat stress induces unique metabolic alterations in the small intestines, intestinal digesta, and plasma of broiler chicks

Possible authors: Courtney J. Christopher, Elizabeth S. Greene, Hector Castro, Shawn R. Campagna, Sami Dridi

Author contributions

SD, SRC, and CJC designed the experiment. ESG and SD conducted the trial and processed the animals at the end of the trial. CJC wrote the manuscript. SRC and HFC edited the manuscript. CJC performed metabolomics extractions, mass spectral analysis, and data processing and analysis.

2.1 Abstract

Heat stress is devastating to poultry production sustainability worldwide. In addition to its adverse effects on growth, welfare, meat quality, and mortality, HS alters the gut integrity, leading to dysbiosis and leaky gut syndrome; however, the underlying mechanisms are not fully defined. Here, a high-throughput mass spectrometric metabolomics approach was utilized to probe the metabolite profile in the small intestines (duodenum, jejunum, and ileum), intestinal digesta (ileal and cecal), and plasma of modern male broilers exposed to acute heat stress (AHS, 2 h/day for 2 weeks) or chronic cyclic heat stress (CHS, 8 h/day for 2 weeks) in comparison with thermoneutral (TN-control) and pair-fed (PF) birds. Ultra high-performance liquid chromatography coupled with high resolution mass spectrometry (UHPLC–HRMS) identified a total of 218 metabolites. Partial least squares discriminant analysis (PLS-DA) plots (both 2D and 3D maps) showed clear separation between the TN-control and each treated group, indicating a

unique metabolic profile in heat stressed birds. PLS-DA analysis revealed that the small intestines showed the greatest impact from heat stress exposure. Heat stress induced metabolic changes were apparent in the intestinal digesta and plasma, though changes in the cecal digesta were minimal. Within the heat stress groups, PLS-DA displayed different clusters when comparing metabolite profiles from AHS and CHS birds, suggesting that the metabolite signatures were also dependent on HS duration. Further analyses revealed pathways affected by heat stress, with a clear impact on energy and purine metabolism. Taken together, these data showed that, independently of feed intake depression, heat stress systemically induced significant changes in the metabolite profile in a duration-dependent manner and demonstrated mitochondrial mediated cellular reprogramming in response to heat stress.

2.2 Introduction

Poultry meat is highly regarded as an efficient source for high quality proteins with affordable prices and without religious taboos. With a global annual average production of $99,901 \times 10^3$ metric tons, strengthened by intensive genetic selection and long-term genetic gain (growth rate, breast yield, feed efficiency) and improvement of housing and management, broiler (meat-type) chickens are a central component of the worldwide meat production market and support the livelihoods and food security of billions of people.⁷⁶ However, these unprecedented and successful advances were associated with several unexpected and undesirable changes, such as the emergence of metabolic disorders (muscle myopathies, etc.) and hypersensitivity to high environmental temperatures.⁷⁷

Climate change and global warming are real concerns, as unusually warm hot seasons and temperature anomalies have markedly increased and broadened over the past decades.⁷⁸⁻⁸² Global warming and heat stress are adversely affecting every biological system, including birds, large animals, insects, and crops, and thereby threatening the sustainability of global agricultural production.⁸²⁻⁸⁴ Of particular interest, broiler chickens are very susceptible to heat stress, as they lack sweat glands, are covered with feathers, and have high metabolic activity and core body temperatures.⁸⁵⁻⁸⁷ The strong adverse effects of heat stress on poultry performance, well-being, mortality, meat yield and quality are well documented.⁸⁸⁻⁹⁴ One of the prominent negative effects of heat stress is gut injury; however, its underlying mechanisms are not well understood.^{95, 96} The brain–gut axis, involving the enteric nervous system (ENS), the autonomic nervous system (ANS), the hypothalamus–pituitary axis (HPA), and the central nervous system (CNS), is very responsive to any stress, including heat load.⁹⁷⁻¹⁰⁰ Although the complexity of the brain–gut interactions, functionality, and network is still at the beginning of unraveling, there is evidence that heat stress triggers the activation of HPA and ANS, leading to increased corticosterone levels and pro-inflammatory cytokines, which in turn affect the intestinal homeostatic functions.¹⁰¹ For instance, it has been shown that the abovementioned changes, in combination with depressed feed intake induced by heat stress, alter gut motility, flux patterns, secretory activity,

content viscosity, and pH.^{96, 102, 103} It is important to highlight that, to dissipate heat during high ambient temperature, heat-stressed birds divert blood flow to the periphery (skin).¹⁰⁴⁻¹⁰⁷ This, in turn, leads to a hypoxia-like state in several internal organs, including the gut.^{17, 108} Combined with low nutrient supply, which is exacerbated by depression in energy intake, hypoxia would result in adenosine triphosphate (ATP) depletion, promoting oxidative and nitrosative stress that leads to leaky gut syndrome.¹⁰⁹⁻¹¹¹ The integrity of the intestinal barrier and its effective functionality are vital for the overall health and performance of broilers.¹¹²⁻¹¹⁴ As heat stress is a global socio-economic burden that jeopardizes poultry welfare, profitability, and global food security, and as larger and widespread heat waves are predicted for the next century, there is a critical need to define the mechanisms of heat stress responses and their effect on poultry intestinal permeability.¹¹⁵⁻¹¹⁷

Previous studies have shown that heat stress alters the expression of intestinal heat-shock proteins, cyto(chemo)kines, tight junction proteins, and nutrient transporters, thereby inducing leaky gut syndrome.^{88, 118, 119} To gain further in-depth insights into heat stress responses and intestinal barrier integrity, the present study was conducted using an ultra-high performance liquid chromatography–high resolution mass spectrometry (UHPLC–HRMS) based metabolomics approach to determine the metabolic profiles of the duodenum, jejunum, ileum, ileal digesta, cecal digesta, and plasma of modern broilers exposed to acute (2 h) or chronic cyclic (8 h/day for 2 weeks) heat stress in comparison with thermoneutral and pair-fed birds (Fig. 2.1). To date, this is the first study to utilize UHPLC–HRMS based metabolomics to examine the systemic impact heat stress has on the broiler metabolome. Recent advances in mass spectrometry have allowed metabolomics to become a vital tool for systems biology.¹²⁰ The metabolome is dynamic and highly sensitive to environmental alterations, which makes metabolomics an ideal tool to use for uncovering the impact of heat stress at the molecular level.¹²¹ This study bridges the knowledge gap between the physiological and systemic metabolic impacts of heat stress on broiler chicks.

2.3 Results

2.3.1 Significant differences between small intestine, intestinal digesta, and plasma

UHPLC–HRMS based metabolomics analysis was utilized to investigate the systemic impact of heat stress on the metabolome of the duodenum, jejunum, ileum, ileal digesta, cecal digesta, and plasma of broiler chicks. This study also included the following groups: pre-heat stress (PHS), thermoneutral control (TN-control), pair fed (PF), acute heat stress (AHS), and cyclic heat stress (CHS). This analysis identified a total of 218 metabolites with 128 (58.7%) metabolites detected in all matrices. Of the 218 identified metabolites, 17 (7.8%) were unique to the samples collected from the small intestine tissue (duodenum, jejunum, and ileum) and 15 (6.9%) were unique to the digesta samples (ileal and cecal) (Fig. 2.2).

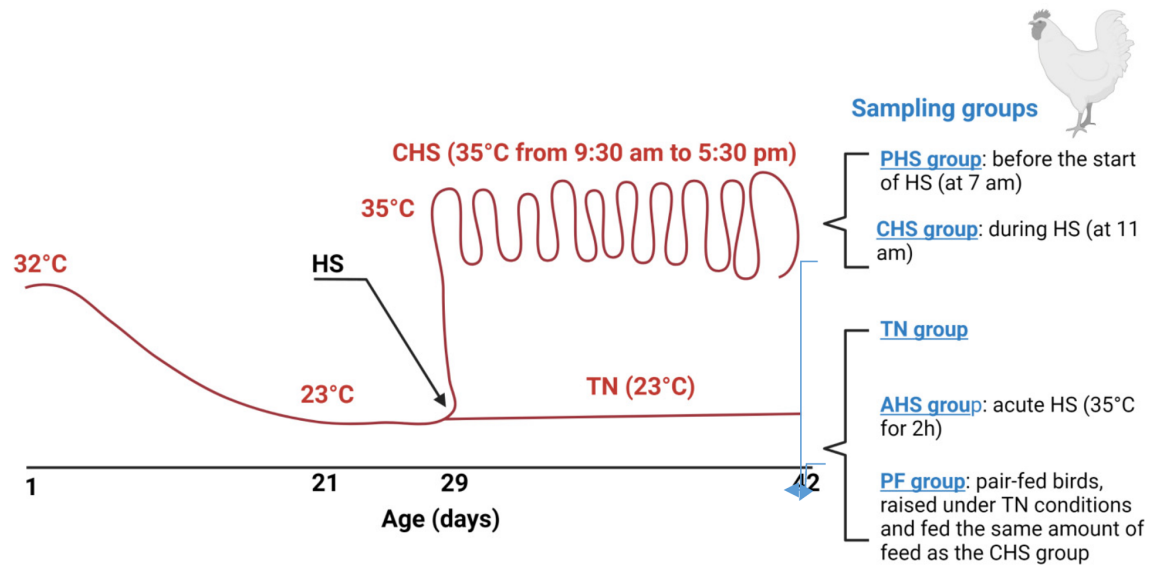


Figure 2.1 Experimental design representation and heat stress challenge. Temperature was gradually reduced from 32 °C to approximately 23 °C on d 21. At d 29, the experiment followed a completely randomized design with three treatments (8 replicate pens/treatment, 28 birds/pen): a control group (TN) where the birds were raised under thermoneutral condition (23 °C) from d 29–42, a chronic cyclic heat-stressed group (CHS) where the birds were exposed to high ambient temperature (35 °C) for 8 h/d (9:30 am to 5:30 pm) from d 29–42, and a pair-fed group (PF) where the birds were raised like the control group (similar environmental conditions, 23 °C) and fed the same amount of feed as the CHS group. Two additional groups were also used: an acute heat-stressed group (AHS) where some TN birds were exposed to 35 °C for 2 h before sampling on d 42, and a preheat-stressed group (PHS) where CHS birds were sampled before starting the heat stress on d 42. AHS, acute heat stress; CHS, chronic cyclic heat stress; HS, heat stress; PHS, preheat stress; PF, pair fed.

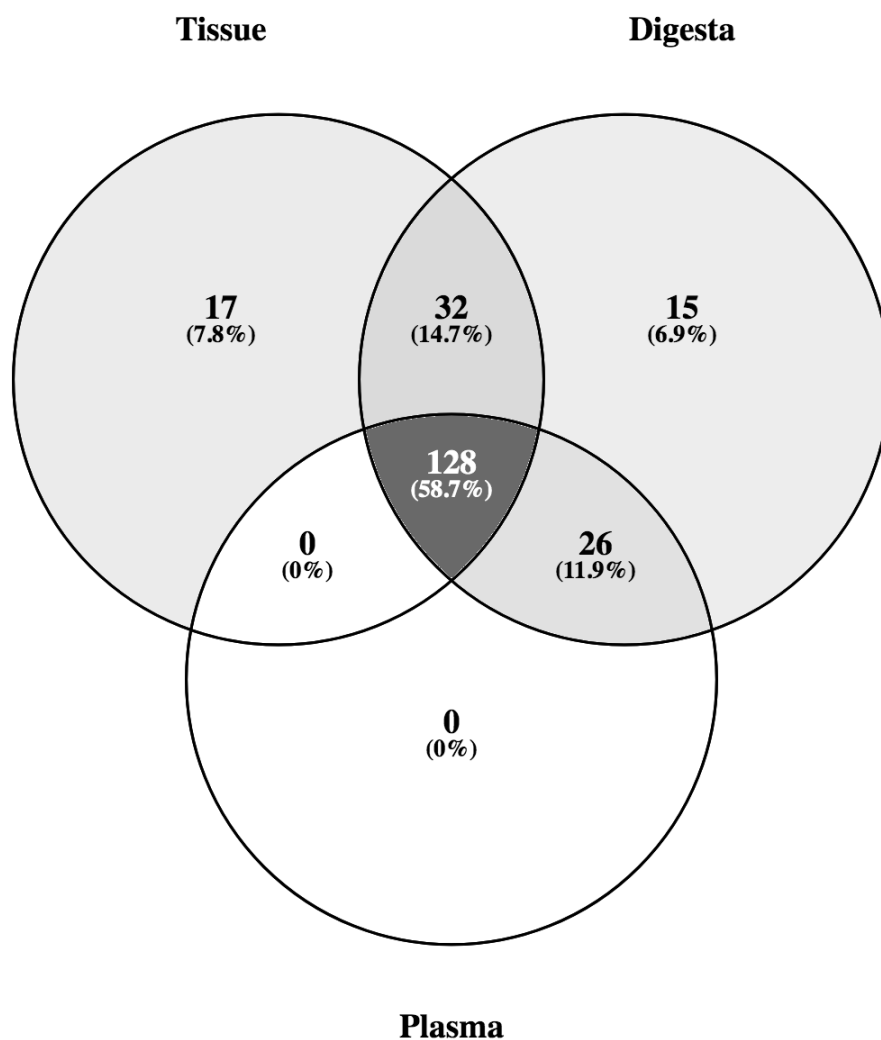


Figure 2. 2 Venn diagram comparing the detected metabolites in each region. There were 17 metabolites unique to the tissue (duodenum, jejunum, and ileum), 15 metabolites unique to the digesta (ileal and cecal), and metabolites unique to the plasma.

There were not any identified metabolites unique to the plasma samples. Initially, PLS-DA was utilized to pinpoint features contributing to metabolome differences of all samples collected in this experiment. All samples within a defined cluster in the PLS-DA model share a similar metabolic profile, and the separation of clusters indicates that each cluster has a metabolic profile that is unique from the other clusters. When using groupings for sample location (duodenum, jejunum, ileum, ileal digesta, cecal digesta, and plasma) along with treatment (TN-control, PHS, PF, AHS, and CHS) in a PLS-DA (Fig. 2.3), four distinct clusters are evident. As expected, these four clusters correspond to the small intestine (duodenum, jejunum, and ileum), ileal digesta, cecal digesta, and plasma indicating that the factor with the most impact on the metabolic profile was the sample biological location regardless of heat stress. Within each of the four clusters, the impact of heat stress is nonexistent. Similarly, when using PLS-DA to analyze each treatment (PHS, TN-control, PF, AHS, and CHS) individually (Fig. 2.4), the same four distinct clusters were evident – small intestine, ileal digesta, cecal digesta, and plasma. However, the impact of heat stress on the broiler chick gut metabolome becomes clearly evident when analyzing each location independently.

2.3.2 Heat stress induces a significant impact on the metabolic profile of broiler chicks

Small Intestines

Metabolomics analysis of the duodenum, jejunum, and ileum identified 177 metabolites. Of these 177 metabolites, 17 were unique to the tissue of the small intestine. Heatmaps, which display the \log_2 fold change in metabolite relative abundance, were used to provide a general overview of the metabolite relative abundances for each treatment group compared to TN-control group for the duodenum, jejunum, and ileum (Figs. 2.19-2.21). Based on the heatmaps, the region of the small intestine with the greatest impact from heat stress is the jejunum as the brightness of colors on the heatmap correspond to the magnitude of change in metabolite relative abundance.

Moreover, the number of metabolites that were considered to be significantly altered by heat stress ($p < 0.05$ and fold change $> |1.5|$) in the duodenum and ileum were similar while it was revealed that the duodenum had 12 and 14 metabolites significantly altered by AHS and CHS, respectively, and the ileum had 9 and 13 metabolites significantly altered by AHS and CHS, respectively (Table 2.1). The metabolites that are unique to each region could be used as potential signatures of either AHS or CHS for each region. Specifically, four metabolites were significantly increased in relative abundance in the duodenum due to the impact of AHS (prephenate, pimelic acid, 3-Hydroxyisovalerate, and ADP-glucose) while eight metabolites were significantly decreased (homocarnosine, N-Carbamoyl-L-aspartate, dihydroorotate, dAMP, glycinamide ribotide (GAR), AICAR, S-Adenosyl-L-homocysteine, and orotate). The impact of CHS on the

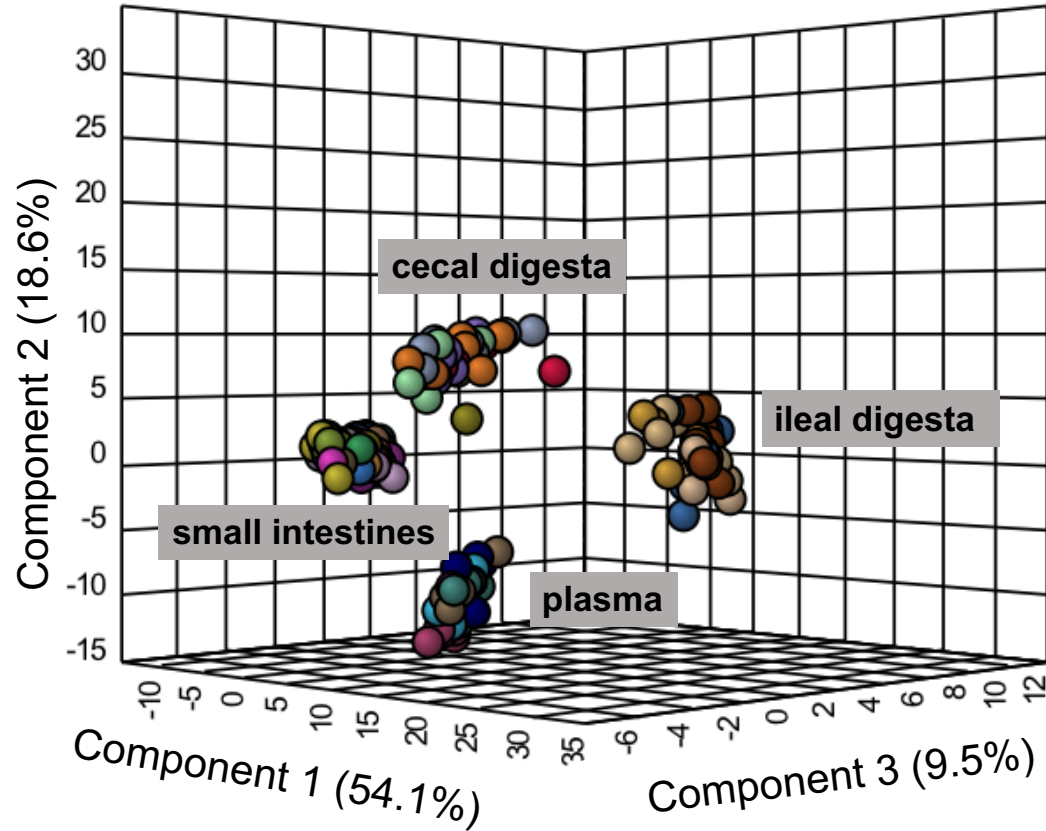


Figure 2. 3 3D partial least-squares discriminant analysis (PLS-DA) displays that biological location, rather than HS, has the greatest impact on the metabolic profiles as four distinct clusters are present (small intestines, ileal digesta, cecal digesta, and plasma) when all samples are plotted with treatment and biological location information used for grouping. Within each cluster, there is no apparent distinction for heat stress.

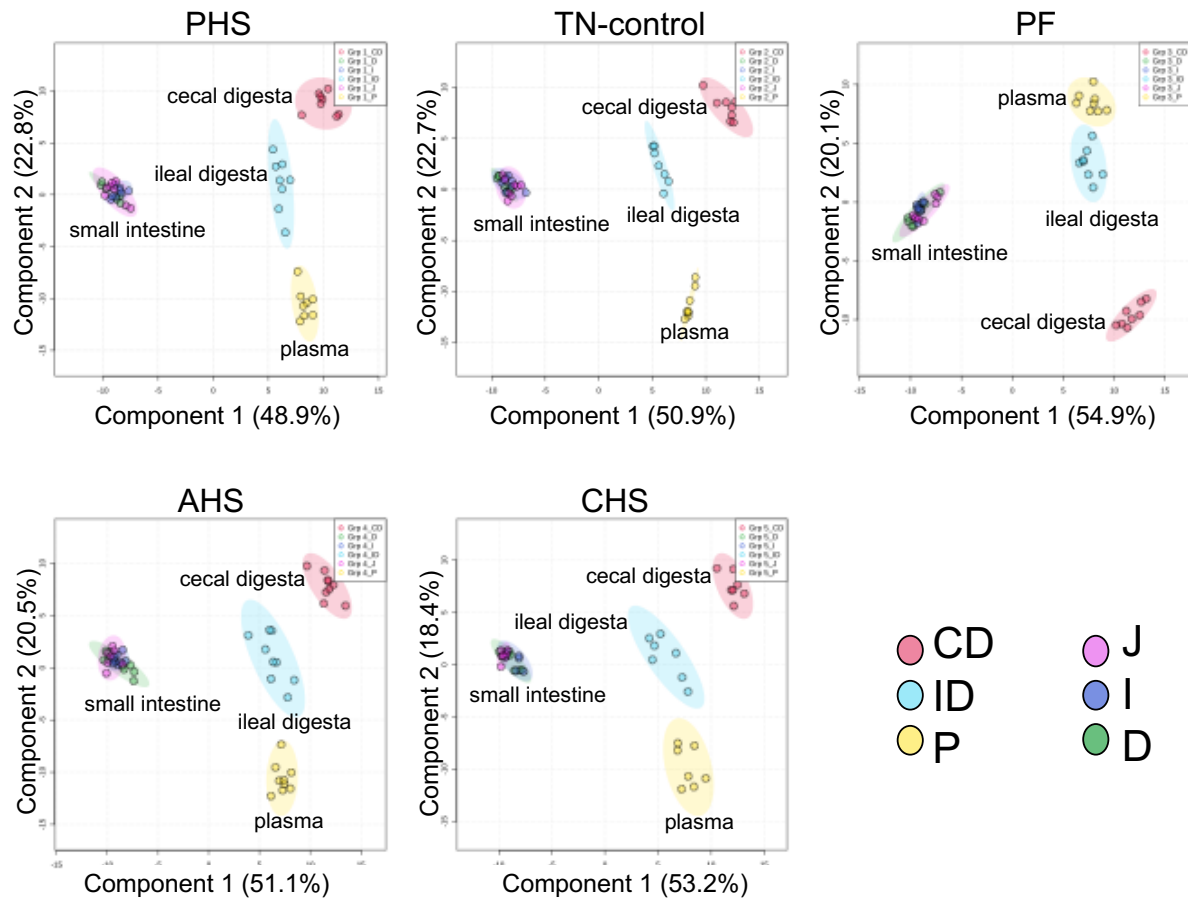


Figure 2.4 *Partial least-squares discriminant analysis (PLS-DA) plots for each treatment. Within each treatment, samples were grouped by biological location (duodenum, jejunum, ileum, ileal digesta, cecal digesta, and plasma). Each plot shows 4 distinct clusters that correspond to the small intestines, cecal digesta, ileal digesta, and plasma. Pre-heat stress (PHS), TN-control (TN-control), pair-fed (PF), acute heat stress (AHS), cyclic heat stress (CHS), cecal digesta (CD), ileal digesta (ID), plasma (P), jejunum (J), ileum (I), duodenum (D).*

Table 2.1 Overview of metabolites significantly altered by heat stress. Metabolites were considered to be significantly altered if $p < 0.05$ and had a fold change of ≥ 1.5 . Pre-heat stress (PHS), TN-control (TN-control), pair-fed (PF), acute heat stress (AHS), cyclic heat stress (CHS), heat stress (HS)

	Duodenum		Jejunum		Ileum		Ileal digesta		Cecal digesta		Plasma	
	AHS	CHS	AHS	CHS	AHS	CHS	AHS	CHS	AHS	CHS	AHS	CHS
Total identified metabolites	177	177	177	177	177	177	201	201	201	201	154	154
Significantly altered metabolites	12	14	73	74	9	13	5	9	15	9	6	7
Significantly increased in HS	4	7	64	70	6	3	3	7	7	2	5	4
Significantly decreased in HS	8	7	9	4	3	10	2	2	8	7	1	3

duodenal metabolome led to seven metabolites having a significant increase in relative abundance (prephenate, cysteate, NADH, ADP-glucose, NAD⁺, NADP⁺, and D-erythrose 4-phosphate) and seven having a significantly decreased abundance in the duodenum due to CHS exposure (homocarnosine, N-acetylputrescine, 1-methylhistidine, histidine, phosphothreonine, glucose phosphate, and aconitate). Likewise, AHS induced a significant increase in six metabolites (salicylate, homocysteic acid, N-acetylglucosamine, 3-hydroxyisovalerate, 1-methyladenosine, and xanthosine) and a decrease in three metabolites (N-carbamoyl-L-aspartate, taurodeoxycholate, and GAR) in the ileum. CHS exposure resulted in an increased abundance of three metabolites (hydroxyphenylacetate, salicylate, and oxaloacetate) and a decreased abundance of 10 metabolites (homocarnosine, 1-methylhistidine, glutamine, ophthalmate, taurodeoxycholate, NADH, UDP, CMP, IMP, and CDP) in the ileal metabolome. In contrast to the duodenum and ileum, the jejunum showed the most impact from heat stress with roughly six times more metabolites significantly altered by heat stress with 73 and 74 metabolites significantly altered by AHS and CHS, respectively (Table 2.2)

To visualize the impact of heat stress on the individual regions of the small intestines, PLS-DA was used to compare all treatments (PHS, PF, TN-control, AHS, and CHS) within the duodenum, jejunum, and ileum separately (Fig. 2.5). This analysis shows that heat stress induces the greatest impact on the jejunum in the small intestines as the AHS and CHS groups show complete separation from the TN and PHS groups. In the duodenum, only the CHS group showed complete separation from the PHS and PF group, while the AHS and CHS groups showed overlap with the TN-control group. In contrast, the AHS group in the ileum showed complete overlap with all other groups (PHS, TN-control, PF, and CHS) while the CHS group showed overlap with all groups, excluding the PF group.

In order to identify specific metabolites or metabolic pathways directly impacted by heat stress, pairwise comparisons were made using PLS-DA plots along with variable importance in projection (VIP) scores. Each metabolite is assigned a VIP score, and a VIP score >1 indicates that metabolite is significantly driving the separation of groups in the PLS-DA. For the duodenum, jejunum, and ileum pairwise comparisons (Fig. 2.6-2.8), there is clear separation of the TN-control group from all other treatment groups in the 3D PLS-DA plots with AHS and CHS exhibiting the greatest separation.

All metabolites with a VIP score >1 for each region of the small intestines were used to compare metabolites altered most by heat stress across the small intestines. Using a Venn diagram¹²² (Fig. 2.9), five metabolites were found to be conserved between the duodenum, jejunum, and ileum and have a convincing impact on the separation of the TN-control and AHS groups. These metabolites are prephenate, phenyllactic acid, 3-hydroxyisovalerate, histamine, and phosphoenolpyruvate. With the exception of histamine, exposure to heat stress induced a consistent increase in these metabolite relative abundances in all three regions of the small intestine. Histamine did not follow this same trend as its

Table 2.2 Metabolites significantly increased or decreased by acute heat stress (AHS) or cyclic heat stress (CHS) in the jejunum.

Jejunum			
AHS		CHS	
Increased	Decreased	Increased	Decreased
Creatinine	3-Phosphoserine	Creatinine	Dephospho-CoA
N-Acetylputrescine	Dihydroorotate	N-Acetylputrescine	Thymidine
Phenyllactic acid	Taurodeoxycholate	Cystathionine	CMP
Phenylpyruvate	dCMP	Indole	7-Methylguanosine
Acetylphosphate	Dephospho-CoA	Acetylphosphate	
2-Amino adipate	Glycinamide ribotide (GAR)	2-Amino adipate	
Dimethylglycine	Thymidine	Glutamate	
Glutamate	CMP	Glutamine	
Glutamine	7-Methylguanosine	Glutathione disulfide	
Glutathione		Homoserine/Threonine	
Glutathione disulfide		Methionine	

Table 2.2 continued

Homoserine/Threonine

Methionine

N-Acetylornithine

Pyroglutamic acid

Aspartate

Hydroxyproline

Ornithine

Phenylalanine

Tyrosine

Acetyllysine

Alanine/Sarcosine

Citrulline

Creatine

Leucine/Isoleucine

N-Acetyl-beta-alanine

N-Acetylornithine

Ophthalmate

Pyroglutamic acid

Aspartate

Cystine

Hydroxyproline

Lysine

Ornithine

Phenylalanine

Proline

Tyrosine

Valine/betaine

Acetyllysine

Table 2.2 continued

N-Acetylglutamate

Serine

Histamine

aminoisobutyric acid

Cysteine

Glycine

Taurine

Xylitol

N-Acetylglucosamine

Sedoheptoluse bisphosphate

Lactate

2-Hydroxy-2-methylsuccinate

aminocaproic acid

Hydroxyisocaproic acid

Alanine/Sarcosine

Citrulline

Creatine

Leucine/Isoleucine

N-Acetylglutamate

Serine

Histamine

Tryptophan

Arginine

Cysteine

Glycine

Taurine

Xylitol

xylose

Table 2.2 continued

methyl succinic acid

3-Hydroxyisovalerate

GDP

UDP

UDP-glucose

UDP-glucuronate

Uridine

Xanthosine 5'-phosphate

cAMP

ADP

GMP

UDP-N-acetylglucosamine

AMP/dGMP

Guanine

N-Acetylglucosamine

Sedoheptoluse bisphosphate

Phosphoenolpyruvate

Lactate

2-Hydroxy-2-methylsuccinate

aminocaproic acid

Carnitine

methyl succinic acid

3-Hydroxyisovalerate

Deoxyuridine

dTMP

dUMP

GDP

Inosine

Table 2.2 continued

Hypoxanthine

2-hydroxyglutaric acid

Glycolate

homocitrulline

glutaric acid

Uric acid

Uracil

Homovanillic acid (HVA)

Malate

Riboflavin

Biotin

UDP-glucose

Uridine

Xanthosine 5'-phosphate

GMP

UDP-N-acetylglucosamine

Guanine

Hypoxanthine

Octulose biphosphate

2-hydroxyglutaric acid

homocitrulline

glutaric acid

Uric acid

Uracil

Ribose phosphate

Table 2.2 continued

Malate

Riboflavin

Biotin

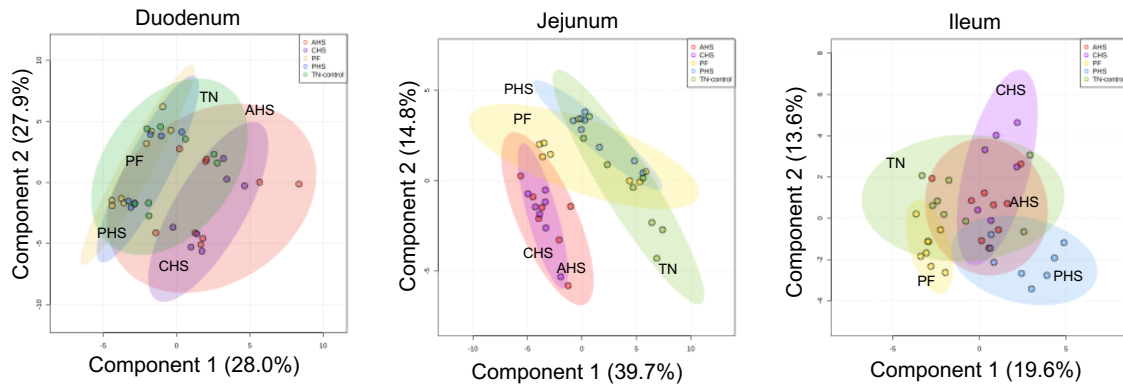
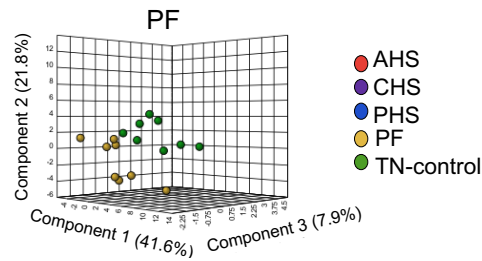
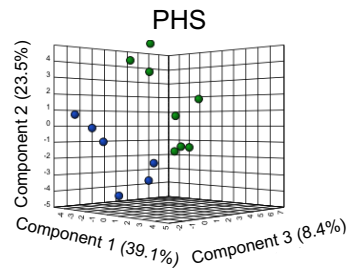
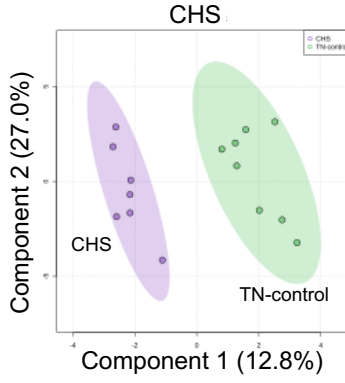
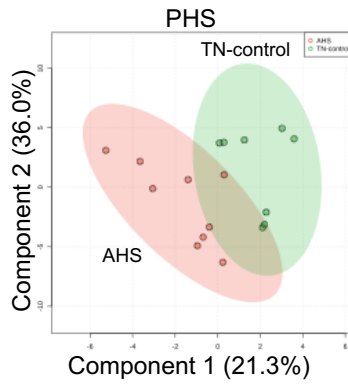
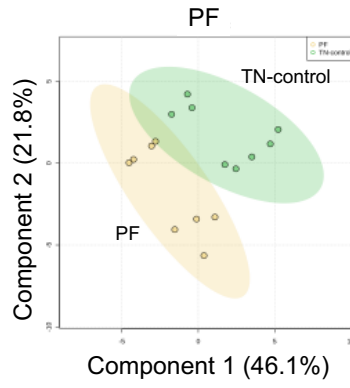
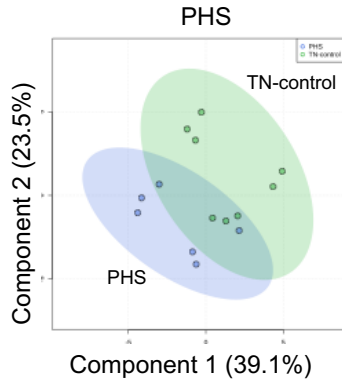


Figure 2.5 *Partial least-squares discriminant analysis (PLS-DA) plots for each region of the small intestines (duodenum, jejunum, and ileum). Within each treatment, samples were grouped by treatment Pre-heat stress (PHS), TN-control (TN-control), pair-fed (PF), acute heat stress (AHS), cyclic heat stress (CHS). The heat stress samples were most clearly separated from the other treatment groups in the jejunum.*

Figure 2.6 2D (top) *Partial least-squares discriminant analysis (PLS-DA)* plots for pairwise comparisons of each treatment to the TN-control in the duodenum. CHS has the most separation from the control. The treatment groups show more separation from the TN-control in 3D (bottom) PLS-DA plots. Pre-heat stress (PHS), TN-control (TN-control), pair-fed (PF), acute heat stress (AHS), cyclic heat stress (CHS), cecal digesta (CD), ileal digesta (ID), plasma (P), jejunum (J), ileum (I), duodenum (D)



- AHS
- CHS
- PHS
- PF
- TN-control

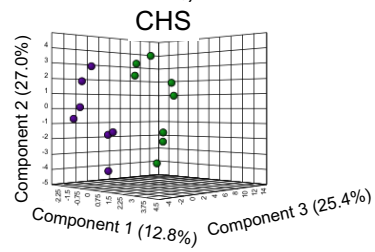
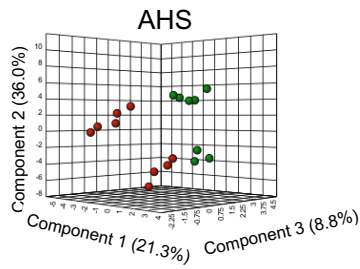
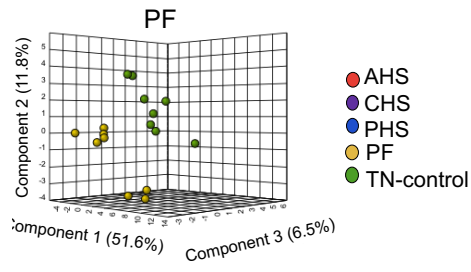
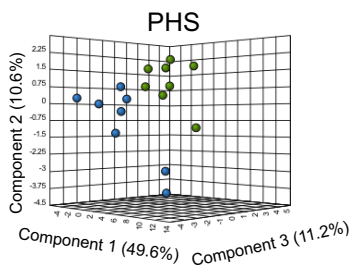
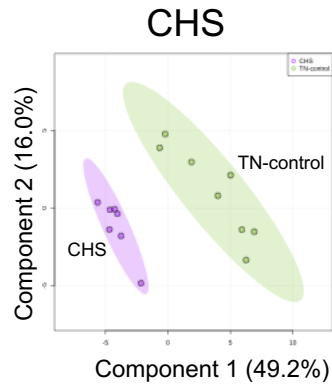
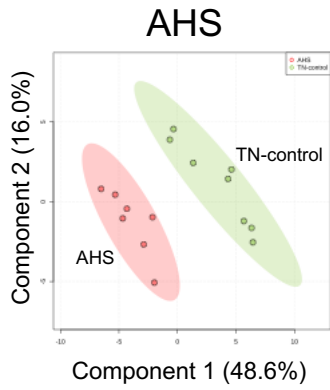
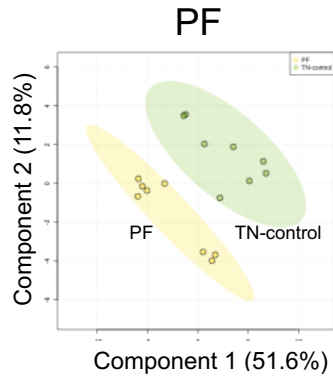
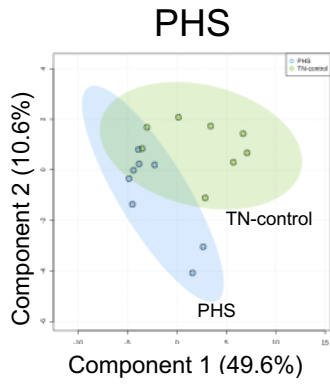


Figure 2.7 2D (top) *Partial least-squares discriminant analysis (PLS-DA)* plots for pairwise comparisons of each treatment to the TN-control in the jejunum. CHS and AHS had the most separation from the control. The treatment groups show more separation from the TN-control in 3D (bottom) PLS-DA plots. Pre-heat stress (PHS), TN-control (TN-control), pair-fed (PF), acute heat stress (AHS), cyclic heat stress (CHS), cecal digesta (CD), ileal digesta (ID), plasma (P), jejunum (J), ileum (I), duodenum (D)



- AHS
- CHS
- PHS
- PF
- TN-control

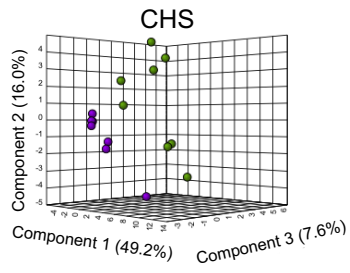
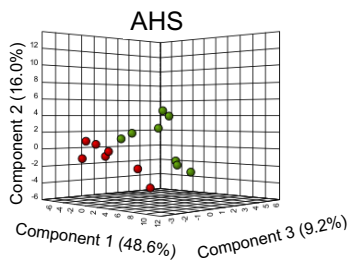
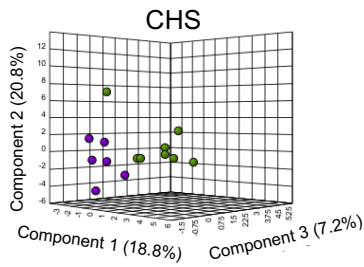
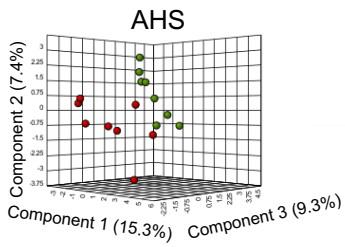
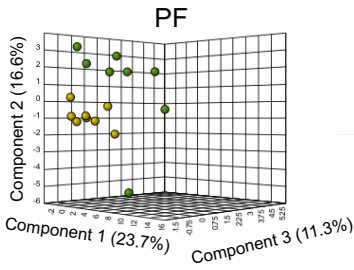
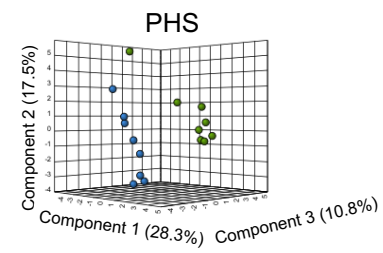
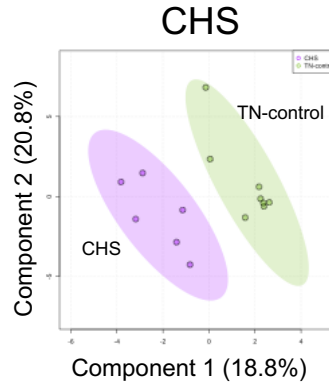
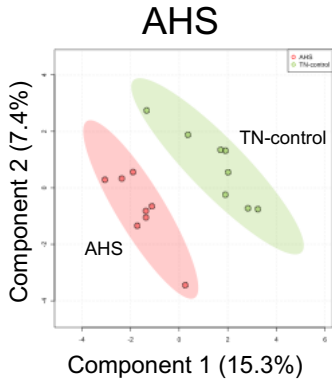
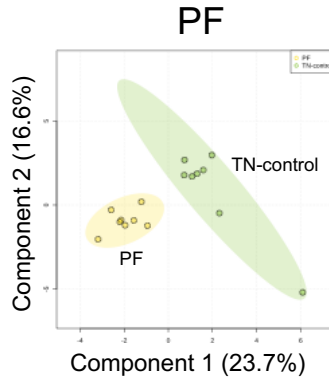
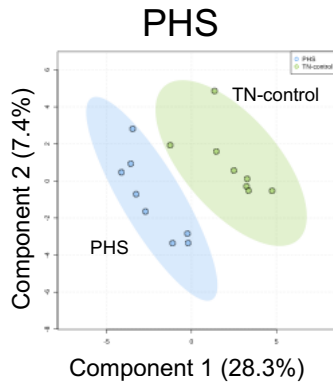


Figure 2.8 2D (top) *Partial least-squares discriminant analysis (PLS-DA)* plots for pairwise comparisons of each treatment to the TN-control in the ileum. CHS and AHS had the most separation from the control. The treatment groups show more separation from the TN-control in 3D (bottom) PLS-DA plots. Pre-heat stress (PHS), TN-control (TN-control), pair-fed (PF), acute heat stress (AHS), cyclic heat stress (CHS), cecal digesta (CD), ileal digesta (ID), plasma (P), jejunum (J), ileum (I), duodenum (D)



- AHS
- CHS
- PHS
- PF
- TN-control

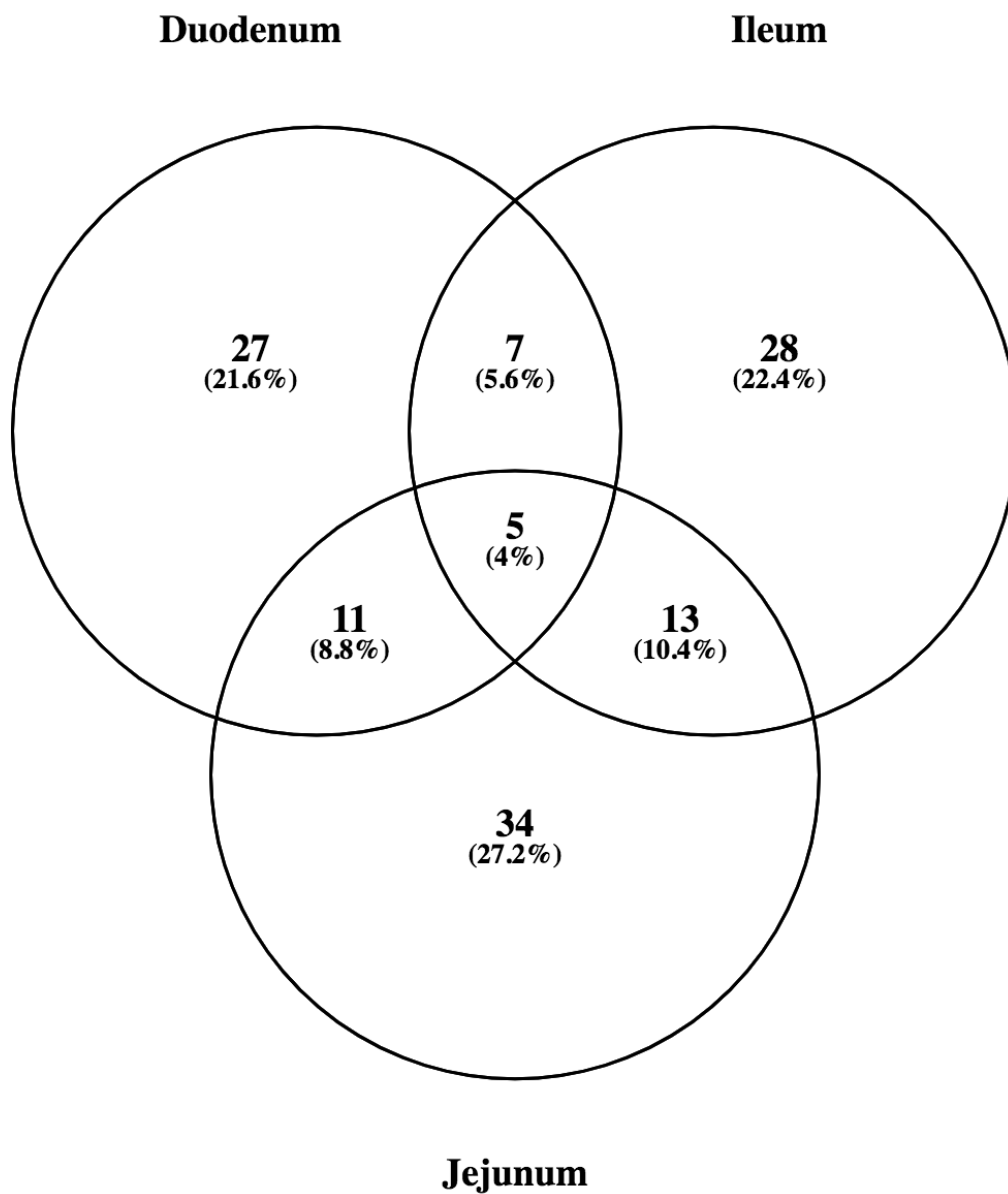


Figure 2.9 Metabolites with a variable importance in projection (VIP) score >1 in each pairwise comparison within the small intestine regions was used to generate a Venn diagram to determine metabolites that significantly contributed to the differences between the acute heat stress (AHS) and TN-control (TN-control) metabolic profiles in all three regions.

abundance was decreased by heat stress exposure in the duodenum and ileum but increased in the jejunum. Furthermore, seven metabolites were found to be highly influential in driving the separation of the TN-control and CHS groups across the small intestines (Fig. 10). These metabolites are phosphothreonine, NAD⁺, ADP-glucose, 2-isopropylmalate, cystathionine, uric acid, and deoxyinosine and of these only three displayed consistent trends. Unlike the trends induced by AHS, only one metabolite, deoxyinosine, consistently increased in response to exposure to CHS throughout the small intestines. Two other metabolites with a consistent trend in response to heat stress, ADP glucose and uric acid, which were increased in the duodenum and jejunum but decreased in the ileum.

Intestinal Digesta

The intestinal digesta (contents) metabolome is also altered by heat stress exposure, though it does show more resilience to perturbations in metabolism. Of the 218 metabolites identified in this study, 201 were detected in the digesta, and 15 of these were unique to the digesta (Fig. 2.2). The heatmaps provide an overview of the identified metabolite relative abundances for each treatment compared to the TN-control group in the ileal and cecal digesta (Fig. 2.22-2.23). There was a total of 5 and 9 metabolites in the ileal digesta significantly altered in response to AHS and CHS, respectively. AHS exposure led to three metabolites (acetylphosphate, xylitol, and 1-methyladenosine) having a significantly increased relative abundance and two (2-oxoisovalerate and nicotinate) metabolites having a significantly decreased relative abundance (Table 2.1). Similarly, CHS exposure led to seven metabolites (cystathionine, hydroxyphenylacetate, carbamoyl phosphate, N-acetylglucosamine, 1-methyladenosine, uracil, and D-gluconate) having a significantly increased relative abundance and two (2-oxoisovalerate and nicotinate) metabolites having a significantly decreased relative abundance. Interestingly, the only two metabolites that were significantly decreased in the ileal digesta were conserved in both AHS and CHS exposure. In the cecal digesta, there were 15 and 9 metabolites significantly altered in response to AHS and CHS, respectively. AHS induced a significant increase in the relative abundance of seven metabolites (citraconate, 2-isopropylmalate, NADP⁺, 7-methylguanosine, octulose 8,1 phosphate, (iso)citrate, and folate) and a significant decrease in eight metabolites (N-acetylglutamine, acetyllysine, N-acetylglutamate, pimelic acid, deoxyadenosine, phosphorylethanolamine, pyrophosphate, and pantothenate). Additionally, CHS led to the significant increase of two metabolite ((iso)citrate and folate) and a significant decrease in seven metabolites (2-aminoadipate, 3-phosphoserine, trehalose 6-phosphate, methyl succinic acid, phosphorylethanolamine, glutaric acid, and pyrophosphate).

From PLS-DA analysis of the ileal digesta with all treatment groups, it appears that heat stress minimally impacts the metabolic profile of the ileal digesta as all groups are overlapping (Fig. 2.11). Out of all regions analyzed, heat stress altered metabolism least in the ileal digesta. However, the PLS-DA

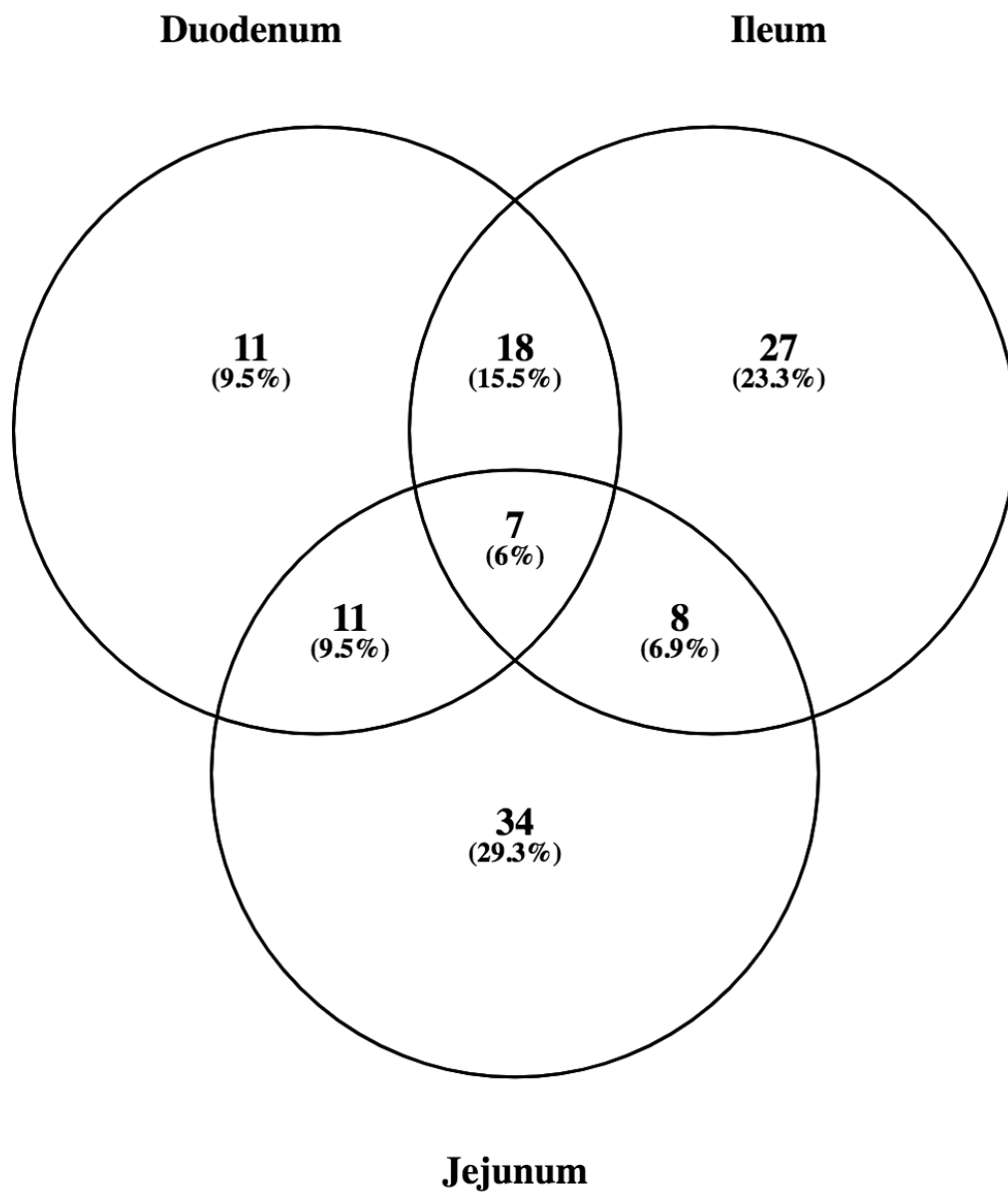
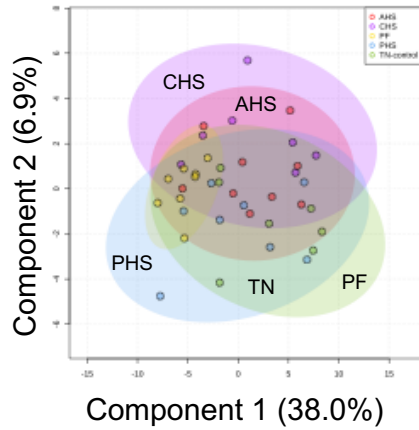


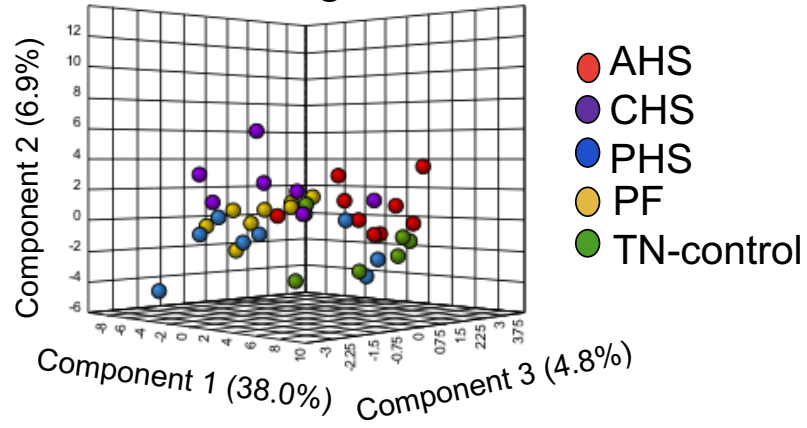
Figure 2.10 Metabolites with a variable importance in projection (VIP) score >1 in each pairwise comparison within the small intestine regions was used to generate a Venn diagram to determine metabolites that significantly contributed to the differences between the cyclic heat stress (CHS) and TN-control (TN-control) metabolic profiles in all three regions.

Figure 2.11 2D (left) *Partial least-squares discriminant analysis (PLS-DA)* plots for the ileal digesta. 3D (right) PLS-DA plots for the ileal digesta. C) 2D PLS-DA plots for the cecal digesta. D) 3D PLS-DA plots for the cecal digesta (right plot shows the rotated side view for better separation). Pre-heat stress (PHS), TN-control (TN-control), pair-fed (PF), acute heat stress (AHS), cyclic heat stress (CHS).

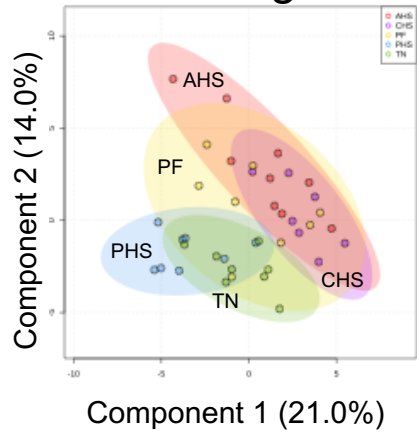
Ileal digesta



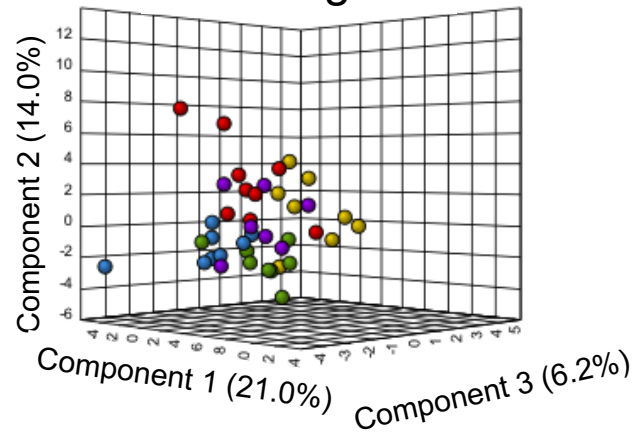
Ileal digesta



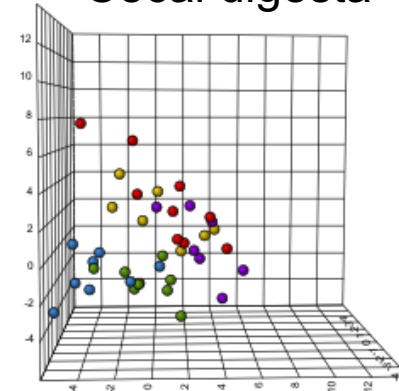
Cecal digesta



Cecal digesta



Cecal digesta



for the cecal digesta shows that there is a clear difference in the metabolic profiles of AHS and CHS birds as these groups are completely separated from the TN-control and PHS groups (Fig. 2.11). The AHS and CHS groups do overlap with the PF group in the cecal digesta.

Pairwise comparisons within the ileal and cecal digesta were used to determine the metabolites impacted most by heat stress in the intestinal contents. Though the impact of heat stress on the ileal digesta was not evident in the PLS-DA with all treatment groups, pairwise comparisons (Fig. 2.12) demonstrated clear separation of the TN-control group from all other treatment groups in the 3D PLS-DA plots, which made it clear that the metabolite profiles in the ileal digesta are moderately different when exposed to heat stress. The PF and CHS groups exhibited the most separation from the TN-control group. Moreover, the pairwise comparisons for the cecal digesta (Fig. 2.13) show that all groups are separated from the TN-control group with AHS and CHS having the most separation. Heat stress exposure does induce a substantial impact on the cecal digesta metabolome.

To better understand how heat stress exposure alters the intestinal digesta metabolome, metabolites with a VIP score >1 for both the ileal and cecal digesta were analyzed. For AHS exposure, there were 16 metabolites with a VIP score >1 conserved between the two regions (Fig. 2.14). These metabolites are: folate, deoxyadenosine, cAMP, dephospho-CoA, (iso)citrate, dTDP, N-acetylglutamate, acetylphosphate, citraconate, norepinephrine, riboflavin, 3,4-dihydroxyphenylacetate (DOPAC), D-gluconate, pyridoxine, aconitate, and CMP. Of these 16 metabolites, 13 were found to have the same trend in response to AHS in the ileal and cecal digesta. Folate, dephospho-CoA, (iso)citrate, acetylphosphate, citraconate, norepinephrine, riboflavin, DOPAC, D-gluconate, pyridoxine, and aconitate increased in relative abundance while cAMP and N-acetylglutamate decreased in relative abundance in response to AHS exposure. These results imply that these metabolites are considerable indicators of AHS in the intestinal digesta.

The other metabolites did not follow the same increasing or decreasing trend for both regions of the digesta. Similarly, CHS exposure had 13 metabolites with a VIP score >1 in both digesta regions that were conserved (Fig. 2.15). These metabolites are: D-glucarate, phosphorylethanolamine, 3-phosphoserine, deoxyadenosine, NAD⁺, adenine, trehalose 6-phosphate, hydroxyphenylacetate, glutathione, nicotinate, and methyl glutaric acid. Only five metabolites had a consistent response to CHS in both the ileal and cecal digesta. As possible indicators of CHS in the intestinal digesta based on these data, acetyl-CoA increased in response to CHS while 3-phosphoserine, NAD⁺, adenine, and methyl glutaric acid decreased in response to CHS.

Plasma

Metabolomics analysis revealed that the plasma metabolome is clearly altered resulting from exposure to heat stress. There were 154 metabolites

Figure 2.12 2D (top) *Partial least-squares discriminant analysis (PLS-DA)* plots for pairwise comparisons of each treatment to the TN-control in the ileal digesta. The treatment groups show more separation from the TN-control in 3D (bottom) PLS-DA plots. Pre-heat stress (PHS), TN-control (TN-control), pair-fed (PF), acute heat stress (AHS), cyclic heat stress (CHS), cecal digesta (CD), ileal digesta (ID), plasma (P), jejunum (J), ileum (I), duodenum (D)

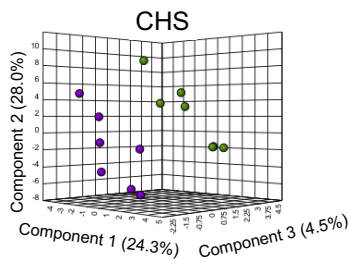
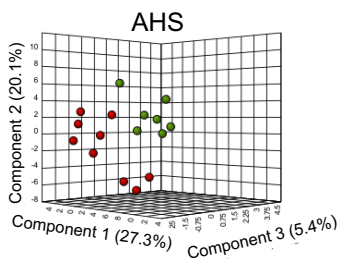
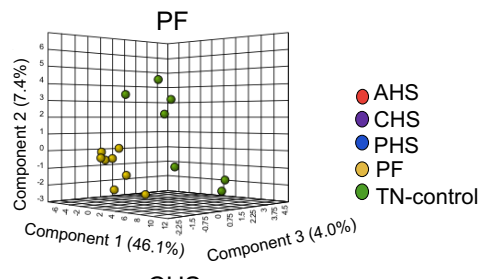
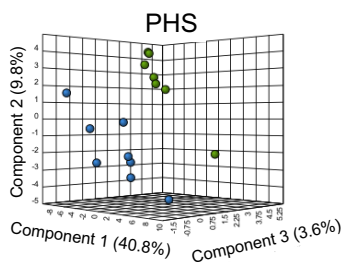
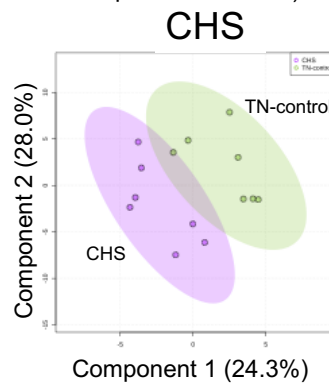
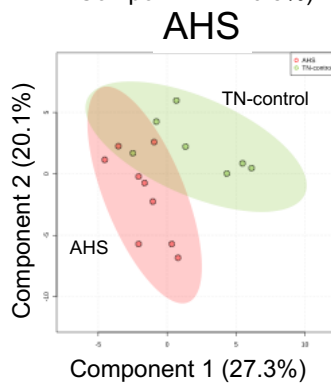
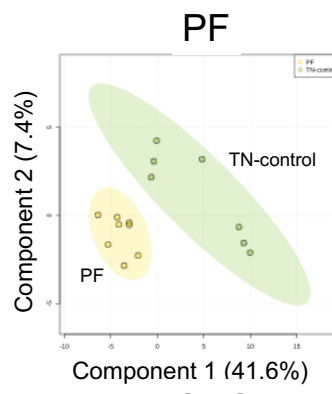
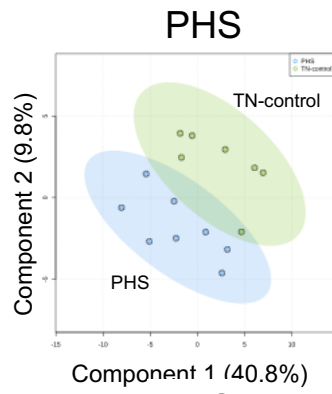
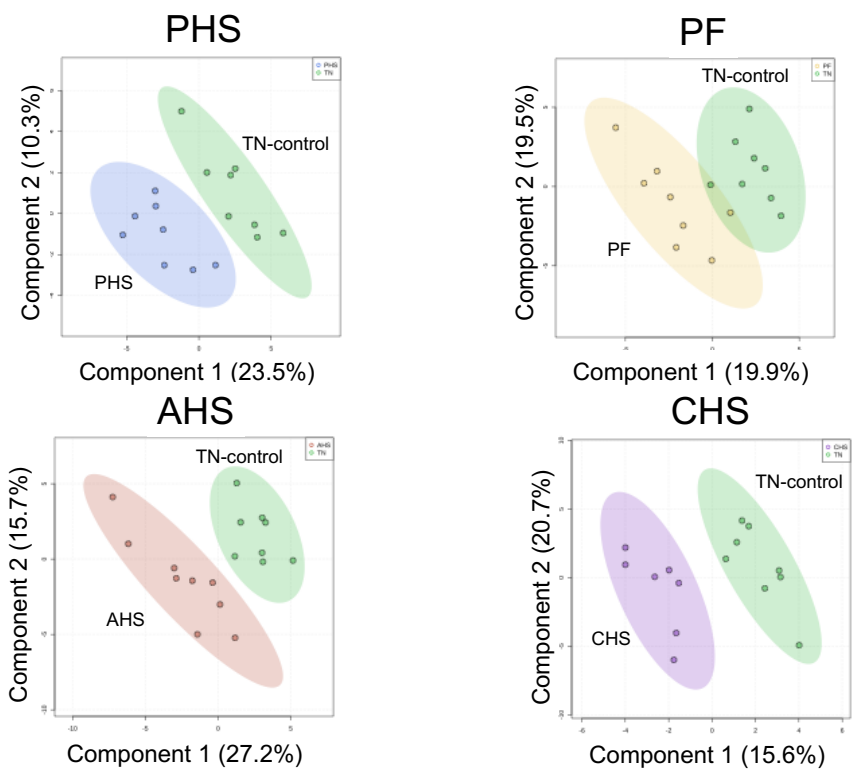
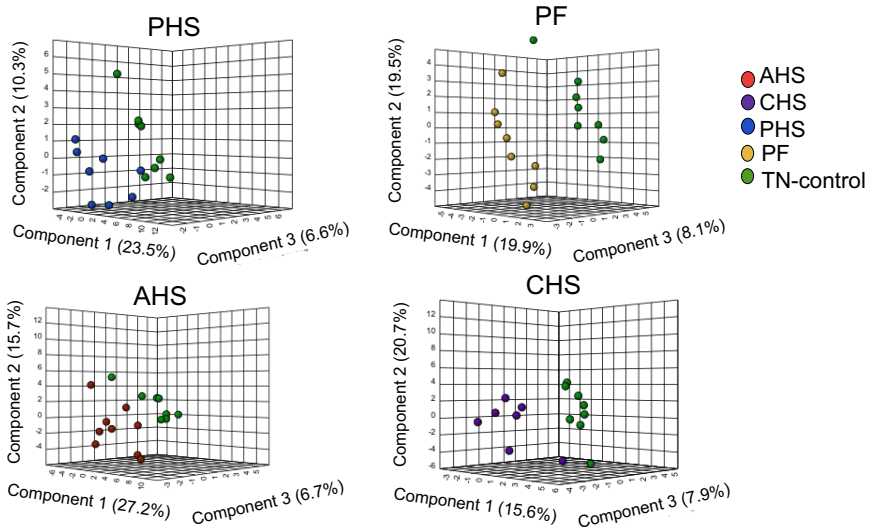


Figure 2.13 2D (top) *Partial least-squares discriminant analysis (PLS-DA)* plots for pairwise comparisons of each treatment to the TN-control in the cecal digesta. CHS and AHS had the most separation from the control. The treatment groups show more separation from the TN-control in 3D (bottom) PLS-DA plots. Pre-heat stress (PHS), TN-control (TN-control), pair-fed (PF), acute heat stress (AHS), cyclic heat stress (CHS), cecal digesta (CD), ileal digesta (ID), plasma (P), jejunum (J), ileum (I), duodenum (D)



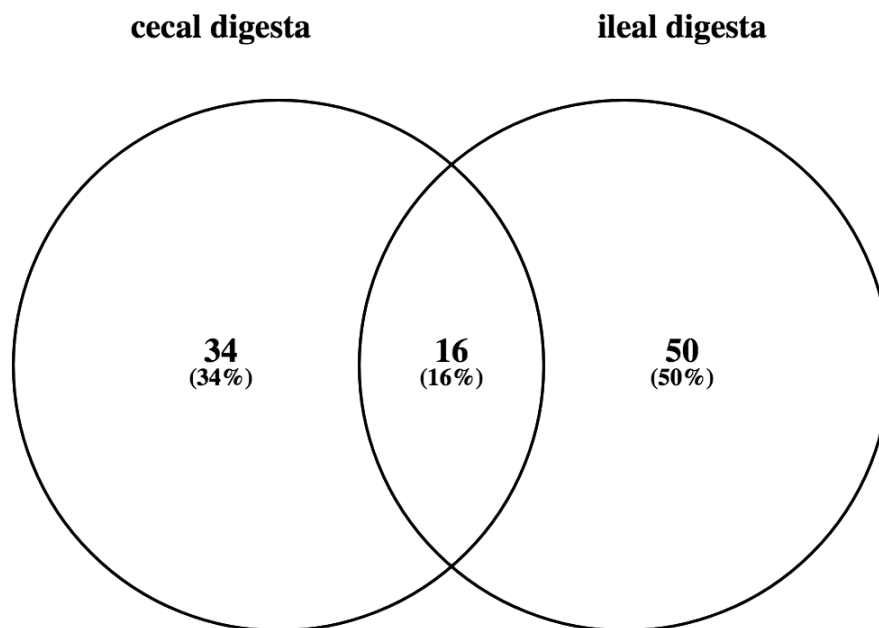


Figure 2.14 Metabolites with a variable importance in projection (VIP) score >1 in each pairwise comparison within the intestinal digesta was used to generate a Venn diagram to determine metabolites that significantly contributed to the differences between the acute heat stress (AHS) and TN-control (TN-control) metabolic profiles in the digesta.

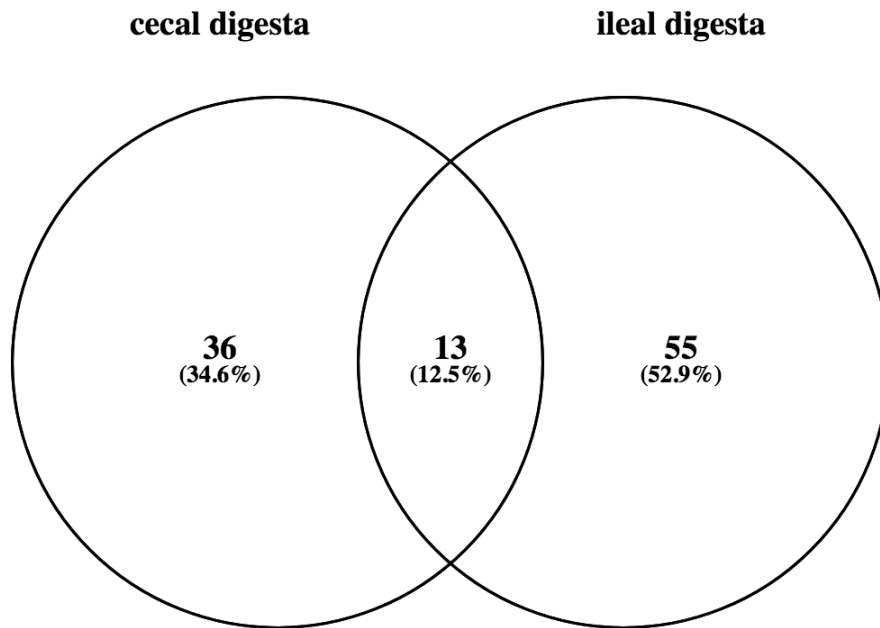


Figure 2.15 Metabolites with a variable importance in projection (VIP) score >1 in each pairwise comparison within the intestinal digesta was used to generate a Venn diagram to determine metabolites that significantly contributed to the differences between the cyclic heat stress (CHS) and TN-control (TN-control) metabolic profiles in the digesta.

identified in the plasma, and the heatmap (Fig. 2.24) depicts an overview of individual metabolite alterations in each treatment group compared to the TN-control. There were six and seven metabolites significantly altered by AHS and CHS, respectively (Table 2.1). Of the six metabolites significantly impacted by AHS in the plasma, five metabolites were increased in relative abundance (N-acetylglutamate, hydroxyisocaproic acid, cytidine, guanosine, and inosine) while one metabolite was significantly decreased in relative abundance (homocitrulline). Similarly, CHS exposure led to the increased relative abundance of four metabolites (inosine, tricarballic acid, 2,3-dihydroxybenzoate, and alpha-ketoglutarate) and decreased relative abundance of three metabolites (homocarnosine, aspartate, and hypoxanthine).

Using the PLS-DA with sample groups for all treatments collected from the plasma, it is evident that heat stress provokes a shift in the metabolic profile of the plasma as there is clear separation of AHS and CHS from the TN-control in the 3D plot (Fig. 2.16). Both the AHS and CHS groups overlap with the PF group, and there is minimal overlap between the PHS and CHS groups. Furthermore, pairwise comparisons (Fig. 2.17) aided in identifying the specific metabolic impact of heat stress exposure. The PF, AHS, and CHS groups showed complete separation from the TN-control group while the PHS group overlapped with the TN-control. The metabolite with the highest VIP score, contributing most to the differences between the metabolic profiles of the AHS and TN-control group in the plasma, is GDP (VIP = 3.2). GDP increased in response to AHS exposure. For CHS, ADP-glucose had the highest VIP score (VIP = 3.3) and was increased in response to CHS exposure.

2.3.3 The impact of heat stress on the metabolome is duration dependent

It is worth noting that, independent of feed depression, the duration of heat stress exposure influences the metabolome. For example, in the duodenum where this trend is especially apparent, the PHS group shows near indistinguishable overlap with the TN-control and PF groups. However, while the AHS group does overlap with the TN-control, PF, and PHS groups, there is more distinct separation from these groups as the exposure to heat stress increases. Then, as the heat stress duration is further increased with the CHS group, clear separation from the PF and PHS groups becomes evident. Furthermore, the only other group overlapping with CHS in the 3D PLS-DA (Fig. 2.18) is the AHS group demonstrating that increased duration of heat stress exposure further modulates the metabolome. In fact, pimelic acid and 3-hydroxyisovalerate, which were elevated, and N-carbamoyl-L-aspartate, dihydroorotate, dAMP, GAR, AICAR, S-adenosyl-L-homocysteine, and orotate, which were depressed, were specific to AHS exposure. Meanwhile, cysteate, NADH, NAD⁺, NADP⁺, and D-erythrose 4-phosphate, which were elevated, and N-acetylputrescine, 1-methylhistidine, histidine, phosphothreonine, glucose phosphate, and aconitate, which were depressed, were specific to birds exposed to CHS. While this duration dependent trend was not as obvious in other regions, there are metabolites unique to AHS or

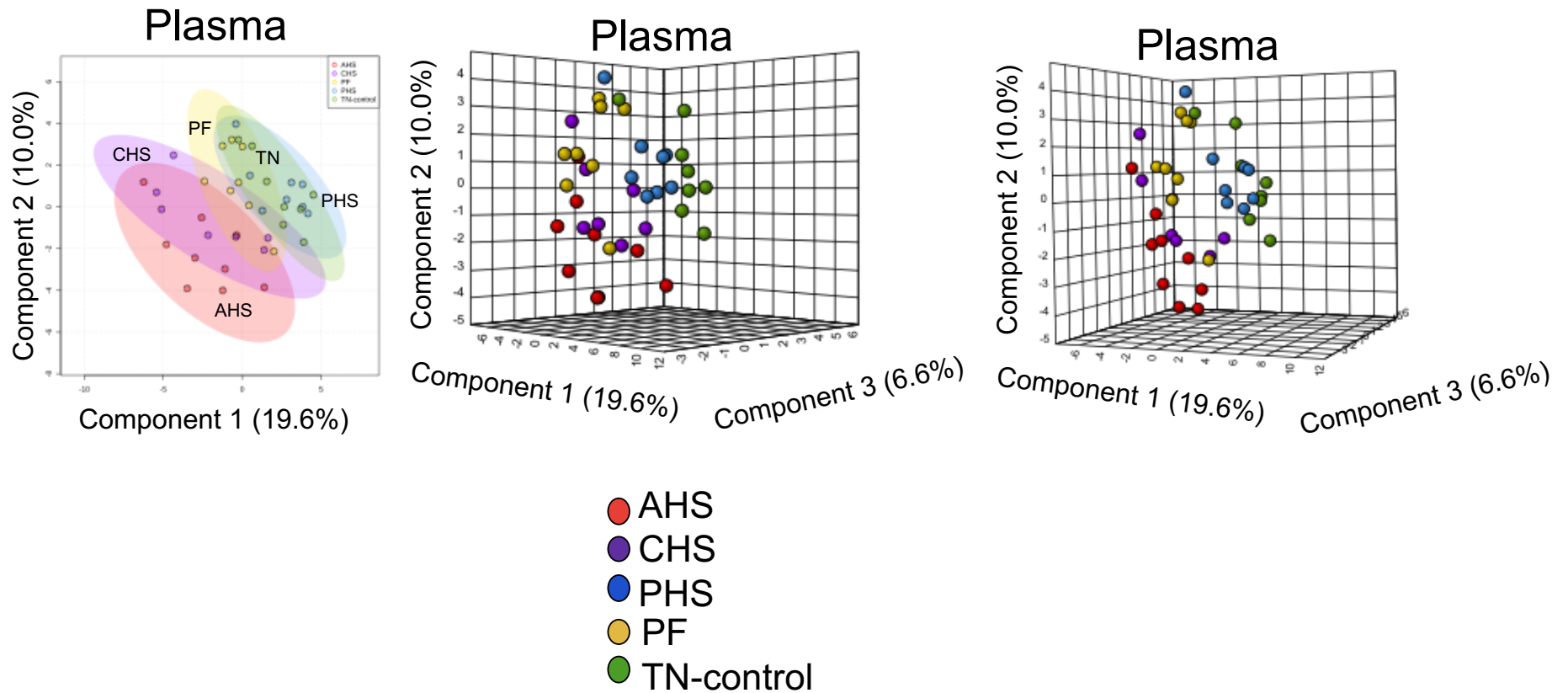


Figure 2.16 2D and 3D *Partial least-squares discriminant analysis* (PLS-DA) plots for the plasma. The side view of the the 3D PLS-DA (right) shows separation of the heat stress groups from the control. Pre-heat stress (PHS), TN-control (TN-control), pair-fed (PF), acute heat stress (AHS), cyclic heat stress (CHS).

Figure 2.17 2D (top) *Partial least-squares discriminant analysis (PLS-DA)* plots for pairwise comparisons of each treatment to the TN-control in the plasma. CHS and AHS had the most separation from the control. The treatment groups show more separation from the TN-control in 3D (bottom) PLS-DA plots. Pre-heat stress (PHS), TN-control (TN-control), pair-fed (PF), acute heat stress (AHS), cyclic heat stress (CHS), cecal digesta (CD), ileal digesta (ID), plasma (P), jejunum (J), ileum (I), duodenum (D)

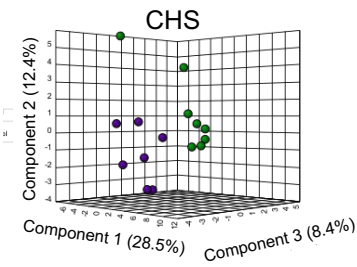
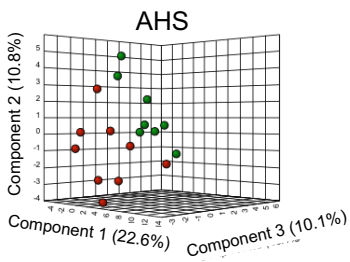
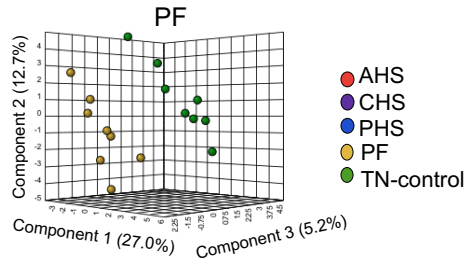
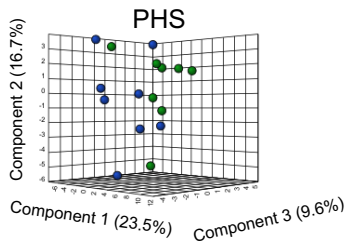
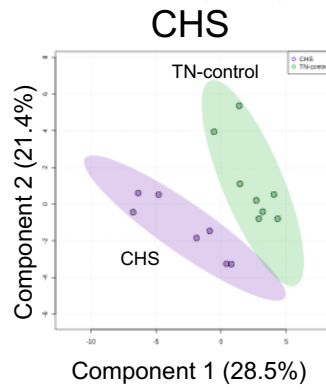
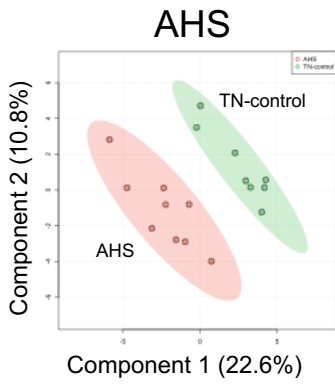
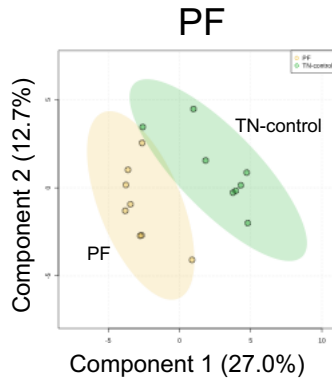
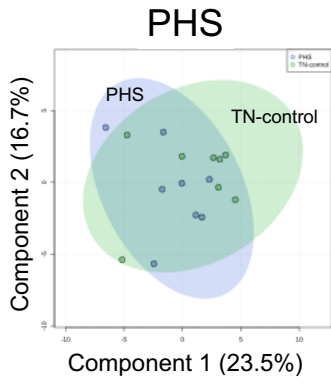
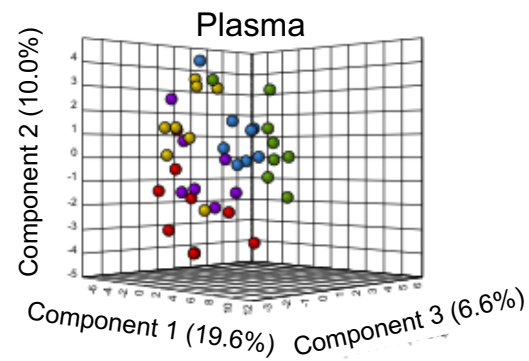
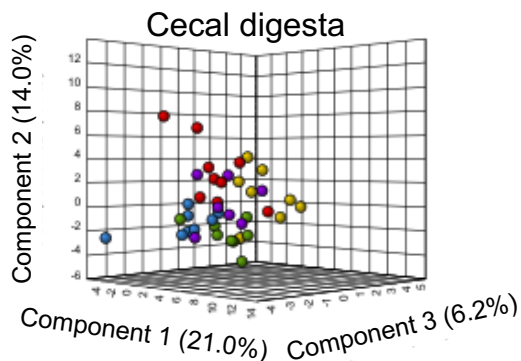
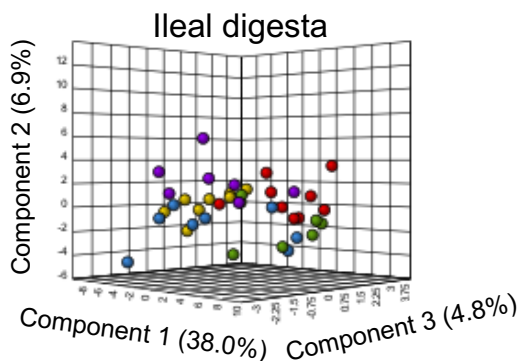
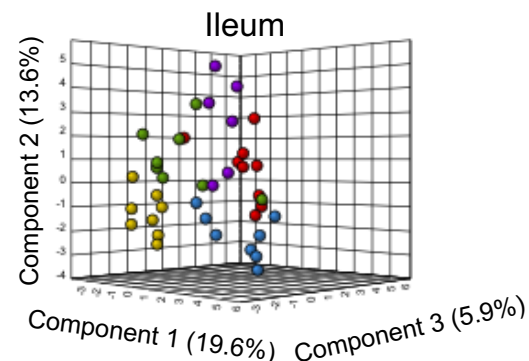
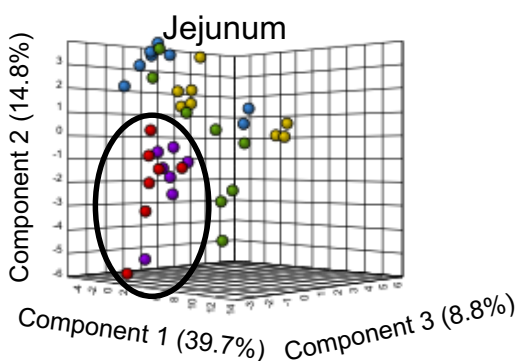
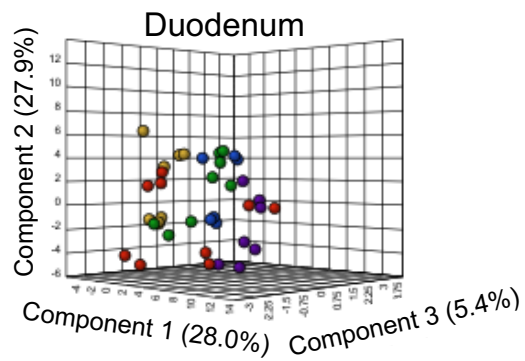


Figure 2.18 3D *Partial least-squares discriminant analysis* (PLS-DA) plots for each biological region. Within each region, samples were grouped by treatment Pre-heat stress (PHS), TN-control (TN-control), pair-fed (PF), acute heat stress (AHS), cyclic heat stress (CHS). This analysis shows the I the jejunum there was clear separation of the heat stress groups from all other groups.



- AHS ● PF
- CHS ● TN-control
- PHS

CHS exposure in all other regions analyzed. The only exception is the ileal digesta where there are not any metabolites uniquely depressed in response to AHS and CHS. Here, only two metabolites (2-oxoisovalerate and nicotinate) are depressed in response to heat stress exposure, and these metabolites are conserved for both AHS and CHS.

2.4 Discussion

Heat stress, which is the most challenging environmental stressor, has recently had a profound detrimental impact on the poultry industry due to the loss of meat production and quality.¹²³ This has caused a disruption in production sustainability which has led to substantial economic burdens worldwide.^{81, 124} In addition to its apparent impact on growth, appetite, and meat quality^{88-91, 125}, heat stress has also been proven to impair body systems and physiology.¹²⁶⁻¹²⁸ Gut injury is one of the most prominent effects of heat stress, though the underlying mechanisms are still not well defined or understood.^{17, 101, 108, 129} It has been shown that heat stress damages the gut by impairing the integrity and permeability of the intestine.^{18, 130} Specifically, previous studies have demonstrated that heat stress induces leaky gut syndrome by altering expression of nutrient transporters, tight junction proteins, cyto(chemo)kines, and intestinal heat-shock proteins.^{88, 118, 119} Leaky gut syndrome increases the permeability of the intestinal mucosa permitting the leakage of toxic digestive metabolites, bacteria, bacterial toxins, and small molecules into circulation in the bloodstream.¹³¹

Since the underlying mechanism of heat stress induced gut injury is still undefined, this study aimed to determine the metabolic profiles of the small intestine, intestinal digesta, and plasma in heat-stressed broilers. The tissue from the small intestine provided information about nutrients being absorbed and metabolic state of the tissue, while the intestinal digesta provided insight to the available nutrients. The data from plasma were used to analyze the metabolic changes to the nutrients in circulation. Studying the heat stress induced metabolome differences serves as a way to understand the underlying physiological impacts of heat stress on the gut and circulating nutrients. Untargeted mass spectrometry-based metabolomics, with its high throughput capabilities, resolution and sensitivity, enabled the study of water-soluble small molecules detected in each biological matrix. This study established that heat stress significantly alters the metabolomes of the small intestine, intestinal digesta, and plasma, with a clear duration dependent impact, specifically on the duodenum.

As expected, metabolomics analysis revealed distinct metabolic profiles for the small intestine, intestinal digesta, and plasma, regardless of heat stress exposure. This distinction is expected due to these biological locations having different physiological functions and microbial populations and activity. Though this separation is anticipated, it is not guaranteed as the metabolites identified in this study were known metabolites related to central carbon metabolism, which only make up a small fraction of total metabolites, and are common among most organisms. Since these data do exhibit obvious separation based on biological

location and function, this is an indicator of reliable, high-quality data. The sum of normalized relative abundances of identified metabolites is the lowest in the plasma compared to other regions (Fig. 2.25), regardless of heat stress exposure. Interestingly, while the ileal digesta had the highest abundance of metabolites, the impact of heat stress was the least evident in this region, likely indicating that the small molecules being passed through the digesta as waste are minimally impacted by heat stress exposure.

2.4.1 Heat stress impacts energy metabolism

Based on the untargeted metabolomics analysis, the impact of heat stress exposure on energy metabolism is quite compelling as alterations in purine, histidine, amino acid, and one-carbon metabolism, glycolysis, and the TCA cycle are evident. Specifically, the impact of heat stress on purine metabolism was highly conserved across the small intestine, intestinal digesta, and plasma for both AHS and CHS exposure. This is in accordance with other studies which have shown that heat stress impacts purine metabolism.¹³² Purine metabolism was the only metabolic pathway altered by heat stress in all analyzed regions for both AHS and CHS. This is intriguing because purines play a crucial role in energy metabolism as they provide a cell with the vital energy and cofactors needed to promote cell growth and maintain cellular metabolism. In addition, purines serve as building blocks for nucleic acids and play a role in intracellular signaling.¹³³ In mammals, the majority of the cellular purine pool is acquired through the recycling of bases via the purine salvage pathway where adenine, guanine, and hypoxanthine are produced from AMP, GMP, and IMP, respectively.¹³³ Purines can also be synthesized using de novo purine biosynthesis in which GAR and AICAR are intermediates and NAD⁺ is needed for these reactions.¹³³ GAR, AICAR, and NAD⁺ were all significantly impacted by heat stress exposure. Similarly, when purines are degraded, uric acid is produced, and uric acid was identified as one of the few metabolites responsible for driving the separation between the CHS exposed birds and TN-control birds in all three regions of the small intestine analyzed. From this, it can be inferred that one of the leading implications of heat stress is the impact on energy metabolism. This is consistent with previous studies as it has been shown that male BALB/c mice exposed to heat stress exhibited impairment of protein synthesis which led to intestinal injury through a mitochondrial-dependent pathway.¹³⁴ It is possible that the alterations to energy metabolism could arise from feed depression that accompanies heat stress as this decreased the nutrient intake. However, some metabolites that were significantly impacted by heat stress were not significantly impacted by the PF group when compared to the TN-control, such as NAD⁺, uric acid, GMP, and xanthosine. From this, it can be suggested that the impact of heat stress, rather than feed depression, more strongly contributes to alterations in energy metabolism.

2.4.2 Heat stress induces considerable changes in the small intestines

Heat stress induced the most dramatic metabolic alterations in the small intestines out of all regions analyzed. This could be attributed to the villi present in the epithelial cells of the intestines. Intestinal villi contain large numbers of mitochondria which function to provide ATP for active transport of nutrients.¹³⁵ Villi are most numerous in the duodenum and jejunum of the small intestines, which provides a possible explanation as to why heat stress has a greater impact on the duodenum and jejunum than the ileum.¹³⁵ This also helps explain why the impact on energy metabolism is most apparent in the duodenum and jejunum. It is clear that, in the small intestines, the jejunum was impacted most by heat stress as the PLS-DA analysis of the small intestines revealed that there was an undeniable impact of heat stress on the jejunum (Fig 2.18). In addition, the jejunum had nearly five times more metabolites significantly altered by heat stress than any other region analyzed (Table 2.1).

Using the pathway analysis feature in MetaboAnalyst 5.0 and metabolites with a VIP score >1 for each pairwise comparison (TN-control vs (AHS or CHS)), the metabolic pathways impacted most by heat stress in the small intestines were determined for both AHS and CHS. Purine, pyrimidine, glutathione, and arginine metabolism were impacted by both AHS and CHS. There were not any pathways uniquely impacted by AHS, however, proline and taurine metabolism and the TCA cycle were unique to CHS exposure. This provides evidence that heat stress impacts the small intestines in a duration dependent manner.

For example, all metabolites conserved in all analyzed regions of the small intestines that had the most impact on driving the separation of the TN-control birds and heat stress birds differed between AHS and CHS. Specifically, unique to AHS, prephenate was increased in response to AHS exposure. Prephenate is involved in aromatic amino acid biosynthesis and the shikimate pathway and is synthesized by bacteria, plants, and some parasitic protozoans but not mammals.^{136, 137} This provides evidence that microbial derived metabolites are altered in response to AHS. Therefore, it could be suggested that AHS stimulates alterations in gut microbial function or composition which could be related to dysbiosis and leaky gut syndrome as previous studies have demonstrated that the intestinal microbiota in chickens can be altered by environmental factors.^{138, 139} However, to fully understand the correlations among heat stress, gut microbial composition and function, and the metabolome, additional studies with metagenomics sequencing are needed. Additionally, unique to AHS, 3-hydroxyisovalerate, a normal mammalian metabolite that is a byproduct of the leucine degradation pathway, is produced in the mitochondria via a biotin-dependent reaction.¹⁴⁰ Increased levels of 3-hydroxyisovalerate are associated with mitochondrial toxicity and dysfunction, redox dyshomeostasis, aciduria, and ketogenesis disorders¹⁴¹, most of which are induced by AHS.¹⁴² The increased levels of 3-hydroxyisovalerate observed in this study in response to heat stress promotes the conclusion that heat stress impacts energy metabolism.

It is also worth noting that one carbon metabolism, specifically the methionine cycle, was impacted by both AHS and CHS exposure. However, the extent of impact differed by duration. AHS led to a significant increase in methionine, cysteine, and glutathione and a significant decrease in S-adenosylhomocysteine. However, with CHS exposure, there is a significant increase in methionine, and cysteine, and cystathionine. These data likely indicate that the methylation status of macromolecules has been altered in response to heat stress in a duration dependent manner.¹⁴³ These modifications in one carbon metabolism reveal how heat stress redirects cellular metabolism.

NAD⁺, uric acid, deoxyinosine, and cystathionine are involved in purine metabolism and antioxidant defense and have significant VIP scores exclusively with CHS. Deoxyinosine and uric acid are both increased in response to CHS exposure in the duodenum and jejunum. Deoxyinosine is also increased in the ileum, but uric acid is decreased in the ileum, though this decrease is not significant ($p=0.13$). As, the ileum is the region of the small intestines impacted least by heat stress, and this could potentially be attributed to the reduction in epithelial villi which plays a role in energy metabolism. The increase in deoxyinosine and uric acid provide evidence that CHS promotes purine degradation, which is in accordance with other studies showing that heat stress affects purine metabolism.¹³² Under oxidative stress, the mitochondria may redirect cellular metabolism to increase uric acid production to defend against reactive oxygen species (ROS) as uric acid is a powerful antioxidant.⁵⁷ Additionally, cystathionine, which was significantly increased in the jejunum ($p= 0.0045$), is involved in the transsulfuration pathway and leads to the production of glutathione stimulating the antioxidant defense system.¹⁴⁴ Combined, this further supports the conclusion of mitochondrial reprogramming in response to heat stress.

In addition to mitochondrial origin, the observed high levels of NAD⁺, NADH, and NADP⁺, which were in agreement with previous studies¹⁴⁵, suggest that CHS induced ROS via the nicotinamide adenine dinucleotide phosphate oxidase pathway.¹⁴⁵ In this pathway, NADPH is converted to NADP⁺.¹⁴⁶ These metabolites have multiple roles, for instance, NAD⁺ plays a crucial role in the maintenance of mitochondrial function.¹⁴⁷ NAD⁺ and NADPH play essential roles in immunity and inflammation, mainly dependent on the redox signaling.¹⁴⁸ NADH is a central hydride donor that drives the mitochondrial oxidative phosphorylation (OXPHOS) for ATP generation along with ROS production and the conversion of lactic acid to pyruvate.¹⁴⁹ Beyond its crucial role as a coenzyme in energy metabolism, NAD⁺ has been shown in recent years to play a vital role in stress resistance, DNA repair, cell death, and regulating cellular metabolism through mitochondrial mediated epigenetic modifications and histone demethylations.¹⁵⁰⁻¹⁵⁴ Together, there is strong evidence to support the impact of heat stress on mitochondrial energy metabolism in the small intestines.

2.4.3 Intestinal digesta and plasma metabolomes are affected by heat stress

Metabolites with a VIP score >1 for each pairwise comparison (TN-control vs either AHS or CHS) were used to pinpoint metabolic pathways impacted most by heat stress in the intestinal digesta and plasma for both AHS and CHS. For the ileal and cecal digesta, the TCA cycle and purine metabolism were impacted by both AHS and CHS. As mentioned previously, the impact on purine metabolism was conserved across all regions and discussed in depth. However, the TCA cycle is unique to the intestinal digesta. Specifically, (iso)citrate was elevated in response to both AHS and CHS in the ileal and cecal digesta. However, the change in abundance of (iso)citrate was only significant in the cecal digesta. This is not surprising because, as previously mentioned, the ileal digesta displays the least impact of heat stress out of all analyzed regions. (Iso)citrate is a precursor to glutamate, and glutamate is one of the amino acids that is needed for the synthesis of glutathione.¹⁵⁵ Since glutathione is an antioxidant that is synthesized to help prevent oxidative damage by neutralizing ROS, this further validates that heat stress stimulates the antioxidant defense system.

In contrast to the small intestines, there are pathways unique to AHS exposure in the intestinal digesta. These pathways are riboflavin and pyrimidine metabolism, the pentose phosphate pathway (PPP), and one carbon pool by folate. The PPP has been demonstrated to be a major regulator for cellular reduction-oxidation (redox) homeostasis and biosynthesis and promotes nucleotide synthesis.¹⁵⁶ The involvement of the PPP was evidenced by the increased abundance of riboflavin, which is an intermediate in the PPP.¹⁵⁷ This supports the notion of a metabolic steady-state adaptation under AHS, rerouting from glycolysis to the PPP as a metabolic transition to counteract heat stress.¹⁵⁸⁻¹⁶⁰ Similarly, riboflavin, or vitamin B₂, has been shown to play a crucial role in boosting the antioxidant and immune systems under stress conditions.^{161, 162} It is also possible that riboflavin could be involved in cellular oxidation and mitochondrial energy production via the electron transport chain (ETC)¹⁶³ to sustain membrane stability and adequate energy-related cellular functions under AHS; however, further studies associated with the riboflavin/FAD cycle are warranted. Also, it is not surprising to see that one carbon metabolism by folate is impacted by AHS because riboflavin plays a crucial role in folate recycling as it acts as a cofactor in the conversion of 5,10 methyleneTHF to 5-methylTHF.¹⁶⁴ It is also worth pointing out that in the intestinal digesta, methylated amino acids, acetylated amino acids, and methylated nucleosides appear to be significantly altered by AHS exposure. These compounds are used in mitochondrial mediated epigenetic regulation to redirect cellular metabolism.¹⁵² Further confirming that cellular metabolism is reprogrammed in response to AHS exposure.

Similarly, for the impact of CHS exposure on the intestinal digesta cysteine, methionine, arginine, glutathione, and pyruvate metabolism are altered in response to CHS. A possible explanation for alterations in cysteine, methionine, and glutathione metabolism could be a result of metabolism is being rerouted to

produce antioxidants to defend against ROS. Cystathionine and folate were significantly increased in response to CHS, which is likely indicating the switch from glycolysis to the PPP in order to conserve energy. Arginine can be converted to glutamate which is needed for glutathione synthesis, and pyruvate is precursor to acetyl-CoA which is used for epigenetic modifications and histone acetylation.¹⁵²

The plasma follows a similar trend with altered purine metabolism conserved between AHS and CHS. In the plasma, there no significantly altered pathways unique to AHS. However, cysteine, methionine, alanine, aspartate, glutamate, pyruvate and riboflavin metabolism and glycolysis are unique to CHS. This provides another example of the duration dependent impacts of heat stress. Here, it is evident the CHS impacts the nutrients in circulation as a result of cellular reprogramming.

2.5 Methods

2.5.1 Ethics Statement

The present study was conducted in accordance with the recommendations in the guide for the care and use of laboratory animals of the National Institutes of Health, and the protocol was approved by the Institutional Animal Care and Use Committee (#21050) at the University of Arkansas.

2.5.2 Birds, Diets, and Heat Stress Challenge

One-day old male broiler (meat-type) chicks (n = 672) were obtained from commercial Cobb-Vantress hatchery (Siloam Springs, Arkansas), neck tagged, individually weighed, and randomly allocated to 12 environmental chambers (2 floor pens/chamber, 24 pens in total, 28 birds/pen). Each pen was covered with 7 cm fresh pine shavings and equipped with a plastic hanging poultry feeder and an automatic vacuum-sealing O-ring drinker. Birds were given ad libitum access to clean and fresh water and a corn–soybean meal basal diet (starter d 1–14, grower d 15–28, and finisher d 29–42). The diet composition has been previously described.⁸⁸ Temperature was maintained at 32 °C for the first 3 days, and then gradually reduced approximately 3 °C each week until it reached 23 °C on d 21. The average relative humidity was 30%. The lighting program was 24 h light for the first 3 days, reduced to 23 h light:1 h dark during d 4–7, and reduced further to 18 h light: 6 h dark thereafter. The experiment followed a completely randomized design with three treatments (8 replicate pens/treatment): a control group (TN) where the birds were raised under thermoneutral condition (23 °C) from d 29–42, a chronic cyclic heat-stressed group (CHS) where the birds were exposed to high ambient temperature (35 °C) for 8 h/d (9:30 am to 5:30 pm) from d 29–42 to mimic summer time in Arkansas, and a pair-fed group (PF) where the birds were raised like the control group (similar environmental conditions, 23 °C) and fed the same amount of feed as the CHS group. Using the pair-fed TN group would help to distinguish between the effect of feed depression and the effect of heat stress. Feed intake and water consumption were recorded daily. Individual body weight

was recorded weekly. Body core temperature was continuously monitored using ThermoChron temperature logger (iButton, DS19221, Embedded Data Systems, Lawrenceburg, KY, USA). The environmental temperature and humidity were also continuously recorded in each chamber. At the end of the experiment (d 42), duodenum, jejunum, and ileum segments, ileal and cecal digesta, and plasma from each group (TN, CHS, PF, n = 8/group) were collected, rinsed in PBS 1x, snap frozen in liquid nitrogen, and stored at $-80\text{ }^{\circ}\text{C}$ for metabolomics analysis. Samples were also collected from two additional groups: an acute heat-stressed group (AHS), where some TN birds were exposed to $35\text{ }^{\circ}\text{C}$ for 2 h before sampling on d 42, and a preheat-stressed group (PHS), where CHS birds were sampled before starting the heat stress on d 42 (Fig. 1).

2.5.3 Sample Collection and Preparation

Tissue samples were ground, and intestinal digesta and plasma samples were aliquoted, snap frozen in liquid nitrogen, and sent to the Biological and Small Molecule Mass Spectrometry Core (BSMMSC, The University of Tennessee, Knoxville, TN, USA). Tissue samples were pre-weighed (50-100 mg), and intestinal digesta and plasma samples were aliquoted ($100\text{ }\mu\text{L}$) prior to extraction. These weights and volumes were used to normalize the raw metabolite peak intensities. Metabolites were extracted with 1.5 mL of extraction solvent (40:40:20 HPLC grade methanol: acetonitrile: water with formic acid at a final concentration of 0.1 M), pre-chilled at $4\text{ }^{\circ}\text{C}$, and incubated at $-20\text{ }^{\circ}\text{C}$ for 20 min. Samples were centrifuged ($13,300\times\text{ g}$, 5 min, $4\text{ }^{\circ}\text{C}$), and supernatants were collected. Solvent was evaporated under a stream of nitrogen, and metabolites were suspended with $300\text{ }\mu\text{L}$ of HPLC-grade water prior to mass analysis.

2.5.4 Ultra-High Performance Liquid Chromatography—High Resolution Mass Spectrometry (UHPLC–HRMS) Metabolomics Analysis

UHPLC–HRMS analysis has been described previously.^{15, 165} Briefly, metabolites were separated on a Dionex UltiMate 3000 RS (Sunnyvale, CA, USA) by injecting a $10\text{ }\mu\text{L}$ sample on a Synergy reverse phase Hydro-RP 100 Å, $100\text{ mm}\times 2.00\text{ mm}$, $2.5\text{ }\mu\text{m}$ pore size LC column (Phenomenex, Torrance, CA, USA) kept at $25\text{ }^{\circ}\text{C}$. The previously validated global metabolomics method ran for 26 min with the application of a multistep gradient.¹⁶⁶ To separate the analytes, two HPLC-grade solvents were used in gradient steps. Solvent A (97:3 H₂O:MeOH with 11 mM tributylamine and 15 mM acetic acid) and solvent B (100% MeOH). The gradient was performed as follows: 0 min, 0% B; 5 min, 20% B; 13 min, 55% B; 15.5 min, 95% B; 19 min, 0% B; 25 min, 0% B with a flow rate of $200\text{ }\mu\text{L}/\text{min}$. The eluent was administered into the mass spectrometer via an electrospray ionization (ESI) source conjoined to an Exactive™ Plus Orbitrap Mass Spectrometer (Thermo Scientific, Waltham, MA, USA) under the following established parameters of aux gas: 8; sheath gas: 25; sweep gas: 3; spray voltage: 3.00 kV; and capillary temperature: $300\text{ }^{\circ}\text{C}$. The parameters of the mass spectrometer were

set as follows: resolution: 140,000; automatic gain control (AGC): 3×10^6 ; maximum IT time: 100; scan range: 85–1000 m/z . Raw data were obtained from the Xcalibur MS software (Thermo Electron Corp, Waltham, MA, USA) and converted to mzML format by ProteoWizard tool MSConverter.^{73, 167} The converted data were analyzed using MAVEN²⁴, and peaks were annotated with a maximum allowed error of ± 5 ppm. Area under the chromatographic curve was integrated based upon an in-house verified list of metabolites using exact mass and known retention times.¹⁶⁸ All metabolite values were normalized based on the mass or volume of the sample extracted prior to all statistical calculations.

2.5.6 Data Processing and Statistical Analysis

Metabolites showing differences higher or lower than 1.5 folds and p -value less than 0.05 in the comparison between each of the treatment groups (AHS, PHS, CHS, and PF) and TN-control birds were considered significantly different. Heatmaps, which displayed \log_2 fold changes for identified metabolites, were created using R (version 1.0.153). p -values were calculated using student's t -test. For group discrimination, partial least squares discriminant analysis (PLS-DA) and variable importance in projection (VIP) scores were constructed using the MetaboAnalyst 5.0.²⁵ Metabolites with VIP values > 1 were the ones that contributed to the group differentiation, and this was considered as a significant VIP score.

2.6 Conclusions

In conclusion, this study is the first to use a high-throughput mass spectrometric metabolomics approach to probe the systemic impact of heat stress-induced metabolic changes in broilers. The metabolic profiles of the small intestines (duodenum, jejunum, and ileum), intestinal digesta (ileal and cecal), and plasma of broilers were characterized in response to heat stress exposure. The results demonstrated that, independently of feed intake depression, heat stress induced significant changes in metabolic pathways in a duration-dependent manner and identified potential markers for heat stress in each region. These data imply that heat stress, having the most impact on the small intestines, modifies the intestinal microbiota and host-dependent metabolites. Specifically, with the results provided from study, it can be speculated that heat stress induces mitochondrial mediated cellular reprogramming, as the impact on purine and energy metabolism was evident in each region. However, this study was limited to only male broilers, preventing analysis of sex-based differences on the impact of heat stress. Although this data-driven approach was not designed to provide mechanistic and functional evidence, pathway analysis provided additional understanding of the systemic heat stress responses in broilers and opened a new vista for future investigations.

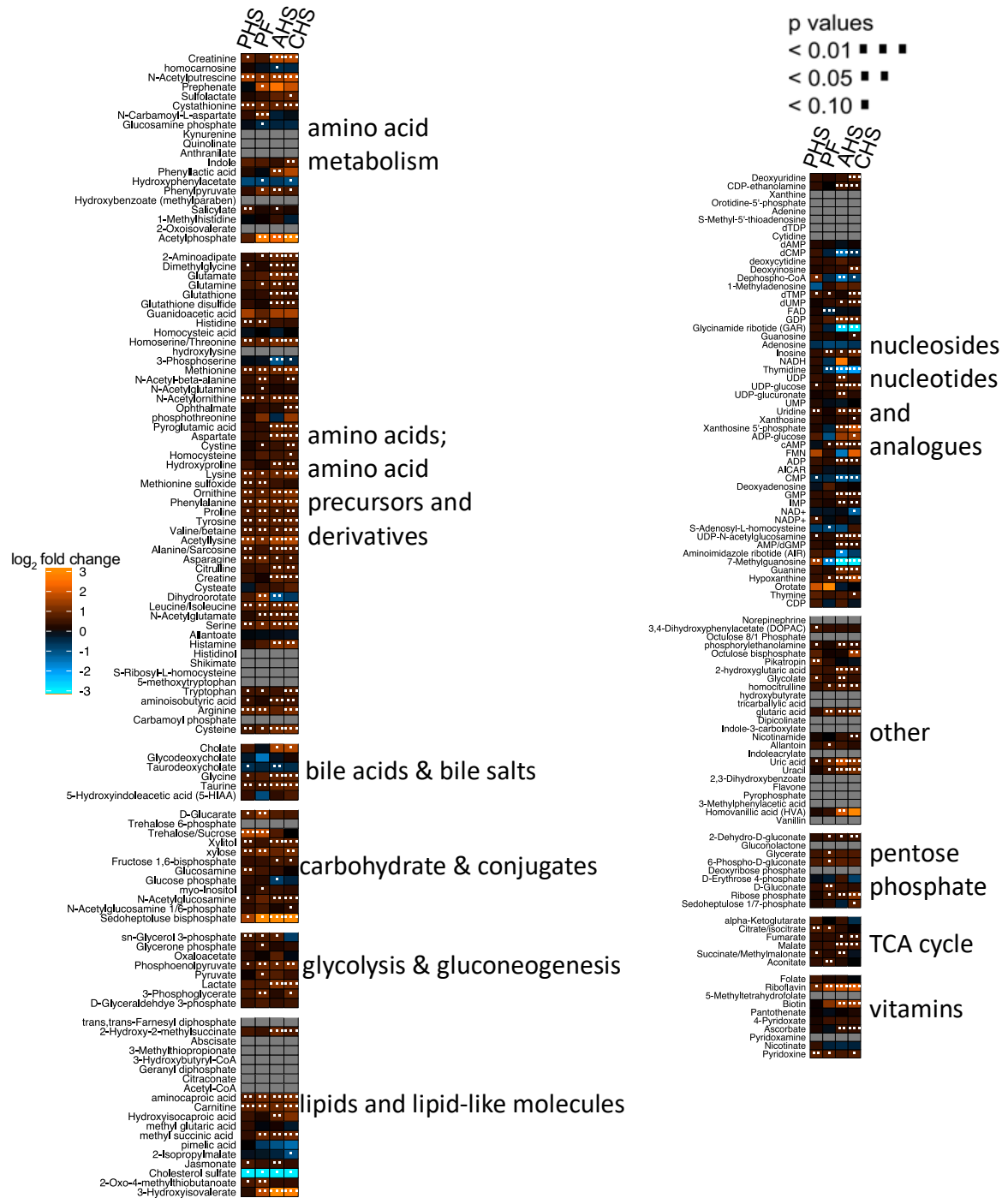


Figure 2.20 Heatmap displaying log₂fold change for all identified metabolites in the jejunum. Pre-heat stress (PHS), TN-control (TN-control), pair-fed (PF), acute heat stress (AHS), cyclic heat stress (CHS)

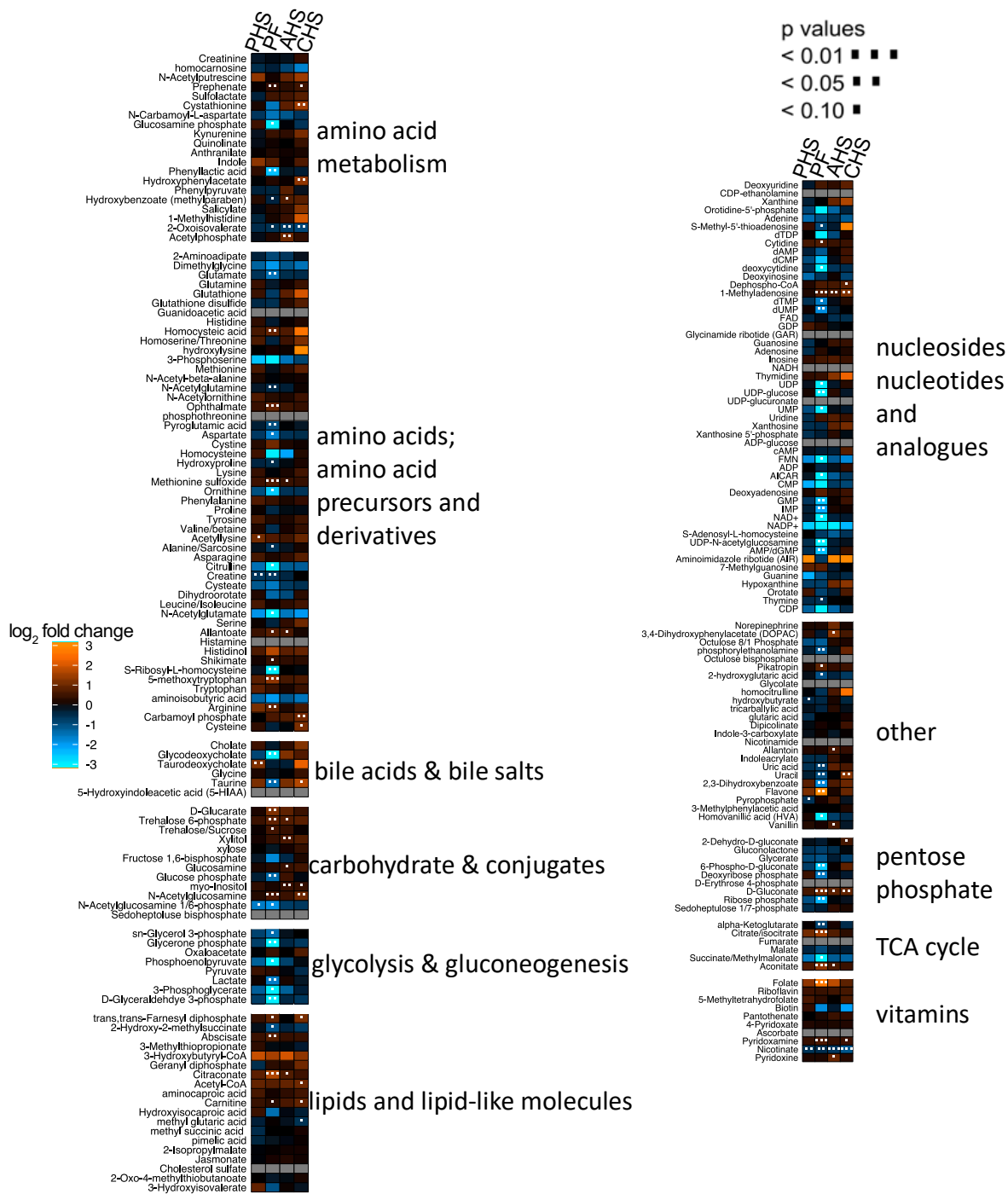


Figure 2.22 Heatmap displaying log₂fold change for all identified metabolites in the ileal digesta. Pre-heat stress (PHS), TN-control (TN-control), pair-fed (PF), acute heat stress (AHS), cyclic heat stress (CHS)

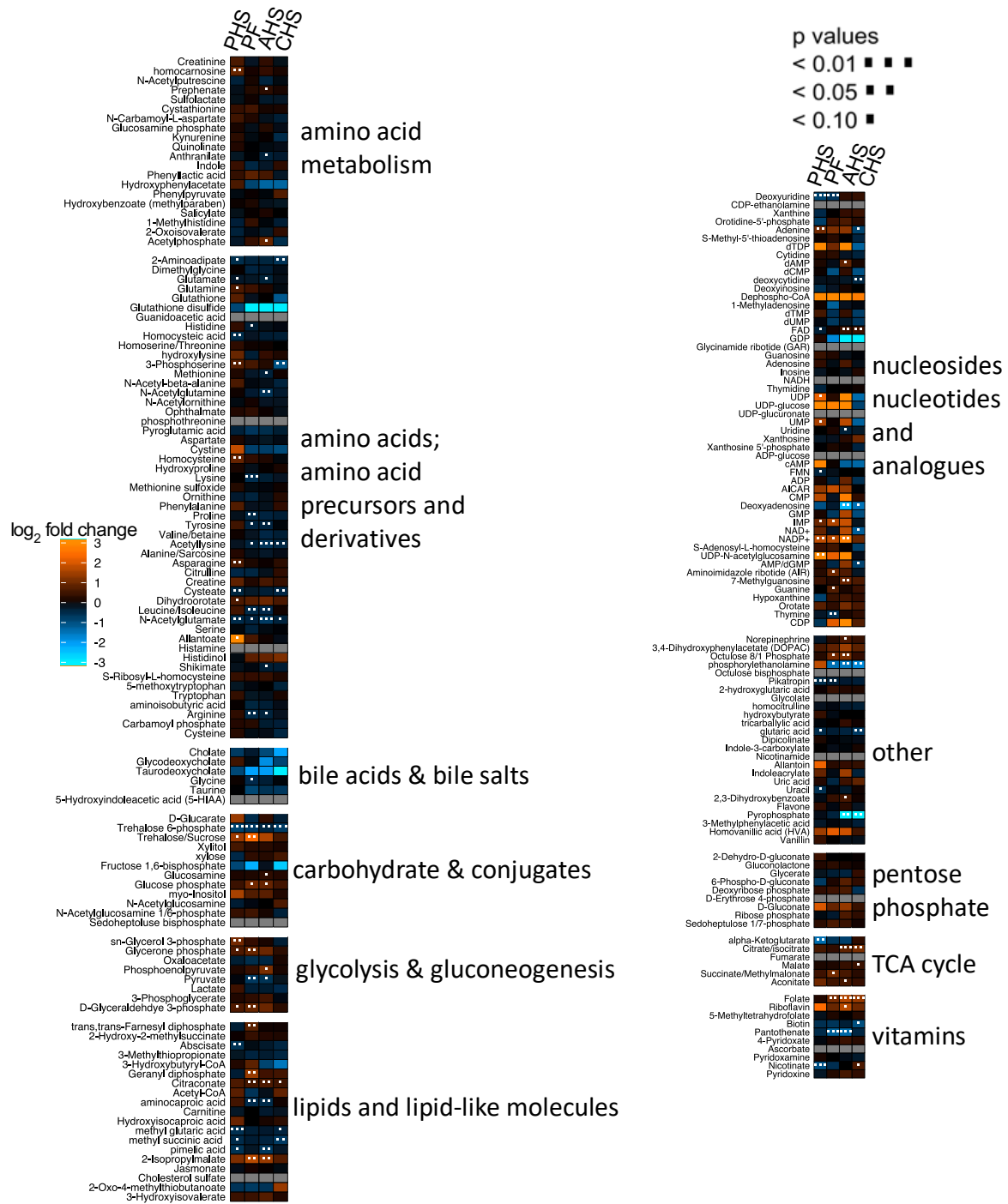


Figure 2.23 Heatmap displaying log₂fold change for all identified metabolites in the cecal digesta. Pre-heat stress (PHS), TN-control (TN-control), pair-fed (PF), acute heat stress (AHS), cyclic heat stress (CHS)

Metabolite abundance by region and treatment

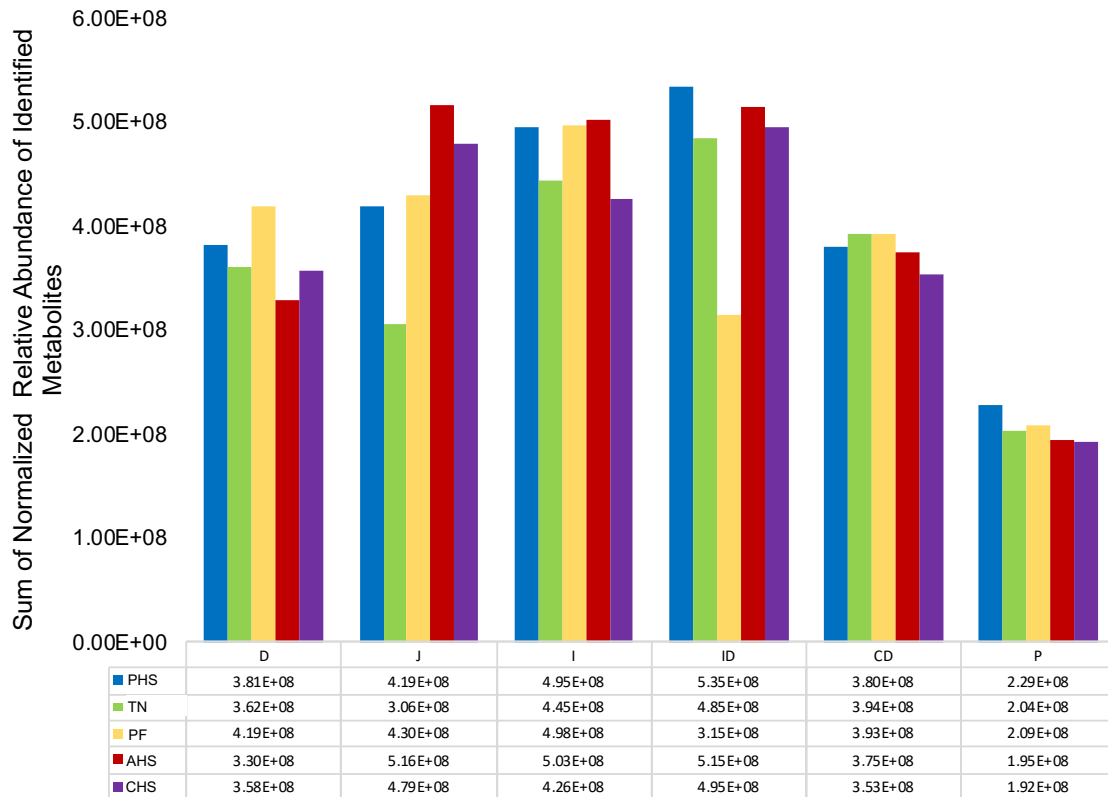


Figure 2.25 The sum of the moralized relative abundance of all identified metabolites for each region and treatment was compared. Pre-heat stress (PHS), TN-control (TN-control), pair-fed (PF), acute heat stress (AHS), cyclic heat stress (CHS), cecal digesta (CD), ileal digesta (ID), plasma (P), jejunum (J), ileum (I), duodenum (D)

CHAPTER 3 METABOLIC PROFILE OF *HISTOMONAS MELEAGRIDIS* AND UNDEFINED BACTERIAL POPULATIONS IN DWYER'S MEDIA WITH AND WITHOUT RICE STARCH IDENTIFIES RIBOFLAVIN AS A POSSIBLE REQUIREMENT FOR AXENIC CULTURES

A version of this chapter will be a part of a future publication titled:

Metabolic profile of *Histomonas meleagridis* and undefined bacterial population in Dwyer's media with and without rice starch identifies riboflavin as a possible requirement for axenic cultures

Potential authors: Sawsan Ammar*, Courtney J. Christopher*, Hector F. Castro, Shawn R. Campagna, Richard Gerhold

*Authors contributed equally to this work

Author contributions

RG, SA SRC, and CJC designed the experiment. SA conducted the experiment. CJC and SA wrote the manuscript. SRC, RG and HFC edited the manuscript. CJC performed metabolomics extractions, mass spectral analysis, and data processing and analysis.

3.1 Abstract

The parasite induced poultry disease, histomonosis, is prevalent worldwide and threatens the poultry industry with serious economic losses due to its impact on the mortality and morbidity in turkey and chicken flocks. Histomonosis is caused by the infection of the unicellular parasite *Histomonas meleagridis* (*H. meleagridis*). Previously, anti-histomonal drugs were available but recently these drugs have been banned due to the issue of consumer protection in countries with strict pharmaceutical regulations, including the US. Consequently, this has led to the reemergence of *H. meleagridis* infection, which poses an eminent threat for the poultry industry. The need for new approaches in treating or preventing histomonosis has opened a new vista for scientific exploration, including understanding the nutrient requirements for *H. meleagridis* survival, which is what this study aimed to elucidate. Here, an ultra-high performance liquid chromatography high resolution mass spectrometry (UHPLC-HRMS) based metabolomics approach was utilized to investigate essential nutrient requirements for *H. meleagridis* growth. Typically, *H. meleagridis*, along with an undefined composition of microbes, is grown in Dwyer's media, which has been used for the last few decades, for lab experiments. Dwyer's media contains rice starch, and it has been found that *H. meleagridis* will not grow if rice starch is omitted from the media. Therefore, this study analyzed *H. meleagridis* grown in Dwyer's media with and without rice starch in order to gain a deeper understanding of why *H. meleagridis* will not grow when rice starch is omitted from the media. Samples were collected from cultures grown with and without rice starch over 166 hours, which encompassed each phase of the growth curve. The growth dynamics in Dwyer's media with and without rice starch of *H. meleagridis* compared to the undefined bacterial population revealed that the absence of rice starch does not affect bacterial growth, however, it does inhibit *H. meleagridis* growth. The untargeted metabolomics data supported this with the heatmap illustrating a significant decrease in nearly all identified metabolites for the culture grown in the absence of rice starch. Further analysis using partial least-squares discriminant analysis (PLS-DA) and variable importance in projection (VIP) revealed that cells grown in Dwyer's media with rice starch had a distinctly different metabolic profile than cells grown with rice starch omitted as the PLS-DA showed two groups with clear separation. Riboflavin (vitamin B₂) contributed most to the separation of cells grown with and without rice starch (VIP = 5.4). Riboflavin is converted to FMN and FAD, which are the main flavin cofactors are essential for all living cells. These data suggest that omission of rice starch from Dwyer's media causes a riboflavin deficiency inhibiting *H. meleagridis* growth. While there is very limited information about the nutrient requirements for *H. meleagridis*, it is plausible that riboflavin is essential for axenic *H. meleagridis* growth.

3.2 Introduction

Histomonas meleagridis (*H. meleagridis*) is an important protozoan parasite of birds that primarily infects the cecum of birds, though infection can also reach

to the liver.^{169, 170} A *H. meleagridis* outbreak can have devastating impacts on the poultry industry, with the mortality rate in turkeys approaching nearly 100%.^{171, 172} In the 1970s, histomonosis was well controlled as drugs were available for the treatment and prevention *H. meleagridis* infection. Since histomonosis no longer posed an eminent threat, there was little research conducted on *H. meleagridis*. However, starting in the late 1990s, there was a ban on all drugs used for the prevention and treatment of histomonosis preventing use in food producing animals.¹⁷³ This has led to the reemergence of *H. meleagridis* infection, with numerous histomonosis outbreaks observed in recent years.^{174, 175} Because of this, there has been a renewed concern regarding *H. meleagridis* leading to new studies with the goal of better understanding *H. meleagridis*.¹⁷¹ Since *H. meleagridis* is a parasite, it depends on its host for survival as it cannot grow, reproduce, or live without the nutrients supplied by the host.¹⁷¹ *H. meleagridis* lacks mitochondria and rely on hydrogenosomes and nutrients provided from the host for energy metabolism.¹⁷⁶⁻¹⁷⁸ This makes it difficult when studying *H. meleagridis* in a lab setting because it challenging to differentiate *H. meleagridis* driven alterations from bacterial host driven alterations.

H. meleagridis has been grown on Dwyer's media for the last few decades.¹⁷⁹ Although the original media described by Dwyer contains chick embryo extract, this component has been omitted later to leave the Dwyer's media with only rice starch, serum and M 199 as main components.¹⁸⁰ Since then, several manipulations were attempted to increase the yield of the parasite in Dwyer's media and to understand *H. meleagridis* growth requirements.¹⁸¹⁻¹⁸³ A starch source and serum were found to be essential components of Dwyer's media and *H. meleagridis* was not able to establish in media lacking any or both of them.^{181, 182} There are ample proposed theories on the role of the rice starch in *H. meleagridis* media. Van der Heijden *et al.* described that *H. meleagridis* are only able to digest rice starch particles with size less than five microns. They proposed that the bigger particles are probably digested by the bacteria to provide *H. meleagridis* with further nutrients.¹⁸¹ The role played by bacteria is also not completely understood. The bacteria are introduced to the cultures with the inoculum from the cecum and trials to have axenic *H. meleagridis* cultures were not successful.^{184, 185}

To study *H. meleagridis* in the lab, a cecal swab from an infected bird is obtained. This cecal swab contains *H. meleagridis* as well as undefined bacterial populations. In order to understand the role of the rice starch in Dwyer's media used for *H. meleagridis* lab cultures, a metabolic analysis of intracellular metabolites of *H. meleagridis* and the undefined bacteria grown in Dwyer's media with and without rice starch was conducted. Understanding the role of rice starch in the media will have great implications the ability to modify Dwyer's media to increase its applications and gain a better understanding about the nutrient requirements of *H. meleagridis*. Understanding the small molecule interactions between the bacteria and *H. meleagridis* is crucial in order to aid in identifying the

role the bacteria play in *H. meleagridis* growth. In addition to that, if this experiment were able to understand the essential nutrients required for the organism, this would aid in having axenic cultures, which would open a new vista for scientific exploration of *H. meleagridis*. Using a global metabolomics approach, the goal was to identify essential components required for *H. meleagridis* growth which could allow us to replace or omit the rice starch with a more defined. It is hypothesized that there is a difference in growth of *H. meleagridis* in Dwyer's media with (SD) and without rice (NR) which will lead to difference in the metabolic profiles of cells grown in the SD compared to NR media. Therefore, this study aimed to identify the key metabolites that are driving this difference and altering them in future experiments to eventually replace the rice starch and potentially culture *H. meleagridis* axenically.

3.3 Results

3.3.1 *Histomonas meleagridis* growth

There was a significant difference in *H. meleagridis* growth in SD compared to NR media. At 42, 66, 114, 142, 166 HPI, *H. meleagridis* mean log count was higher in SD than in NR media ($p < 0.001$). There was a decline in *H. meleagridis* growth starting approximately 6 hours after inoculation in media lacking rice. In contrast, *H. meleagridis* grow considerably in SD media and reached the peak at 114 hours which was followed by a rapid decline (Fig. 3.1).

3.3.2 Growth of undefined bacteria

Bacterial growth showed a typical bacterial growth curve (Fig. 3.2) with the lag phase ending at 6 HPI, exponential phase from 6 to 18 HPI and a stationary phase from 18-114 HPI. Bacteria declined starting at 142 HPI. There was no significant difference in mean log count of bacteria in SD and NR media except at 6 HPI where bacterial count was significantly higher in SD compared to NR media ($p = 0.002$).

3.3.3 Metabolic profile of *Histomonas meleagridis* and undefined bacterial populations in Dwyer's media with and without rice

From the intracellular metabolic analysis of samples collected from SD and NR media, there was a total of 170 metabolites identified (Fig. 3.3). The heatmap was used for visualization of the metabolite fold changes between the SD and NR media throughout the various time points. The greatest magnitude of change between the metabolite relative abundances is evident from 66-142 HPI, as indicated by the brightness of the fold changes in the heatmap, which is consistent with the greatest changes in magnitude of the *H. meleagridis* growth curve. Interestingly, almost all of the identified metabolites decreased in NR media compared to SD media at 66-142 HPI.

From the heat map, there is an interesting trend for the samples collected for the blank and 0 timepoint between SD and NR. Though the majority of detected

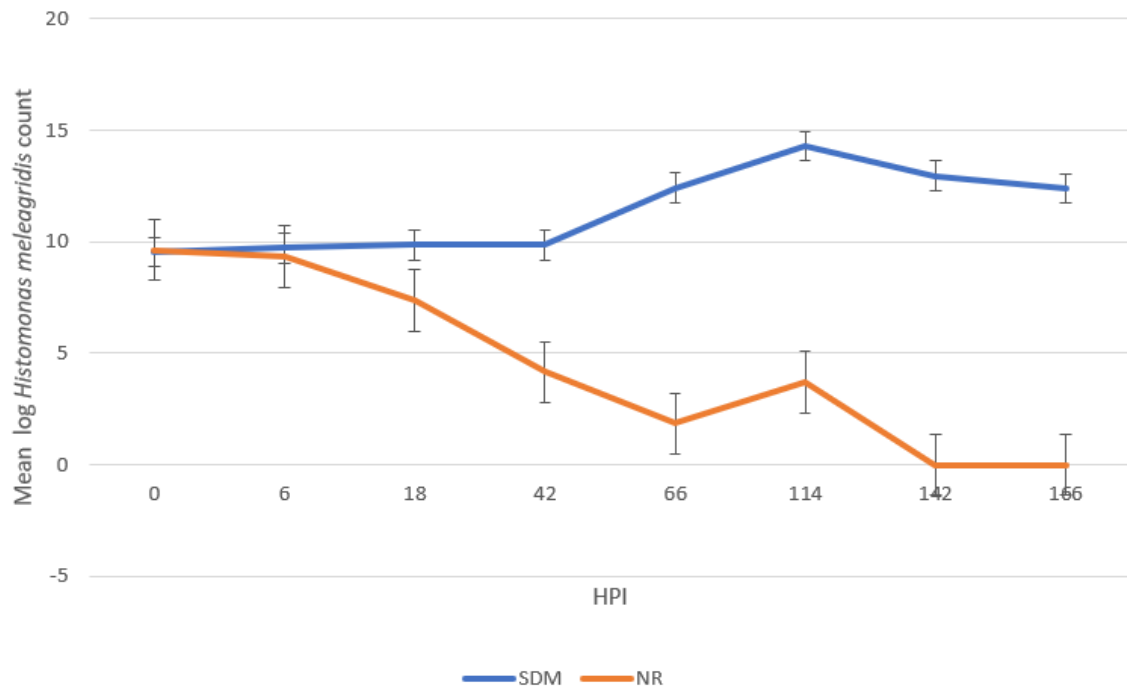


Figure 3. 1 Growth curve of *Histomonas meleagridis* grown in Dwyer's media with (SDM) and without (NR) rice starch. The mean of the log values is represented on the vertical axis and the hours post inoculation (HPI) on the horizontal axis.

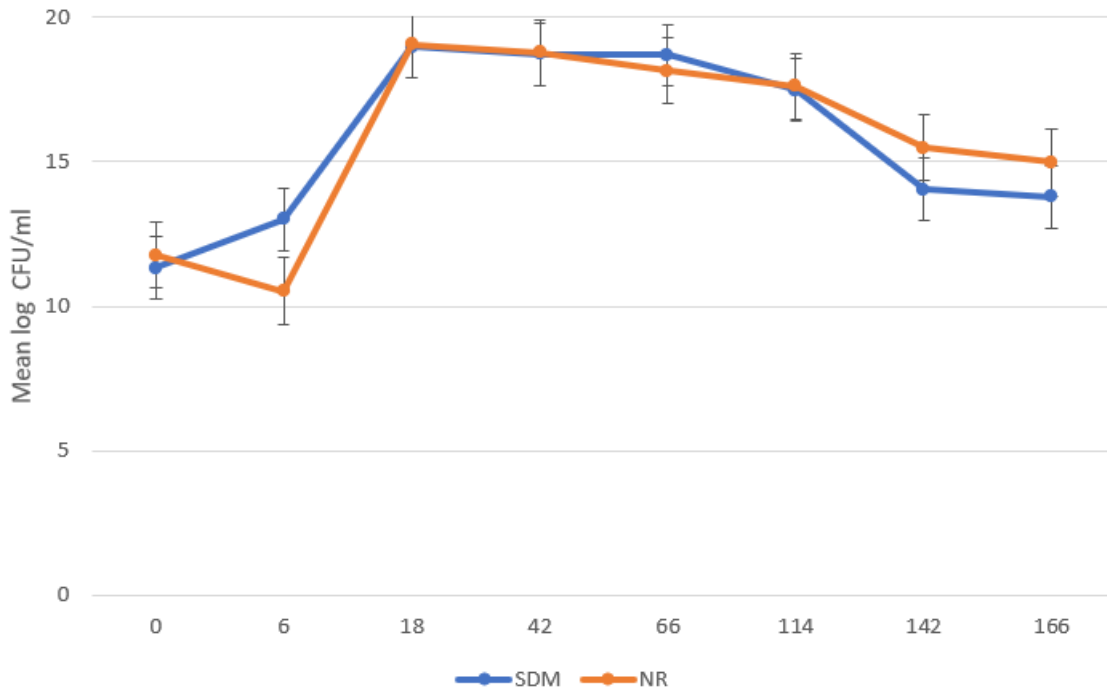
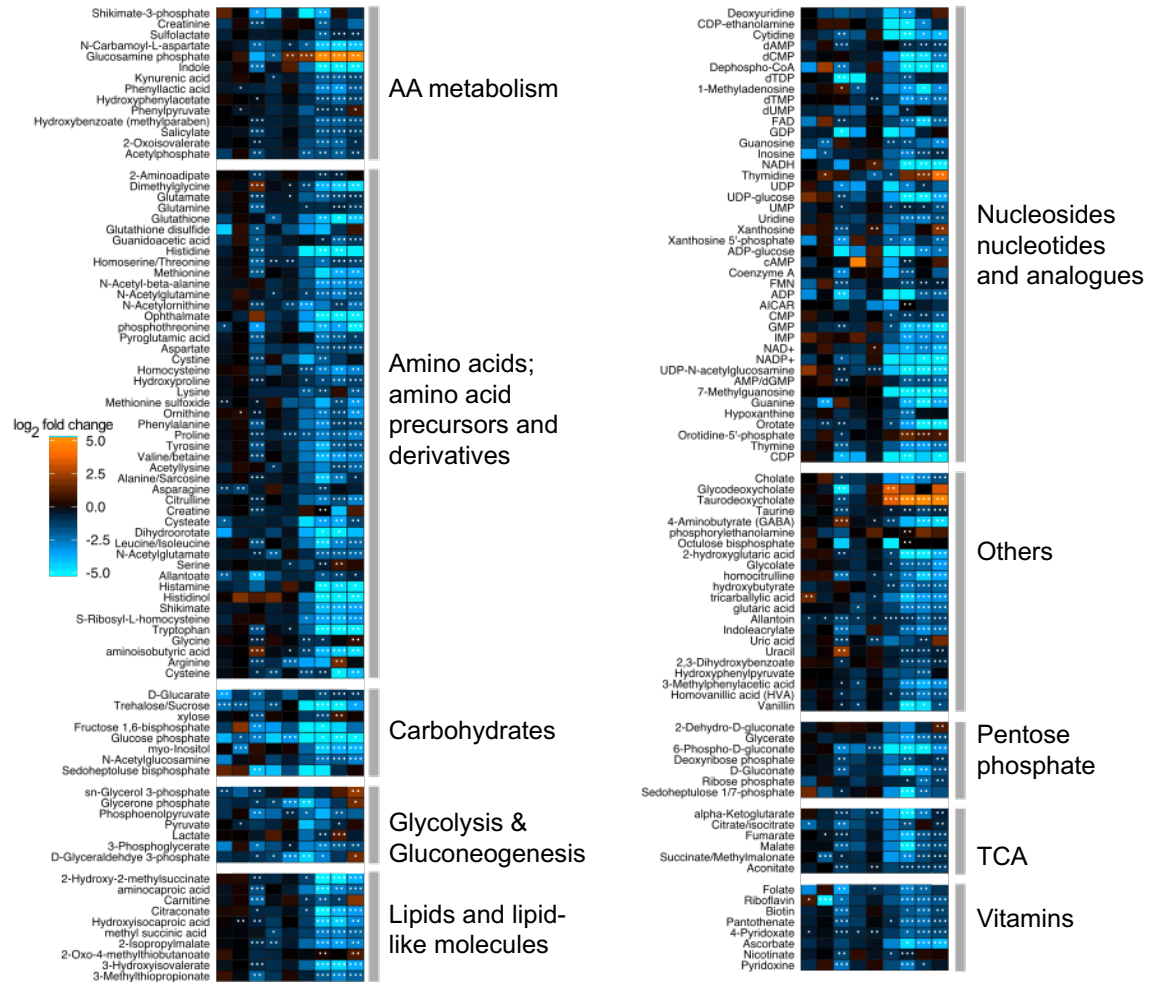


Figure 3.2 Growth curve of undefined bacteria in *H. meleagridis* cultures using Dwyer's media with (SDM) and without (NR) rice starch. The mean of the log values is represented on the vertical axis and the hours post inoculation (HPI) on the horizontal axis. CFU is colony forming unit.

Figure 3.3 Heatmap of intracellular metabolites of *Histomonas meleagridis* and undefined bacteria in Dwyer's media with (SD) and without (NR) rice starch showing the change in relative abundance of metabolites between the two media at various timepoints. Fold change equals \log_2 (average relative abundance for NR / average relative abundance for SD). Orange indicates metabolite has higher relative abundance in NR treatment, while blue indicates the metabolite has lower abundance in NR treatment, and black represents metabolite that do not change in relative abundance between the two treatments. The brightness represents the magnitude of change. P-values indicate if the change in relative metabolite abundance is significantly different between media conditions as follows, * ≤ 0.1 , ** ≤ 0.05 , * ≤ 0.01 . NR is no rice media, SD is standard Dwyer's media, AA is amino acids and TCA is tricarboxylic acid cycle.**



metabolites are not significantly different at these timepoints, it is still noteworthy that some metabolites are significantly different. That was further investigated using PLS-DA to identify differences in the metabolic profiles and the metabolites responsible for driving these differences (Fig. 3.4). There were distinct metabolic profiles between SD and NR media for the blank and 0 HPI as indicated in Fig. 3.4 by visual separation of groups. From this PLS-DA analysis, all detected metabolites are assigned a variable importance in projection (VIP) score and any metabolite with a VIP score > 1 significantly contributes to the separation of groups and drives the differences in the metabolic profiles. Riboflavin was the metabolite with the highest VIP score in the comparison for the blank and 0 HPI (Fig. 3.5).

3.4 Discussion

Histomonosis is a reemerging disease caused by infection of the parasite *H. meleagridis* and poses a serious threat to the poultry industry.¹⁸⁶ *H. meleagridis* infection is most problematic in turkeys and chickens, with nearly a 100% mortality rate in turkeys. If one bird in a flock becomes infected, within two weeks, the entire flock could be infected leading to the loss of an entire flock.¹⁷¹ Previously, histomonosis was well controlled by nitroimidazoles and nitrofurans. During this period, the amount of research on *H. meleagridis* significantly decreased. However, in recent years, these drugs used for the treatment and prevention of *H. meleagridis* have been banned for use in animals used for food production due to consumer safety concerns. The reemergence of *H. meleagridis* infection, along with the potential impact of economic loss infection poses, has encouraged more research in the last few years. One specific avenue of research has focused on gaining a better understanding of *H. meleagridis* nutrient requirements. However, this is complicated by the inability to grow axenic cultures of *H. meleagridis*, as it is a parasite that depends on the host for survival. Understanding the specific nutrient requirements would greatly advance the current knowledge of *H. meleagridis* and potentially lead to new preventative or treatment methods for *H. meleagridis* infection as studies on axenic *H. meleagridis* would be possible. Lab experiments studying *H. meleagridis* use Dwyer's media containing rice starch, and is known that *H. meleagridis* will not grow if the rice starch is omitted from the media.¹⁸⁰ Therefore, this study was conducted to investigate the metabolome of *H. meleagridis* grown in Dwyer's media with and without rice starch in order to gain a deeper understanding of why *H. meleagridis* will not grow when rice starch is omitted from the media, which would provide insight into specific nutrient requirements of *H. meleagridis*.

Dwyer's media has been used since the 1970s for cultivation of *Histomonas meleagridis* and is the routinely used media in most laboratories

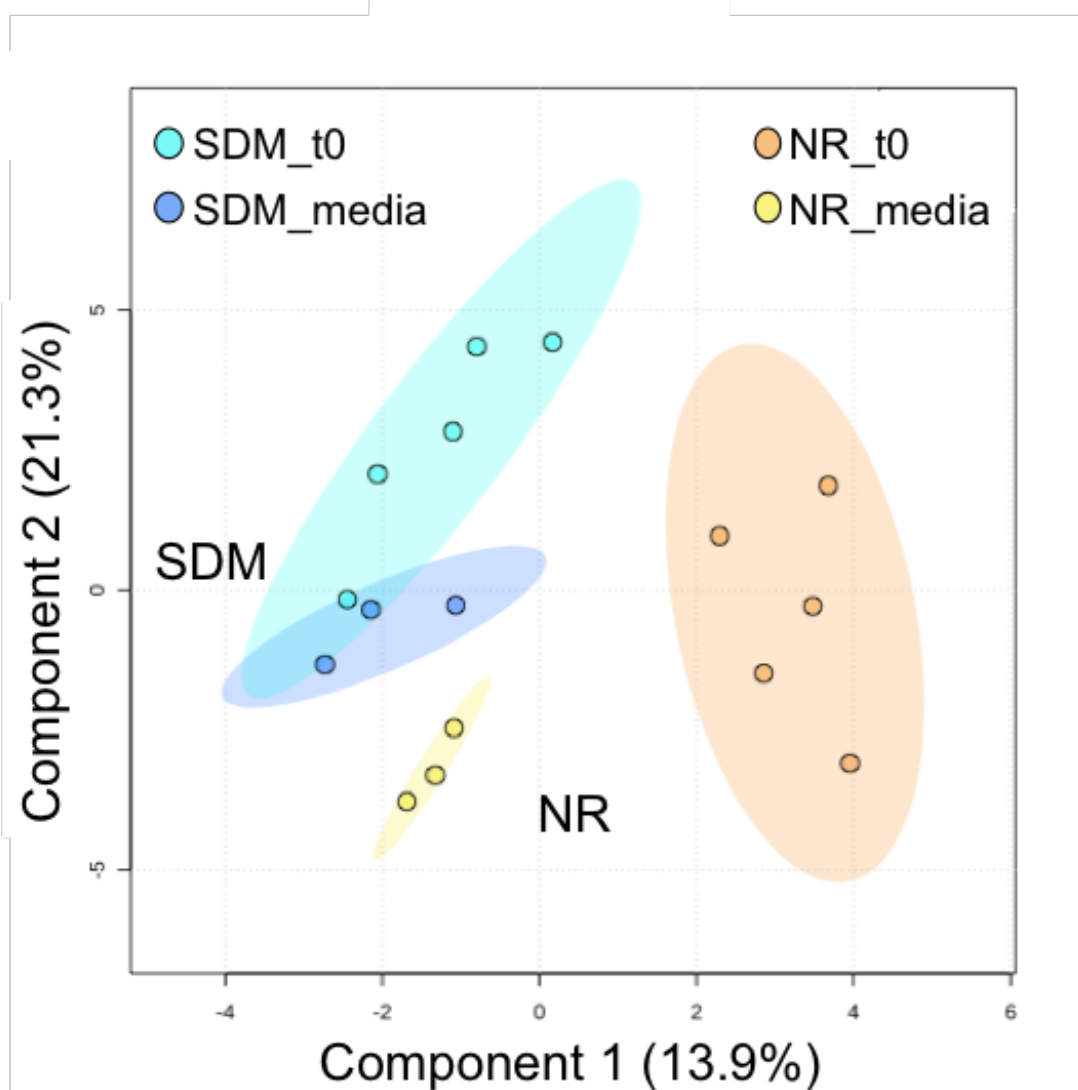


Figure 3.4 Partial least squares discriminant analysis (PLS-DA) of metabolites in Dwyer's media with (SD) and without (NR) rice inoculated with *H. meleagridis* and undefined bacterial population at blank and 0 HPI (t0). Ellipse represents 95% confidence interval.

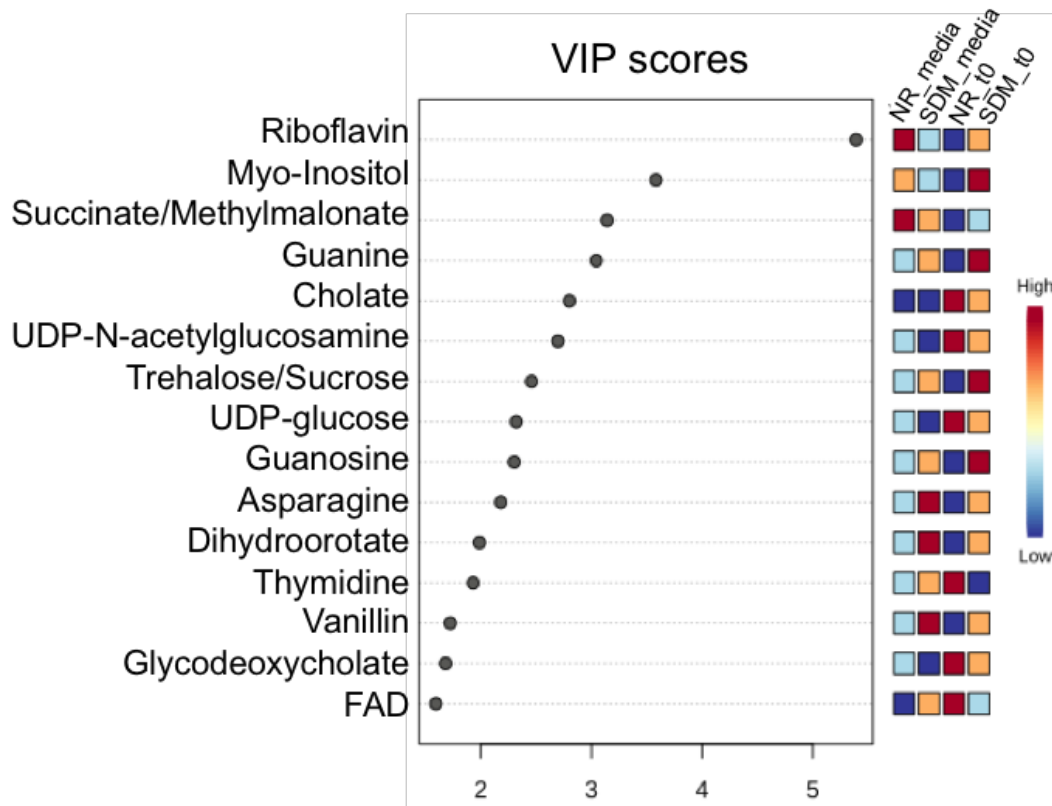


Figure 3.5 Variable importance in projection (VIP) scores for the top 15 metabolites contributing most to the differences in the metabolic profile between Dwyer's media with and without rice inoculated with *H. meleagridis* and undefined bacteria in the media blank and 0 HPI. Metabolites with a VIP score over 1 are driving the separation in the PLS-DA plot. Riboflavin has the highest VIP score in all 5 components (5.3907-1.1438).

today with minor modifications.¹⁷⁹ In this study, a modified formula of the original Dwyer's media recipe was used to cultivate *H. meleagridis*. This modified recipe contains rice starch and no chick embryo extract. It has been confirmed that rice starch is an impurity and rice granules' size have some implications on the *H. meleagridis* yield in media.¹⁸¹ In this study, a global metabolomics analysis of the *H. meleagridis* intracellular metabolome grown in Dwyer's media with or without rice was compared to investigate the role of rice starch in media. It is important to note that these cultures contained undefined bacteria that was inoculated in media from when the *Histomonas* strain was originally isolated through obtaining a cecal swab from an infected bird. Although the biomass in the cultures consisted of *H. meleagridis* and the bacteria, the heat map shows that it is likely that *H. meleagridis* is responsible for driving the changes in the metabolic profile as the metabolite fold changes and greatly correspond to the growth curve of *H. meleagridis*. Specifically, from 114-166 HPI nearly all detected metabolites are significantly less abundant in NR which is indicative of the lack of *H. meleagridis* growth.

Researchers propose a mutualistic relationship between *Histomonas* and bacteria as opposed to a predator-prey relationship.¹⁸⁴ From the current study, it is proposed that the bacteria may be playing a role in providing the *Histomonas* with riboflavin (B₂) which is required for many biological processes in the cell as flavins are crucial for energy metabolism and fatty acid oxidation. Riboflavin is a water-soluble vitamin that can be found in three forms, non-phosphorylated riboflavin that is not incorporated with protein and found in the intestine of animals, flavin mononucleotide (FMN) that is taken up by enterocytes and transferred to the liver on albumin where it is incorporated into flavoproteins or metabolized into flavin adenine dinucleotide (FAD) that is incorporated into flavoproteins in the liver.¹⁸⁷ Although riboflavin is present in the intestine and animal cells have specialized transporter proteins, mammalian cells are not capable of synthesizing riboflavin and depend completely on uptake of it from the intestine. Microbiota residing in the intestinal tract of animals are capable of synthesizing riboflavin, and studies have indicated that gut microbes can play important roles in providing micronutrients like vitamin B₂.¹⁸⁸ Bacteria are capable of acquiring vitamin B₂ through two different mechanisms: either through a specific riboflavin biosynthetic pathway (RBP) or through using specialized importer proteins if the riboflavin is abundant in its microenvironment thus saving energy.^{189, 190} However, it has been shown that if riboflavin is environmentally available, bacteria will shut down riboflavin biosynthesis because bacteria prefer to import exogenous riboflavin to save on energy.¹⁹¹

Additionally, bacterial secreted flavins are key metabolites in a variety of physiological processes in pro and eukaryotes.¹⁹⁰ A deficiency in riboflavin would inhibit cellular growth and metabolism as FMN and FAD synthesis would be inhibited. This could explain the decreased abundance of nearly all metabolites in the NR treatment on the heatmap. FMN and FAD act as important cofactors and play a major role in energy metabolism, cellular function, growth and development,

neurotransmitters metabolism and metabolism of carbohydrates.^{190, 192} In fact, deficiency of vitamin B₂ in birds presents as neurological symptoms.¹⁹³ It is likely that *H. meleagridis* requires riboflavin for its biological processes and depends on bacteria to provide this essential component as it's known that parasites in the gut depend on bacterial hosts for riboflavin. It was observed in this experiment that riboflavin was higher in NR media than SD only in blank samples. The media used in this experiment was prepared in clean non-sterile conditions and although the bacteria in blank samples was less than our ability to detect, media left in incubator for the next day changes in color without the addition of any histomonads. This means the media have living bacteria. The increase in riboflavin in NR media may be attributed to the lack of external source of riboflavin for the bacteria. In response, the bacteria could be actively synthesizing it. In the SD media, the white rice starch is a good source of riboflavin providing an environment rich in riboflavin precursors for the bacteria.¹⁹⁴ However, the addition of *Histomonas* in cultures causes increase in the requirements for riboflavin which is could be followed by increase riboflavin synthesis by the bacteria. It is clear that in SD media, the riboflavin amount corresponds to the *Histomonas* growth and that decline in bacterial populations at 114 HPI is followed by *Histomonas* decline at 142HPI (Fig. 3.6). Higher abundance of a metabolite may be due to one of two factors, increased production of the metabolite or decreased consumption. With respect to the importance of riboflavin in cells, it is proposed that riboflavin is excessively produced by the bacteria to benefit both the bacterial and *Histomonas* cells. Labeled isotope tracing experiments may be helpful in investigating this proposal.

There is little is known about the growth requirement of *H. meleagridis*. However, it has been shown that *H. meleagridis* depends on bacteria in vitro, as in vivo studies have observed that *H. meleagridis* will only cause lesions in chicken if bacteria is present.¹⁹⁵ This supports the idea that *H. meleagridis* relies on the bacteria to provide riboflavin, which is a necessity for energy metabolism. In addition, it is unknown if *H. meleagridis* has the necessary cellular machinery to synthesize riboflavin or if it completely dependent on the host to fulfill its riboflavin requirements.

H. meleagridis infects the ceca and liver of birds¹⁹⁶, and the highest concentration of riboflavin is found in these two organs. In these organs, riboflavin is either produced by bacteria in gut or carried on various proteins to the liver. *H. meleagridis* may be competing with the host on these essential nutrients. That may explain the weakness and dullness seen in the birds infected with the parasite¹⁹⁷ as they could experience riboflavin depletion. More specifically, *H. meleagridis* causes lesions in bird ceca and it was found that the cecum of turkeys and chickens have double the riboflavin amount compared to the rest of the intestine.¹⁹⁸ However, fecal material from cecectomized birds contained approximately the same content as in normal birds.¹⁹⁸ Laying hens transfer riboflavin into the yolk and albumen then to embryos. Liver and eggs are an important source of Vitamin B₂ and the chicken embryo extract was used in *Histomonas* culture media for a

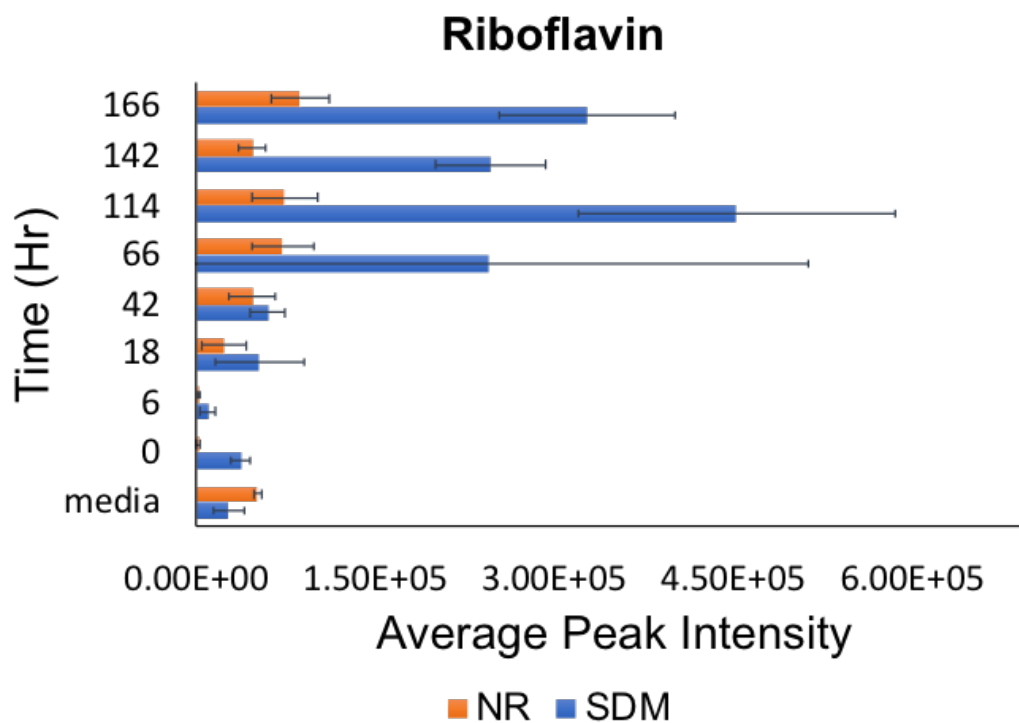


Figure 3.6 Average peak intensity vs time for riboflavin in Dwyer’s media with (SD) and without (NR) rice before (media) and after inoculation with *H. meleagridis* and undefined bacteria showing an increase in SDM from t0-t166 hours.

long time to replace the hamster liver¹⁷⁹, which further supports our hypothesis that *Histomonas* cannot grow in the absence of rice starch from SD media due to the lack of riboflavin.

3.5 Methods

3.5.1 *Histomonas meleagridis* strain preparation

Histomonas meleagridis strain used is UGA-Histo strain isolated from a domestic turkey in Georgia, US. The isolate was propagated on Dwyer's media (M199, sodium bicarbonate, rice starch and inactivated horse serum) at 40 C in our laboratory and passed multiple times. The isolates were cryopreserved in liquid nitrogen and successfully resuscitated for various experiments.

The strain was incubated in Dwyer's media (SD) at 40-42°C to reach logarithmic growth (after 48-72 hours) in 21 T25 flasks. Then, the contents of T25 flasks were transferred with a plastic pipette to a 500 mL tube. Histomonads were counted in the 500 mL tube using hemocytometer. The tube was centrifuged at 200xg for 2 minutes and the supernatant was discarded. The pellet was resuspended in warm 50 mL Dwyer's media with no rice added (NR), centrifuged and the supernatant was discarded. This washing step was repeated one more time before final resuspension in ten mL of warm NR media. One mL of the final suspension (count adjusted to 109.9875×10^4 cells/ mL) was added to each of ten T75 flasks full of 100 mL of either SD (five flasks) or NR media (five flasks). The flasks were then immediately sampled (zero sample) and incubated at 40-42°C for the rest of the experiment.

3.5.2 Sample collection and preparation

Three T75 flasks were sampled from each treatment (six flasks total) before inoculating them with *Histomonas meleagridis* to be used as blanks. Then all the flasks were sampled immediately after *H. meleagridis* inoculation (zero timepoint) and at 6, 18, 42, 66, 114, 142 and 166 hours post inoculation (HPI).

Four mL of each T75 flask were filtered through Whatman® Nuclepore™ Track-Etched Membranes with a 0.4 µm pore size (Sigma Millipore, US). The filter was then folded with the cell carrying surface inside in a 2 mL cryovial and flash frozen in liquid nitrogen. The cryovials were stored in -80°C until the extraction process. Global metabolomics analysis was performed at the Biological and Small Molecule Mass Spectrometry Core (BSMMSC), University of Tennessee, Knoxville, TN (RRID: SCR_021368). Using an acidic acetonitrile extraction procedure, metabolites were extracted from the filters using methanol, acetonitrile, and water (2:2:1) with 0.1% formic acid. A Synergy Hydro-RP column (100 × 2 mm, 2.5 µm particle size) was used to separate metabolites based on retention time, with 10 µL of sample injected into the Dionex UltiMate 3000 UPLC system (Thermo Fisher Scientific, Waltham, MA). An Exactive™ Plus Orbitrap MS (Thermo Fisher Scientific, Waltham, MA) was used for mass spectral analysis with

negative mode electrospray ionization, using an established ultra-high-performance liquid chromatography high resolution mass spectrometry (UHPLC-HRMS) global metabolomics method of water-soluble metabolites method.^{166, 199}

H. meleagridis count (histomonads/mL) was recorded at each time point in each flask using a hemocytometer. At each time point, 200 μ L of each flask were stored at -20°C and were used later to prepare ten-fold serial dilutions that were plated on Columbia blood agar with 5% sheep blood (Thermo Scientific™, US) to detect the bacterial colony forming unit per mL of media. Plates were incubated at 35°C in CO_2 incubator and colonies were counted after 24 hours incubation.

3.5.2 Data analysis

Growth curves of undefined bacteria and *H. meleagridis* were generated in Excel using log of values (CFU/mL for bacteria or cells/mL for *H. meleagridis*). Mixed model analysis and pairwise comparisons were performed using IBM SPSS statistics 27 to compare the different media used across various time points.

Following the preliminary mass analysis, raw spectral files were converted to mzML files using msConvert, a package from ProteoWizard.^{73, 167} These files were imported into an open-source software, Metabolomics Analysis and Visualization Engine (MAVEN), to visualize extracted ion chromatograms (EICs) for data processing, in which peak areas were integrated for each identified metabolite.^{24, 74} Metabolites were identified in MAVEN by exact mass (± 5 ppm mass accuracy) and chromatographic retention time from an in-house standard library. Peak areas were averaged for biological replicates. From these data, heatmaps and partial least squares discriminant analysis (PLS-DA) plots were generated. R (version 1.0.153) was used to generate heatmaps expressing \log_2 fold changes for each metabolite and p-values determined by a Student's T-test. Prior to performing PLS-DA analysis, the data were filtered using interquartile range (IQR), log transformed, and Pareto scaled using features in MetaboAnalyst 5.0.²⁰⁰

3.6 Conclusion

In conclusion, physiological changes are observed when rice starch is omitted from the media. Omission of rice starch inhibits *H. meleagridis* growth, yet it does not induce a change in the bacterial growth. Riboflavin is an important nutrient that may be supplemented by rice starch. Riboflavin has been reported as a requirement for axenic cultivation of the anaerobic parasitic, *Entamoeba histolytica*, a protozoan closely related to *H. meleagridis*.^{196, 201} This further supports our hypothesis that *H. meleagridis* will not grow if rice starch is omitted from the media due to a riboflavin deficiency. From these data, it can also be hypothesized that Riboflavin is required for axenic cultivation of *H. meleagridis*. Experiments on replacing rice starch with various forms and concentrations of riboflavin are warranted. If this is possible, that may allow us in the future to use

antibiotics in media and grow axenic cultures with no bacteria. That will have great implication on future research on *H. meleagridis*.

CONCLUSION

This dissertation has shown how untargeted mass spectrometry-based metabolomics can be applied to different biological systems to answer unique and complex biological questions. Untargeted metabolomics is a hypothesis generating technique and the data acquired from these studies can be used to inform future experiments. It also has shown how metabolomics is a beneficial tool for studying the gut microbiome as there is an intrinsic link between the gut microbiome and the metabolome. The metabolome is predictive of phenotype as it is dynamic and responsive environmental alterations. This makes metabolomics an attractive technique for studying the gut microbiome.

In the first chapter, a metagenomics and metabolomics approach were utilized to gain a baseline understanding of how protein supplementation impacts the gut microbiome and metabolome. This study was also used to investigate if there was a unique gut microbial and metabolomic profile that corresponded with traits energy and fatigue. Here, fecal sample were collected from both male and female young physically active adults who did and did not report consuming protein supplements. This multi-omics analysis revealed the nitrogen metabolism, specifically purine degradation, was impacted most by protein supplementation. Both uric acid and allantoin, which are purine degradation products, were increased in those who reported consuming protein. To further support this result, *Lactobacillales*, which facilitates purine absorption and uric acid decomposition, was higher in those who reported consuming protein supplements. These data suggest that consuming protein supplements impacts nitrogen metabolism, favoring the degradation of purines. Also, it was noted that traits energy and fatigue did not result in distinct fecal metabolic profiles, but *Anaerostipes* could be correlated with the traits, suggesting that energy and fatigue are unique traits that could be defined by distinct bacterial communities.

The second chapter studied the systemic impact of heat stress on the broilers. Heat stress poses a serious threat to the poultry industry with the reduction in meat quality and production. Samples were collected from the duodenum, jejunum, ileum, ileal digesta, cecal digesta, and plasma of birds. There were five different treatments: pre-heat stress (PHS), thermoneutral-control (TN-control), pair-fed (PF), acute heat stress (AHS), and cyclic heat stress (CHS). Metabolomics analysis revealed that heat stress had the greatest impact on the jejunum out of all regions analyzed. There was also a duration-dependent impact of heat stress observed, especially clear in the duodenum. For all regions and both AHS and CHS, energy metabolism was impacted. The impact of heat stress on purine metabolism was conserved throughout the study, implying that mitochondrial mediated cellular reprogramming is a response to heat stress that can lead to gut damage.

The third chapter of this dissertation investigated the essential nutrient requirements of a gut parasite *Histomonas meleagridis* (*H. meleagridis*). In recent years, *H. meleagridis* has reemerged and poses an eminent threat to the

poultry industry as there are no drugs available to prevent or treat *H. meleagridis* infection. This infection has close to a 100% mortality rate in turkeys, so there is a critical need for research regarding the gut parasite. To investigate the specific nutrient requirements for *H. meleagridis* survival, *H. meleagridis* and an undefined gut bacterial population were grown in Dwyer's media with and without rice starch because it is known that *H. meleagridis* cannot grow if rice starch is omitted from the media. Samples were collected throughout the full growth curve to analyze the metabolic profiles. It was found that omission rice starch did not significantly impact bacterial growth, though it was evident that *H. meleagridis* was not growing based off of growth curves. Metabolomics analysis revealed that riboflavin was responsible for driving the difference in metabolic profiles between the cells grown in Dwyer's media with and without rice starch. Riboflavin plays a key role in energy metabolism as it is used for the synthesis on cofactors responsible for energy metabolism. It was also noted that nearly all metabolites had a decreased relative abundance from the cells grown in Dwyer's media without rice starch, and this would be consistent with a riboflavin deficiency. These data imply that riboflavin is an essential nutrient for *H. meleagridis* growth and is required for axenic *H. meleagridis* growth.

In summary, untargeted metabolomics was used to expand the current understanding of metabolism. The first and second chapter focused on how extrinsic factors such as diet (protein supplementation and heat stress exposure) alter the gut microbial metabolism. The third study set out determine the essential nutrient requirements for a gut parasite using a metabolomics approach. Future research can expand upon these findings by designing experiments to test the hypotheses that were generated.

Moving forward, to further determine the health implications of protein supplementation on young physically active adults, serum samples should be collected. Uric acid was found to be increased in the fecal metabolome in response to protein supplementation, however, it is unknown if this is beneficial or harmful to humans. Though uric acid is a powerful antioxidant, accumulation can lead to negative health consequences such as gout. The quantification of uric acid in serum samples would allow for conclusions to be made about the impact of protein supplementation on human health. In addition, to expand upon the heat stress study, it would be beneficial to include female broiler chicks in future studies as it can be concluded from the data and results in this dissertation that mitochondrial mediated cellular reprogramming could be a response to heat stress that leads to gut damage. There is a growing amount of evidence showing sexual dimorphisms in mitochondrial function in diseases such as neurological diseases, cardiovascular diseases, and metabolic diseases. Therefore, it is important to determine if the metabolic impacts of heat stress on mitochondrial function is consistent between males and females. Lastly, to determine if riboflavin is an essential nutrient requirement for *H. meleagridis* growth, as the data described here suggest, additional experiments should be conducted to analyze *H. meleagridis* growth in Dwyer's media with rice starch omitted and

riboflavin supplemented. It would also be beneficial to sequence the genome of *H. meleagridis* to determine if *H. meleagridis* has the cellular machinery necessary for synthesizing riboflavin.

REFERENCES

1. Guinane, C. M.; Cotter, P. D., Role of the gut microbiota in health and chronic gastrointestinal disease: understanding a hidden metabolic organ. *Therap Adv Gastroenterol* **2013**, *6* (4), 295-308.
2. Thursby, E.; Juge, N., Introduction to the human gut microbiota. *Biochemical Journal* **2017**, *474* (11), 1823-1836.
3. Bull, M. J.; Plummer, N. T., Part 1: The Human Gut Microbiome in Health and Disease. *Integr Med (Encinitas)* **2014**, *13* (6), 17-22.
4. Gomma, E. Z., Human gut microbiota/microbiome in health and diseases: a review. *Antonie van Leeuwenhoek* **2020**, *113* (12), 2019-2040.
5. Shreiner, A. B.; Kao, J. Y.; Young, V. B., The gut microbiome in health and in disease. *Curr Opin Gastroenterol* **2015**, *31* (1), 69-75.
6. Makki, K.; Deehan, E. C.; Walter, J.; Bäckhed, F., The Impact of Dietary Fiber on Gut Microbiota in Host Health and Disease. *Cell Host & Microbe* **2018**, *23* (6), 705-715.
7. Carding, S.; Verbeke, K.; Vipond, D. T.; Corfe, B. M.; Owen, L. J., Dysbiosis of the gut microbiota in disease. *Microbial Ecology in Health and Disease* **2015**, *26* (1), 26191.
8. Leeming, E. R.; Johnson, A. J.; Spector, T. D.; Le Roy, C. I., Effect of Diet on the Gut Microbiota: Rethinking Intervention Duration. *Nutrients* **2019**, *11* (12).
9. Zhang, C.; Zhang, M.; Wang, S.; Han, R.; Cao, Y.; Hua, W.; Mao, Y.; Zhang, X.; Pang, X.; Wei, C., Interactions between gut microbiota, host genetics and diet relevant to development of metabolic syndromes in mice. *ISME J* **2010**, *4* (2), 232-241.
10. David, L. A.; Materna, A. C.; Friedman, J.; Campos-Baptista, M. I.; Blackburn, M. C.; Perrotta, A.; Erdman, S. E.; Alm, E. J., Host lifestyle affects human microbiota on daily timescales. *Genome biology* **2014**, *15* (7), 1-15.
11. Sonnenburg, J. L.; Bäckhed, F., Diet–microbiota interactions as moderators of human metabolism. *Nature* **2016**, *535* (7610), 56-64.
12. Wu, G. D.; Chen, J.; Hoffmann, C.; Bittinger, K.; Chen, Y.-Y.; Keilbaugh, S. A.; Bewtra, M.; Knights, D.; Walters, W. A.; Knight, R., Linking long-term dietary patterns with gut microbial enterotypes. *Science* **2011**, *334* (6052), 105-108.
13. David, L. A.; Maurice, C. F.; Carmody, R. N.; Gootenberg, D. B.; Button, J. E.; Wolfe, B. E.; Ling, A. V.; Devlin, A. S.; Varma, Y.; Fischbach, M. A., Diet rapidly and reproducibly alters the human gut microbiome. *Nature* **2014**, *505* (7484), 559-563.
14. Walker, A. W.; Ince, J.; Duncan, S. H.; Webster, L. M.; Holtrop, G.; Ze, X.; Brown, D.; Stares, M. D.; Scott, P.; Bergerat, A., Dominant and diet-responsive groups of bacteria within the human colonic microbiota. *ISME J* **2011**, *5* (2), 220-230.

15. Byerley, L. O.; Gallivan, K. M.; Christopher, C. J.; Taylor, C. M.; Luo, M.; Dowd, S. E.; Davis, G. M.; Castro, H. F.; Campagna, S. R.; Ondrak, K. S., Gut Microbiome and Metabolome Variations in Self-Identified Muscle Builders Who Report Using Protein Supplements. *Nutrients* **2022**, *14* (3), 533.
16. Kårlund, A.; Gómez-Gallego, C.; Turpeinen, A. M.; Palo-oja, O.-M.; El-Nezami, H.; Kolehmainen, M., Protein Supplements and Their Relation with Nutrition, Microbiota Composition and Health: Is More Protein Always Better for Sportspeople? *Nutrients* **2019**, *11* (4), 829.
17. Rostagno, M. H., Effects of heat stress on the gut health of poultry. *Journal of Animal Science* **2020**, *98* (4).
18. Liu, Z.; Sun, X.; Tang, J.; Tang, Y.; Tong, H.; Wen, Q.; Liu, Y.; Su, L., Intestinal inflammation and tissue injury in response to heat stress and cooling treatment in mice. *Mol Med Rep* **2011**, *4* (3), 437-443.
19. Naveed, A.; Abdullah, S., Impact of parasitic infection on human gut ecology and immune regulations. *Translational Medicine Communications* **2021**, *6* (1), 11.
20. Riekeberg, E.; Powers, R., New frontiers in metabolomics: from measurement to insight. *F1000Res* **2017**, *6*, 1148.
21. Patti, G. J.; Yanes, O.; Siuzdak, G., Innovation: Metabolomics: the apogee of the omics trilogy. *Nat Rev Mol Cell Biol* **2012**, *13* (4), 263-269.
22. Koal, T.; Deigner, H.-P., Challenges in mass spectrometry based targeted metabolomics. *Current molecular medicine* **2010**, *10* (2), 216-226.
23. Caudy, W. L. M. F. C. E. M. D. A.-N. A. A., Metabolomic Analysis via Reversed-Phase Ion-Pairing Liquid Chromatography Coupled to a Stand Alone Orbitrap Mass Spectrometer. *Anal. Chem* **2010**, *82* (8), 3212-3221.
24. Clasquin, M. F.; Melamud, E.; Rabinowitz, J. D., LC-MS data processing with MAVEN: a metabolomic analysis and visualization engine. *Curr Protoc Bioinformatics* **2012**, *Chapter 14*, Unit14.11.
25. Pang, Z.; Chong, J.; Zhou, G.; de Lima Morais, D. A.; Chang, L.; Barrette, M.; Gauthier, C.; Jacques, P.-É.; Li, S.; Xia, J., MetaboAnalyst 5.0: narrowing the gap between raw spectra and functional insights. *Nucleic Acids Research* **2021**, *49* (W1), W388-W396.
26. Viant, M. R.; Kurland, I. J.; Jones, M. R.; Dunn, W. B., How close are we to complete annotation of metabolomes? *Current Opinion in Chemical Biology* **2017**, *36*, 64-69.
27. Clarke, S. F.; Murphy, E. F.; O'Sullivan, O.; Lucey, A. J.; Humphreys, M.; Hogan, A.; Hayes, P.; O'Reilly, M.; Jeffery, I. B.; Wood-Martin, R.; Kerins, D. M.; Quigley, E.; Ross, R. P.; O'Toole, P. W.; Molloy, M. G.; Falvey, E.; Shanahan, F.; Cotter, P. D., Exercise and associated dietary extremes impact on gut microbial diversity. *Gut* **2014**, *63* (12), 1913-20.
28. Tu, P.; Bian, X.; Chi, L.; Gao, B.; Ru, H.; Knobloch, T. J.; Weghorst, C. M.; Lu, K., Characterization of the Functional Changes in Mouse Gut Microbiome Associated with Increased Akkermansia muciniphila Population Modulated by Dietary Black Raspberries. *ACS Omega* **2018**, *3* (9), 10927-10937.

29. Conlon, M. A.; Bird, A. R., The Impact of Diet and Lifestyle on Gut Microbiota and Human Health. *Nutrients* **2015**, *7* (1), 17-44.
30. Mazidi, M.; Rezaie, P.; Kengne, A. P.; Mobarhan, M. G.; Ferns, G. A., Gut microbiome and metabolic syndrome. *Diabetes & Metabolic Syndrome: Clinical Research & Reviews* **2016**, *10* (2, Supplement 1), S150-S157.
31. Subramanian, I.; Verma, S.; Kumar, S.; Jere, A.; Anamika, K., Multi-omics Data Integration, Interpretation, and Its Application. *Bioinform Biol Insights* **2020**, *14*, 1177932219899051.
32. Garthe, I.; Maughan, R. J., Athletes and Supplements: Prevalence and Perspectives. *Int J Sport Nutr Exerc Metab* **2018**, *28* (2), 126-138.
33. Messina, M.; Lynch, H.; Dickinson, J. M.; Reed, K. E., No Difference Between the Effects of Supplementing With Soy Protein Versus Animal Protein on Gains in Muscle Mass and Strength in Response to Resistance Exercise. *Int J Sport Nutr Exerc Metab* **2018**, *28* (6), 674-685.
34. Cronin, O.; Barton, W.; Skuse, P.; Penney, N. C.; Garcia-Perez, I.; Murphy, E. F.; Woods, T.; Nugent, H.; Fanning, A.; Melgar, S.; Falvey, E. C.; Holmes, E.; Cotter, P. D.; O'Sullivan, O.; Molloy, M. G.; Shanahan, F., A Prospective Metagenomic and Metabolomic Analysis of the Impact of Exercise and/or Whey Protein Supplementation on the Gut Microbiome of Sedentary Adults. *mSystems* **2018**, *3* (3).
35. Clauss, M.; Gérard, P.; Mosca, A.; Leclerc, M., Interplay Between Exercise and Gut Microbiome in the Context of Human Health and Performance. *Front Nutr* **2021**, *8*, 637010.
36. Clark, A.; Mach, N., Exercise-induced stress behavior, gut-microbiota-brain axis and diet: a systematic review for athletes. *Journal of the International Society of Sports Nutrition* **2016**, *13* (1), 43.
37. Boolani, A.; Manierre, M., An exploratory multivariate study examining correlates of trait mental and physical fatigue and energy. *Fatigue: Biomedicine, Health & Behavior* **2019**, *7* (1), 29-40.
38. O'Connor, P. J.; Kennedy, D. O.; Stahl, S., Mental energy: plausible neurological mechanisms and emerging research on the effects of natural dietary compounds. *Nutr Neurosci* **2021**, *24* (11), 850-864.
39. Baguley, B. J.; Skinner, T. L.; Jenkins, D. G.; Wright, O. R. L., Mediterranean-style dietary pattern improves cancer-related fatigue and quality of life in men with prostate cancer treated with androgen deprivation therapy: A pilot randomised control trial. *Clin Nutr* **2021**, *40* (1), 245-254.
40. Medicine, I. o., *Dietary Reference Intakes for Energy, Carbohydrate, Fiber, Fat, Fatty Acids, Cholesterol, Protein, and Amino Acids*. The National Academies Press: Washington, DC, 2005; p 1358.
41. Jang, L. G.; Choi, G.; Kim, S. W.; Kim, B. Y.; Lee, S.; Park, H., The combination of sport and sport-specific diet is associated with characteristics of gut microbiota: an observational study. *J Int Soc Sports Nutr* **2019**, *16* (1), 21.

42. Medicine, I. o., *Dietary Reference Intakes for Energy, Carbohydrate, Fiber, Fat, Fatty Acids, Cholesterol, Protein, and Amino Acids*. The National Academies Press: Washington, DC, 2005.
43. Thomas, D. T.; Erdman, K. A.; Burke, L. M., Position of the Academy of Nutrition and Dietetics, Dietitians of Canada, and the American College of Sports Medicine: Nutrition and Athletic Performance. *J Acad Nutr Diet* **2016**, *116* (3), 501-528.
44. Gibson, J. A.; Sladen, G. E.; Dawson, A. M., Protein absorption and ammonia production: the effects of dietary protein and removal of the colon. *Br J Nutr* **1976**, *35* (1), 61-5.
45. Yao, C. K.; Muir, J. G.; Gibson, P. R., Review article: insights into colonic protein fermentation, its modulation and potential health implications. *Aliment Pharmacol Ther* **2016**, *43* (2), 181-96.
46. Laitinen, K.; Morkkala, K., Overall Dietary Quality Relates to Gut Microbiota Diversity and Abundance. *Int J Mol Sci* **2019**, *20* (8).
47. Rettedal, E. A.; Cree, J. M. E.; Adams, S. E.; MacRae, C.; Skidmore, P. M. L.; Cameron-Smith, D.; Gant, N.; Blenkiron, C.; Merry, T. L., Short-term high-intensity interval training exercise does not affect gut bacterial community diversity or composition of lean and overweight men. *Exp Physiol* **2020**, *105* (8), 1268-1279.
48. Tzemah Shahar, R.; Koren, O.; Matarasso, S.; Shochat, T.; Magzal, F.; Agmon, M., Attributes of Physical Activity and Gut Microbiome in Adults: A Systematic Review. *Int J Sports Med* **2020**, *41* (12), 801-814.
49. Das, B.; Ghosh, T. S.; Kedia, S.; Rampal, R.; Saxena, S.; Bag, S.; Mitra, R.; Dayal, M.; Mehta, O.; Surendranath, A.; Travis, S. P. L.; Tripathi, P.; Nair, G. B.; Ahuja, V., Analysis of the Gut Microbiome of Rural and Urban Healthy Indians Living in Sea Level and High Altitude Areas. *Sci Rep* **2018**, *8* (1), 10104.
50. Walter, J.; Ley, R., The human gut microbiome: ecology and recent evolutionary changes. *Annu Rev Microbiol* **2011**, *65*, 411-29.
51. Parada Venegas, D.; De la Fuente, M. K.; Landskron, G.; Gonzalez, M. J.; Quera, R.; Dijkstra, G.; Harmsen, H. J. M.; Faber, K. N.; Hermoso, M. A., Short Chain Fatty Acids (SCFAs)-Mediated Gut Epithelial and Immune Regulation and Its Relevance for Inflammatory Bowel Diseases. *Front Immunol* **2019**, *10*, 277.
52. Yamauchi, T.; Oi, A.; Kosakamoto, H.; Akuzawa-Tokita, Y.; Murakami, T.; Mori, H.; Miura, M.; Obata, F., Gut Bacterial Species Distinctively Impact Host Purine Metabolites during Aging in Drosophila. *iScience* **2020**, 101477.
53. Hsieh, M.-W.; Chen, H.-Y.; Tsai, C.-C., Screening and Evaluation of Purine-Nucleoside-Degrading Lactic Acid Bacteria Isolated from Winemaking Byproducts In Vitro and Their Uric Acid-Lowering Effects In Vivo. *Fermentation* **2021**, *7* (2), 74.

54. Chen, Y.-r.; Zheng, H.-m.; Zhang, G.-x.; Chen, F.-l.; Chen, L.-d.; Yang, Z.-c., High Oscillospira abundance indicates constipation and low BMI in the Guangdong Gut Microbiome Project. *Scientific Reports* **2020**, *10* (1), 9364.
55. Gophna, U.; Konikoff, T.; Nielsen, H. B., Oscillospira and related bacteria - From metagenomic species to metabolic features. *Environ Microbiol* **2017**, *19* (3), 835-841.
56. Wu, F.; Guo, X.; Zhang, J.; Zhang, M.; Ou, Z.; Peng, Y., Phascolarctobacterium faecium abundant colonization in human gastrointestinal tract. *Exp Ther Med* **2017**, *14* (4), 3122-3126.
57. Furuhashi, M., New insights into purine metabolism in metabolic diseases: role of xanthine oxidoreductase activity. *American Journal of Physiology-Endocrinology and Metabolism* **2020**, *319* (5), E827-E834.
58. Yu, Y.; Liu, Q.; Li, H.; Wen, C.; He, Z., Alterations of the Gut Microbiome Associated With the Treatment of Hyperuricaemia in Male Rats. *Front Microbiol* **2018**, *9*, 2233.
59. Villegas, R.; Xiang, Y. B.; Elasy, T.; Xu, W. H.; Cai, H.; Cai, Q.; Linton, M. F.; Fazio, S.; Zheng, W.; Shu, X. O., Purine-rich foods, protein intake, and the prevalence of hyperuricemia: the Shanghai Men's Health Study. *Nutr Metab Cardiovasc Dis* **2012**, *22* (5), 409-16.
60. Nishino, T.; Okamoto, K., Mechanistic insights into xanthine oxidoreductase from development studies of candidate drugs to treat hyperuricemia and gout. *JBIC Journal of Biological Inorganic Chemistry* **2015**, *20* (2), 195-207.
61. Vacca, M.; Celano, G.; Calabrese, F. M.; Portincasa, P.; Gobbetti, M.; De Angelis, M., The Controversial Role of Human Gut Lachnospiraceae. *Microorganisms* **2020**, *8* (4).
62. Loy, B. D.; Cameron, M. H.; O'Connor, P. J., Perceived fatigue and energy are independent unipolar states: Supporting evidence. *Med Hypotheses* **2018**, *113*, 46-51.
63. Subar, A. F.; Kirkpatrick, S. I.; Mittl, B.; Zimmerman, T. P.; Thompson, F. E.; Bingley, C.; Willis, G.; Islam, N. G.; Baranowski, T.; McNutt, S.; Potischman, N., The Automated Self-Administered 24-hour dietary recall (ASA24): a resource for researchers, clinicians, and educators from the National Cancer Institute. *J Acad Nutr Diet* **2012**, *112* (8), 1134-7.
64. Haff, G., Quantifying Workloads in Resistance Training: A Brief Review. *Prof. Strength and Cond.* **2010**, *10*, 31-40.
65. Callahan, B. J.; McMurdie, P. J.; Rosen, M. J.; Han, A. W.; Johnson, A. J.; Holmes, S. P., DADA2: High-resolution sample inference from Illumina amplicon data. *Nat Methods* **2016**, *13* (7), 581-3.
66. Katoh, K.; Standley, D. M., MAFFT multiple sequence alignment software version 7: improvements in performance and usability. *Mol Biol Evol* **2013**, *30* (4), 772-80.
67. McDonald, D.; Price, M. N.; Goodrich, J.; Nawrocki, E. P.; DeSantis, T. Z.; Probst, A.; Andersen, G. L.; Knight, R.; Hugenholtz, P., An improved

Greengenes taxonomy with explicit ranks for ecological and evolutionary analyses of bacteria and archaea. *ISME J* **2012**, 6 (3), 610-8.

68. Bolyen, E.; Rideout, J. R.; Dillon, M. R.; Bokulich, N. A.; Abnet, C. C.; Al-Ghalith, G. A.; Alexander, H.; Alm, E. J.; Arumugam, M.; Asnicar, F.; Bai, Y.; Bisanz, J. E.; Bittinger, K.; Brejnrod, A.; Brislawn, C. J.; Brown, C. T.; Callahan, B. J.; Caraballo-Rodriguez, A. M.; Chase, J.; Cope, E. K.; Da Silva, R.; Diener, C.; Dorrestein, P. C.; Douglas, G. M.; Durall, D. M.; Duvallet, C.; Edwardson, C. F.; Ernst, M.; Estaki, M.; Fouquier, J.; Gauglitz, J. M.; Gibbons, S. M.; Gibson, D. L.; Gonzalez, A.; Gorlick, K.; Guo, J.; Hillmann, B.; Holmes, S.; Holste, H.; Huttenhower, C.; Huttley, G. A.; Janssen, S.; Jarmusch, A. K.; Jiang, L.; Kaehler, B. D.; Kang, K. B.; Keefe, C. R.; Keim, P.; Kelley, S. T.; Knights, D.; Koester, I.; Kosciulek, T.; Kreps, J.; Langille, M. G. I.; Lee, J.; Ley, R.; Liu, Y. X.; Lofffield, E.; Lozupone, C.; Maher, M.; Marotz, C.; Martin, B. D.; McDonald, D.; McIver, L. J.; Melnik, A. V.; Metcalf, J. L.; Morgan, S. C.; Morton, J. T.; Naimey, A. T.; Navas-Molina, J. A.; Nothias, L. F.; Orchanian, S. B.; Pearson, T.; Peoples, S. L.; Petras, D.; Preuss, M. L.; Pruesse, E.; Rasmussen, L. B.; Rivers, A.; Robeson, M. S., 2nd; Rosenthal, P.; Segata, N.; Shaffer, M.; Shiffer, A.; Sinha, R.; Song, S. J.; Spear, J. R.; Swafford, A. D.; Thompson, L. R.; Torres, P. J.; Trinh, P.; Tripathi, A.; Turnbaugh, P. J.; Ull-Hasan, S.; van der Hooff, J. J. J.; Vargas, F.; Vazquez-Baeza, Y.; Vogtmann, E.; von Hippel, M.; Walters, W.; Wan, Y.; Wang, M.; Warren, J.; Weber, K. C.; Williamson, C. H. D.; Willis, A. D.; Xu, Z. Z.; Zaneveld, J. R.; Zhang, Y.; Zhu, Q.; Knight, R.; Caporaso, J. G., Reproducible, interactive, scalable and extensible microbiome data science using QIIME 2. *Nat Biotechnol* **2019**, 37 (8), 852-857.

69. Langille, M. G.; Zaneveld, J.; Caporaso, J. G.; McDonald, D.; Knights, D.; Reyes, J. A.; Clemente, J. C.; Burkpile, D. E.; Vega Thurber, R. L.; Knight, R.; Beiko, R. G.; Huttenhower, C., Predictive functional profiling of microbial communities using 16S rRNA marker gene sequences. *Nat Biotechnol* **2013**, 31 (9), 814-21.

70. Parks, D. H.; Beiko, R. G., Identifying biologically relevant differences between metagenomic communities. *Bioinformatics* **2010**, 26 (6), 715-21.

71. Joshua D. Rabinowitz, E. K., Acidic acetonitrile for cellular metabolome extraction from *Escherichia coli*. *Anal. Chem* **2007**, 79 (16), 6167-6173.

72. Stough, J. M. A.; Dearth, S. P.; Denny, J. E.; LeClerc, G. R.; Schmidt, N. W.; Campagna, S. R.; Wilhelm, S. W., Functional Characteristics of the Gut Microbiome in C57BL/6 Mice Differentially Susceptible to *Plasmodium yoelii*. *Front Microbiol* **2016**, 7 (1520).

73. Martens, L.; Chambers, M.; Sturm, M.; Kessner, D.; Levander, F.; Shofstahl, J.; Tang, W. H.; Römpf, A.; Neumann, S.; Pizarro, A. D.; Montecchi-Palazzi, L.; Tasman, N.; Coleman, M.; Reisinger, F.; Souda, P.; Hermjakob, H.; Binz, P.-A.; Deutsch, E. W., mzML--a community standard for mass spectrometry data. *Molecular & cellular proteomics : MCP* **2011**, 10 (1), R110.000133-R110.000133.

74. Melamud, E.; Vastag, L.; Rabinowitz, J. D., Metabolomic Analysis and Visualization Engine for LC-MS Data. *Analytical Chemistry* **2010**, *82* (23), 9818-9826.
75. Shi, Y., Caught red-handed: uric acid is an agent of inflammation. *J Clin Invest* **2010**, *120* (6), 1809-11.
76. Lara, L. J.; Rostagno, M. H., Impact of Heat Stress on Poultry Production. *Animals (Basel)* **2013**, *3* (2), 356-69.
77. Nawaz, A. H.; Amoah, K.; Leng, Q. Y.; Zheng, J. H.; Zhang, W. L.; Zhang, L., Poultry response to heat stress: its physiological, metabolic, and genetic implications on meat production and quality including strategies to improve broiler production in a warming world. *Frontiers in Veterinary Science* **2021**, 814.
78. Baker, J. S.; Havlík, P.; Beach, R.; Leclère, D.; Schmid, E.; Valin, H.; Cole, J.; Creason, J.; Ohrel, S.; McFarland, J., Evaluating the effects of climate change on US agricultural systems: sensitivity to regional impact and trade expansion scenarios. *Environmental Research Letters* **2018**, *13* (6), 064019.
79. Alley, R. B.; Clark, P. U.; Huybrechts, P.; Joughin, I., Ice-sheet and sea-level changes. *science* **2005**, *310* (5747), 456-460.
80. Karn, M.; Sharma, M., Climate change, natural calamities and the triple burden of disease. *Nature Climate Change* **2021**, *11* (10), 796-797.
81. Moore, F. C.; Baldos, U.; Hertel, T.; Diaz, D., New science of climate change impacts on agriculture implies higher social cost of carbon. *Nature Communications* **2017**, *8* (1), 1607.
82. Nelson, G. C.; Valin, H.; Sands, R. D.; Havlík, P.; Ahammad, H.; Deryng, D.; Elliott, J.; Fujimori, S.; Hasegawa, T.; Heyhoe, E., Climate change effects on agriculture: Economic responses to biophysical shocks. *Proceedings of the National Academy of Sciences* **2014**, *111* (9), 3274-3279.
83. Rosenzweig, C.; Elliott, J.; Deryng, D.; Ruane, A. C.; Müller, C.; Arneth, A.; Boote, K. J.; Folberth, C.; Glotter, M.; Khabarov, N., Assessing agricultural risks of climate change in the 21st century in a global gridded crop model intercomparison. *Proceedings of the national academy of sciences* **2014**, *111* (9), 3268-3273.
84. Stevanović, M.; Popp, A.; Lotze-Campen, H.; Dietrich, J.; Müller, C.; Bonsch, M.; Schmitz, C.; Bodirsky, B.; Humpenöder, F.; Weindl, I., The impact of high-end climate change on agricultural welfare *Sci. Adv* **2016**, *2*, 1-9.
85. Liu, L.; Ren, M.; Ren, K.; Jin, Y.; Yan, M., Heat stress impacts on broiler performance: a systematic review and meta-analysis. *Poultry Science* **2020**, *99* (11), 6205-6211.
86. Deeb, N.; Shlosberg, A.; Cahaner, A., Genotype-by-environment interaction with broiler genotypes differing in growth rate. 4. Association between responses to heat stress and to cold-induced ascites. *Poultry Science* **2002**, *81* (10), 1454-1462.

87. Narita, T.; Weinert, B. T.; Choudhary, C., Functions and mechanisms of non-histone protein acetylation. *Nature Reviews Molecular Cell Biology* **2019**, *20* (3), 156-174.
88. Emami, N. K.; Greene, E. S.; Kogut, M. H.; Dridi, S., Heat Stress and Feed Restriction Distinctly Affect Performance, Carcass and Meat Yield, Intestinal Integrity, and Inflammatory (Chemo)Cytokines in Broiler Chickens. *Front Physiol* **2021**, *12*, 707757.
89. Orłowski, S. K.; Cauble, R.; Tabler, T.; Hiltz, J. Z.; Greene, E. S.; Anthony, N. B.; Dridi, S., Processing evaluation of random bred broiler populations and a common ancestor at 55 days under chronic heat stress conditions. *Poultry Science* **2020**, *99* (7), 3491-3500.
90. Greene, E.; Cauble, R.; Kadhim, H.; de Almeida Mallmann, B.; Gu, I.; Lee, S.-O.; Orłowski, S.; Dridi, S., Protective effects of the phytogetic feed additive “comfort” on growth performance via modulation of hypothalamic feeding-and drinking-related neuropeptides in cyclic heat-stressed broilers. *Domestic Animal Endocrinology* **2021**, *74*, 106487.
91. Baxter, M. F.; Greene, E. S.; Kidd, M. T.; Tellez-Isaias, G.; Orłowski, S.; Dridi, S., Water amino acid-chelated trace mineral supplementation decreases circulating and intestinal HSP70 and proinflammatory cytokine gene expression in heat-stressed broiler chickens. *Journal of Animal Science* **2020**, *98* (3), skaa049.
92. Cahaner, A.; Leenstra, F., Effects of High Temperature on Growth and Efficiency of Male and Female Broilers from Lines Selected for High Weight Gain, Favorable Feed Conversion, and High or Low Fat Content. *Poultry Science* **1992**, *71* (8), 1237-1250.
93. Leenstra, F.; Cahaner, A., Effects of Low, Normal, and High Temperatures on Slaughter Yield of Broilers from Lines Selected for High Weight Gain, Favorable Feed Conversion, and High or Low Fat Content. *Poultry Science* **1992**, *71* (12), 1994-2006.
94. Dale, N. M.; Fuller, H. L., Effect of Diet Composition on Feed Intake and Growth of Chicks Under Heat Stress: II. Constant vs. Cycling Temperatures. *Poultry Science* **1980**, *59* (7), 1434-1441.
95. Quinteiro-Filho, W. M.; Ribeiro, A.; Ferraz-de-Paula, V.; Pinheiro, M. L.; Sakai, M.; Sá, L. R. M.; Ferreira, A. J. P.; Palermo-Neto, J., Heat stress impairs performance parameters, induces intestinal injury, and decreases macrophage activity in broiler chickens. *Poultry Science* **2010**, *89* (9), 1905-1914.
96. Mitchell, M. A.; Carlisle, A. J., The effects of chronic exposure to elevated environmental temperature on intestinal morphology and nutrient absorption in the domestic fowl (*Gallus domesticus*). *Comparative Biochemistry and Physiology Part A: Physiology* **1992**, *101* (1), 137-142.
97. Jones, M.; Dille, J.; Drossman, D.; Crowell, M., Brain–gut connections in functional GI disorders: anatomic and physiologic relationships. *Neurogastroenterology & Motility* **2006**, *18* (2), 91-103.

98. Brzozowski, B.; Mazur-Bialy, A.; Pajdo, R.; Kwiecien, S.; Bilski, J.; Zwolinska-Wcislo, M.; Mach, T.; Brzozowski, T., Mechanisms by which stress affects the experimental and clinical inflammatory bowel disease (IBD): role of brain-gut axis. *Current neuropharmacology* **2016**, *14* (8), 892-900.
99. Breit, S.; Kupferberg, A.; Rogler, G.; Hasler, G., Vagus nerve as modulator of the brain-gut axis in psychiatric and inflammatory disorders. *Frontiers in psychiatry* **2018**, *44*.
100. Mukhtar, K.; Nawaz, H.; Abid, S., Functional gastrointestinal disorders and gut-brain axis: What does the future hold? *World J Gastroenterol* **2019**, *25* (5), 552.
101. Lambert, G., Stress-induced gastrointestinal barrier dysfunction and its inflammatory effects. *Journal of animal science* **2009**, *87* (suppl_14), E101-E108.
102. Tur, J. A.; Rial, R. V., The effect of temperature and relative humidity on the gastrointestinal motility of young broiler. *Comparative Biochemistry and Physiology Part A: Physiology* **1985**, *80* (4), 481-486.
103. Hai, L.; Rong, D.; Zhang, Z.-Y., The effect of thermal environment on the digestion of broilers. *Journal of Animal Physiology and Animal Nutrition* **2000**, *83* (2), 57-64.
104. Hall, D. M.; Baumgardner, K. R.; Oberley, T. D.; Gisolfi, C. V., Splanchnic tissues undergo hypoxic stress during whole body hyperthermia. *American Journal of Physiology-Gastrointestinal and Liver Physiology* **1999**, *276* (5), G1195-G1203.
105. Wolfenson, D., Blood flow through arteriovenous anastomoses and its thermal function in the laying hen. *The Journal of Physiology* **1983**, *334* (1), 395-407.
106. Ophir, E.; Arieli, Y.; Marder, J.; Horowitz, M., Cutaneous blood flow in the pigeon *Columba livia*: its possible relevance to cutaneous water evaporation. *Journal of Experimental Biology* **2002**, *205* (17), 2627-2636.
107. Wolf, B. O.; Walsberg, G. E., The Role of the Plumage in Heat Transfer Processes of Birds. *American Zoologist* **2015**, *40* (4), 575-584.
108. Varasteh, S.; Braber, S.; Akbari, P.; Garssen, J.; Fink-Gremmels, J., Differences in susceptibility to heat stress along the chicken intestine and the protective effects of galacto-oligosaccharides. *PloS one* **2015**, *10* (9), e0138975.
109. Alhenaky, A.; Abdelqader, A.; Abuajamieh, M.; Al-Fataftah, A.-R., The effect of heat stress on intestinal integrity and *Salmonella* invasion in broiler birds. *Journal of Thermal Biology* **2017**, *70*, 9-14.
110. Quinteiro-Filho, W. M.; Gomes, A. V. S.; Pinheiro, M. L.; Ribeiro, A.; Ferraz-de-Paula, V.; Astolfi-Ferreira, C. S.; Ferreira, A. J. P.; Palermo-Neto, J., Heat stress impairs performance and induces intestinal inflammation in broiler chickens infected with *Salmonella* Enteritidis. *Avian Pathology* **2012**, *41* (5), 421-427.
111. Tsiouris, V.; Georgopoulou, I.; Batzios, C.; Pappaioannou, N.; Ducatelle, R.; Fortomaris, P., Heat stress as a predisposing factor for necrotic enteritis in broiler chicks. *Avian Pathology* **2018**, *47* (6), 616-624.

112. Kaldhusdal, M.; Benestad, S. L.; Løvland, A., Epidemiologic aspects of necrotic enteritis in broiler chickens – disease occurrence and production performance. *Avian Pathology* **2016**, *45* (3), 271-274.
113. Kadykalo, S.; Roberts, T.; Thompson, M.; Wilson, J.; Lang, M.; Espeisse, O., The value of anticoccidials for sustainable global poultry production. *International Journal of Antimicrobial Agents* **2018**, *51* (3), 304-310.
114. Skinner, J. T.; Bauer, S.; Young, V.; Pauling, G.; Wilson, J., An Economic Analysis of the Impact of Subclinical (Mild) Necrotic Enteritis in Broiler Chickens. *Avian Diseases* **2010**, *54* (4), 1237-1240, 4.
115. Mora, C.; Frazier, A. G.; Longman, R. J.; Dacks, R. S.; Walton, M. M.; Tong, E. J.; Sanchez, J. J.; Kaiser, L. R.; Stender, Y. O.; Anderson, J. M.; Ambrosino, C. M.; Fernandez-Silva, I.; Giuseffi, L. M.; Giambelluca, T. W., The projected timing of climate departure from recent variability. *Nature* **2013**, *502* (7470), 183-187.
116. Moss, R. H.; Edmonds, J. A.; Hibbard, K. A.; Manning, M. R.; Rose, S. K.; van Vuuren, D. P.; Carter, T. R.; Emori, S.; Kainuma, M.; Kram, T.; Meehl, G. A.; Mitchell, J. F. B.; Nakicenovic, N.; Riahi, K.; Smith, S. J.; Stouffer, R. J.; Thomson, A. M.; Weyant, J. P.; Wilbanks, T. J., The next generation of scenarios for climate change research and assessment. *Nature* **2010**, *463* (7282), 747-756.
117. Trisos, C. H.; Merow, C.; Pigot, A. L., The projected timing of abrupt ecological disruption from climate change. *Nature* **2020**, *580* (7804), 496-501.
118. Ruff, J.; Barros, T. L.; Tellez, G.; Blankenship, J.; Lester, H.; Graham, B. D.; Selby, C. A. M.; Vuong, C. N.; Dridi, S.; Greene, E. S.; Hernandez-Velasco, X.; Hargis, B. M.; Tellez-Isaias, G., Research Note: Evaluation of a heat stress model to induce gastrointestinal leakage in broiler chickens. *Poultry Science* **2020**, *99* (3), 1687-1692.
119. Tabler, T. W.; Greene, E. S.; Orlowski, S. K.; Hiltz, J. Z.; Anthony, N. B.; Dridi, S., Intestinal barrier integrity in heat-stressed modern broilers and their ancestor wild jungle fowl. *Frontiers in Veterinary Science* **2020**, *7*, 249.
120. Ren, J. L.; Zhang, A. H.; Kong, L.; Wang, X. J., Advances in mass spectrometry-based metabolomics for investigation of metabolites. *RSC Adv* **2018**, *8* (40), 22335-22350.
121. Brown, L. P.; May, A. L.; Fisch, A. R.; Campagna, S. R.; Voy, B. H., Chapter 5 - Avian metabolomics. In *Sturkie's Avian Physiology (Seventh Edition)*, Scanes, C. G.; Dridi, S., Eds. Academic Press: San Diego, 2022; pp 49-63.
122. Oliveros, J. C. Venny-An interactive tool for comparing lists with Venn's diagrams. <https://bioinfogp.cnb.csic.es/tools/venny/index.html>.
123. Mottet, A.; Tempio, G., Global poultry production: current state and future outlook and challenges. *World's Poultry Science Journal* **2017**, *73* (2), 245-256.
124. St-Pierre, N. R.; Cobanov, B.; Schnitkey, G., Economic Losses from Heat Stress by US Livestock Industries¹. *Journal of Dairy Science* **2003**, *86*, E52-E77.
125. Zaboli, G.; Huang, X.; Feng, X.; Ahn, D. U., How can heat stress affect chicken meat quality?—a review. *Poultry science* **2019**, *98* (3), 1551-1556.

126. Hirakawa, R.; Nurjanah, S.; Furukawa, K.; Murai, A.; Kikusato, M.; Nochi, T.; Toyomizu, M., Heat stress causes immune abnormalities via massive damage to effect proliferation and differentiation of lymphocytes in broiler chickens. *Frontiers in veterinary science* **2020**, *7*, 46.
127. Piestun, Y.; Patael, T.; Yahav, S.; Velleman, S. G.; Halevy, O., Early posthatch thermal stress affects breast muscle development and satellite cell growth and characteristics in broilers. *Poultry Science* **2017**, *96* (8), 2877-2888.
128. Tang, S.; Zhou, S.; Yin, B.; Xu, J.; Di, L.; Zhang, J.; Bao, E., Heat stress-induced renal damage in poultry and the protective effects of HSP60 and HSP47. *Cell Stress Chaperones* **2018**, *23* (5), 1033-1040.
129. Song, J.; Xiao, K.; Ke, Y.; Jiao, L.; Hu, C.; Diao, Q.; Shi, B.; Zou, X., Effect of a probiotic mixture on intestinal microflora, morphology, and barrier integrity of broilers subjected to heat stress. *Poultry science* **2014**, *93* (3), 581-588.
130. Li, L.; Tan, H.; Gu, Z.; Liu, Z.; Geng, Y.; Liu, Y.; Tong, H.; Tang, Y.; Qiu, J.; Su, L., Heat Stress Induces Apoptosis through a Ca²⁺-Mediated Mitochondrial Apoptotic Pathway in Human Umbilical Vein Endothelial Cells. *PLOS ONE* **2015**, *9* (12), e111083.
131. Obrenovich, M. E. M., Leaky Gut, Leaky Brain? *Microorganisms* **2018**, *6* (4), 107.
132. Ippolito, D. L.; Lewis, J. A.; Yu, C.; Leon, L. R.; Stallings, J. D., Alteration in circulating metabolites during and after heat stress in the conscious rat: potential biomarkers of exposure and organ-specific injury. *BMC physiology* **2014**, *14* (1), 1-17.
133. Pedley, A. M.; Benkovic, S. J., A New View into the Regulation of Purine Metabolism: The Purinosome. *Trends Biochem Sci* **2017**, *42* (2), 141-154.
134. Yi, G.; Li, L.; Luo, M.; He, X.; Zou, Z.; Gu, Z.; Su, L., Heat stress induces intestinal injury through lysosome- and mitochondria-dependent pathway in vivo and in vitro. *Oncotarget* **2017**, *8* (25), 40741-40755.
135. Guerbette, T.; Boudry, G.; Lan, A., Mitochondrial function in intestinal epithelium homeostasis and modulation in diet-induced obesity. *Mol Metab* **2022**, *63*, 101546.
136. Hermes, J. D.; Tipton, P. A.; Fisher, M. A.; O'Leary, M.; Morrison, J.; Cleland, W., Mechanisms of enzymatic and acid-catalyzed decarboxylations of prephenate. *Biochemistry* **1984**, *23* (25), 6263-6275.
137. Maeda, H.; Dudareva, N., The shikimate pathway and aromatic amino acid biosynthesis in plants. *Annual review of plant biology* **2012**, *63*, 73-105.
138. Kers, J. G.; Velkers, F. C.; Fischer, E. A. J.; Hermes, G. D. A.; Stegeman, J. A.; Smidt, H., Host and Environmental Factors Affecting the Intestinal Microbiota in Chickens. *Front Microbiol* **2018**, *9*, 235.
139. Shi, D.; Bai, L.; Qu, Q.; Zhou, S.; Yang, M.; Guo, S.; Li, Q.; Liu, C., Impact of gut microbiota structure in heat-stressed broilers. *Poultry science* **2019**, *98* (6), 2405-2413.

140. Gallardo, M. E.; Desviat, L. R.; Rodríguez, J. M.; Esparza-Gordillo, J.; Pérez-Cerdá, C.; Pérez, B.; Rodríguez-Pombo, P.; Criado, O.; Sanz, R.; Morton, D. H., The molecular basis of 3-methylcrotonylglycinuria, a disorder of leucine catabolism. *The American Journal of Human Genetics* **2001**, *68* (2), 334-346.
141. Bartlett, K.; Ng, H.; Leonard, J., A combined defect of three mitochondrial carboxylases presenting as biotin-responsive 3-methylcrotonyl glycinuria and 3-hydroxyisovaleric aciduria. *Clinica Chimica Acta* **1980**, *100* (2), 183-186.
142. Tamura, Y.; Kitaoka, Y.; Matsunaga, Y.; Hoshino, D.; Hatta, H., Daily heat stress treatment rescues denervation-activated mitochondrial clearance and atrophy in skeletal muscle. *The Journal of physiology* **2015**, *593* (12), 2707-2720.
143. Tehlivets, O.; Malanovic, N.; Visram, M.; Pavkov-Keller, T.; Keller, W., S-adenosyl-L-homocysteine hydrolase and methylation disorders: yeast as a model system. *Biochim Biophys Acta* **2013**, *1832* (1), 204-15.
144. Maclean, K. N.; Greiner, L. S.; Evans, J. R.; Sood, S. K.; Lhotak, S.; Markham, N. E.; Stabler, S. P.; Allen, R. H.; Austin, R. C.; Balasubramaniam, V.; Jiang, H., Cystathionine protects against endoplasmic reticulum stress-induced lipid accumulation, tissue injury, and apoptotic cell death. *J Biol Chem* **2012**, *287* (38), 31994-2005.
145. Moon, E. J.; Sonveaux, P.; Porporato, P. E.; Danhier, P.; Gallez, B.; Batinic-Haberle, I.; Nien, Y.-C.; Schroeder, T.; Dewhirst, M. W., NADPH oxidase-mediated reactive oxygen species production activates hypoxia-inducible factor-1 (HIF-1) via the ERK pathway after hyperthermia treatment. *Proceedings of the National Academy of Sciences* **2010**, *107* (47), 20477-20482.
146. Segal, A. W.; Abo, A., The biochemical basis of the NADPH oxidase of phagocytes. *Trends in biochemical sciences* **1993**, *18* (2), 43-47.
147. Mouchiroud, L.; Houtkooper, Riekelt H.; Moullan, N.; Katsyuba, E.; Ryu, D.; Cantó, C.; Mottis, A.; Jo, Y.-S.; Viswanathan, M.; Schoonjans, K.; Guarente, L.; Auwerx, J., The NAD⁺/Sirtuin Pathway Modulates Longevity through Activation of Mitochondrial UPR and FOXO Signaling. *Cell* **2013**, *154* (2), 430-441.
148. Panday, A.; Sahoo, M. K.; Osorio, D.; Batra, S., NADPH oxidases: an overview from structure to innate immunity-associated pathologies. *Cellular & Molecular Immunology* **2015**, *12* (1), 5-23.
149. Hirst, J., Towards the molecular mechanism of respiratory complex I. *Biochemical Journal* **2010**, *425* (2), 327-339.
150. McCormack, J.; Denton, R., The role of Ca²⁺ in the regulation of intramitochondrial energy production in heart. *Biomedica biochimica acta* **1987**, *46* (8-9), S487-92.
151. Furukawa, A.; Tada-Oikawa, S.; Kawanishi, S.; Oikawa, S., H₂O₂ accelerates cellular senescence by accumulation of acetylated p53 via decrease in the function of SIRT1 by NAD⁺ depletion. *Cellular Physiology and Biochemistry* **2007**, *20* (1-4), 045-054.

152. Wiese, M.; Bannister, A. J., Two genomes, one cell: Mitochondrial-nuclear coordination via epigenetic pathways. *Molecular Metabolism* **2020**, *38*, 100942.
153. Houtkooper, R. H.; Cantó, C.; Wanders, R. J.; Auwerx, J., The secret life of NAD⁺: an old metabolite controlling new metabolic signaling pathways. *Endocrine reviews* **2010**, *31* (2), 194-223.
154. Ying, W., NAD⁺ and NADH in brain functions, brain diseases and brain aging. *FBL* **2007**, *12* (5), 1863-1888.
155. Wu, G.; Fang, Y. Z.; Yang, S.; Lupton, J. R.; Turner, N. D., Glutathione metabolism and its implications for health. *J Nutr* **2004**, *134* (3), 489-92.
156. Ge, T.; Yang, J.; Zhou, S.; Wang, Y.; Li, Y.; Tong, X., The Role of the Pentose Phosphate Pathway in Diabetes and Cancer. *Front Endocrinol (Lausanne)* **2020**, *11*, 365.
157. Horecker, B. L., The pentose phosphate pathway. *Journal of Biological Chemistry* **2002**, *277* (50), 47965-47971.
158. Ralser, M.; Wamelink, M. M.; Kowald, A.; Gerisch, B.; Heeren, G.; Struys, E. A.; Klipp, E.; Jakobs, C.; Breitenbach, M.; Lehrach, H., Dynamic rerouting of the carbohydrate flux is key to counteracting oxidative stress. *Journal of biology* **2007**, *6* (4), 1-18.
159. Ralser, M.; Wamelink, M.; Latkolik, S.; Jansen, E. E.; Lehrach, H.; Jakobs, C., Metabolic reconfiguration precedes transcriptional regulation in the antioxidant response. *Nat Biotechnol* **2009**, *27* (7), 604-605.
160. Cosentino, C.; Grieco, D.; Costanzo, V., ATM activates the pentose phosphate pathway promoting anti-oxidant defence and DNA repair. *The EMBO journal* **2011**, *30* (3), 546-555.
161. Alam, M. M.; Iqbal, S.; Naseem, I., Ameliorative effect of riboflavin on hyperglycemia, oxidative stress and DNA damage in type-2 diabetic mice: Mechanistic and therapeutic strategies. *Archives of biochemistry and biophysics* **2015**, *584*, 10-19.
162. Suwannasom, N.; Kao, I.; Pruß, A.; Georgieva, R.; Bäumlner, H., Riboflavin: The health benefits of a forgotten natural vitamin. *International Journal of Molecular Sciences* **2020**, *21* (3), 950.
163. Powers, H. J., Riboflavin (vitamin B-2) and health. *The American journal of clinical nutrition* **2003**, *77* (6), 1352-1360.
164. McNulty, H.; Strain, J. J.; Hughes, C. F.; Pentieva, K.; Ward, M., Evidence of a Role for One-Carbon Metabolism in Blood Pressure: Can B Vitamin Intervention Address the Genetic Risk of Hypertension Owing to a Common Folate Polymorphism? *Curr Dev Nutr* **2020**, *4* (1), nzz102.
165. Greene, E.; Cauble, R.; Dhamad, A. E.; Kidd, M. T.; Kong, B.; Howard, S. M.; Castro, H. F.; Campagna, S. R.; Bedford, M.; Dridi, S., Muscle Metabolome Profiles in Woody Breast-(un)Affected Broilers: Effects of Quantum Blue Phytase-Enriched Diet. *Frontiers in Veterinary Science* **2020**, *7* (458).
166. Lu, W.; Clasquin, M. F.; Melamud, E.; Amador-Noguez, D.; Caudy, A. A.; Rabinowitz, J. D., Metabolomic analysis via reversed-phase ion-pairing liquid

- chromatography coupled to a stand alone orbitrap mass spectrometer. *Anal Chem* **2010**, *82* (8), 3212-21.
167. Chambers, M. C.; Maclean, B.; Burke, R.; Amodei, D.; Ruderman, D. L.; Neumann, S.; Gatto, L.; Fischer, B.; Pratt, B.; Egertson, J.; Hoff, K.; Kessner, D.; Tasman, N.; Shulman, N.; Frewen, B.; Baker, T. A.; Brusniak, M.-Y.; Paulse, C.; Creasy, D.; Flashner, L.; Kani, K.; Moulding, C.; Seymour, S. L.; Nuwaysir, L. M.; Lefebvre, B.; Kuhlmann, F.; Roark, J.; Rainer, P.; Detlev, S.; Hemenway, T.; Huhmer, A.; Langridge, J.; Connolly, B.; Chadick, T.; Holly, K.; Eckels, J.; Deutsch, E. W.; Moritz, R. L.; Katz, J. E.; Agus, D. B.; MacCoss, M.; Tabb, D. L.; Mallick, P., A cross-platform toolkit for mass spectrometry and proteomics. *Nat Biotechnol* **2012**, *30* (10), 918-920.
168. Bazurto, J. V.; Dearth, S. P.; Tague, E. D.; Campagna, S. R.; Downs, D. M., Untargeted metabolomics confirms and extends the understanding of the impact of aminoimidazole carboxamide ribotide (AICAR) in the metabolic network of *Salmonella enterica*. *Microb Cell* **2017**, *5* (2), 74-87.
169. Hess, M.; McDougald, L. R., Histomoniasis (Blackhead) and other protozoan diseases of the intestinal tract. In *Diseases of Poultry*, Swayne, D. E., Ed. 2013; pp 1147-1201.
170. Daş, G.; Wachter, L.; Stehr, M.; Bilic, I.; Grafl, B.; Wernsdorf, P.; Metges, C. C.; Hess, M.; Liebhart, D., Excretion of *Histomonas meleagridis* following experimental co-infection of distinct chicken lines with *Heterakis gallinarum* and *Ascaridia galli*. *Parasites & Vectors* **2021**, *14* (1), 323.
171. Hauck, R.; Hafez, H. M., Experimental infections with the protozoan parasite *Histomonas meleagridis*: a review. *Parasitology Research* **2013**, *112* (1), 19-34.
172. McDougald, L., Histomoniasis (Blackhead) and other protozoan diseases of the intestinal tract. *Diseases of Poultry. Ames: Blackwell Academic Publishing Professional* **2008**, *2008*, 1095-1105.
173. Hafez, H. M.; Hauck, R.; Gad, W.; De Gussem, K.; Lotfi, A., Pilot study on the efficacy of paromomycin as a histomonostatic feed additive in turkey poults experimentally infected with *Histomonas meleagridis*. *Archives of Animal Nutrition* **2010**, *64* (1), 77-84.
174. Callait-Cardinal, M. P.; Leroux, S.; Venereau, E.; Chauve, C.; Le Pottier, G.; Zenner, L., Incidence of histomonosis in turkeys in France since the bans of dimetridazole and nifursol. *Veterinary Record* **2007**, *161* (17), 581-585.
175. Hauck, R.; Balczulat, S.; Hafez, H. M., Detection of DNA of *Histomonas meleagridis* and *Tetratrichomonas gallinarum* in German poultry flocks between 2004 and 2008. *Avian Diseases* **2010**, *54* (3), 1021-1025.
176. Tyzzer, E. E., The flagellate character and reclassification of the parasite producing "Blackhead" in turkeys: *Histomonas* (Gen. nov.) *meleagridis* (Smith). *The journal of parasitology* **1920**, *6* (3), 124-131.
177. Taylor, M. A.; Coop, R. L.; Wall, R. L., *Veterinary parasitology*. John Wiley & Sons: 2015.

178. Klodnicki, M.; McDougald, L.; Beckstead, R., A genomic analysis of *Histomonas meleagridis* through sequencing of a cDNA library. *The Journal of Parasitology* **2013**, *99* (2), 264-269.
179. Dwyer, D. M., An improved method for cultivating *Histomonas meleagridis*. *J Parasitol* **1970**, *56* (1), 191-2.
180. van der Heijden, H. M.; Landman, W. J., Improved culture of *Histomonas meleagridis* in a modification of Dwyer medium. *Avian Dis* **2007**, *51* (4), 986-8.
181. van der Heijden, H. M.; McDougald, L. R.; Landman, W. J., High yield of parasites and prolonged in vitro culture of *Histomonas meleagridis*. *Avian Pathol* **2005**, *34* (6), 505-8.
182. Hauck, R.; Armstrong, P. L.; McDougald, L. R., *Histomonas meleagridis* (Protozoa: Trichomonadidae): analysis of growth requirements in vitro. *J Parasitol* **2010**, *96* (1), 1-7.
183. Barrios, M. A.; Kenyon, A.; Beckstead, R., Development of a Dry Medium for Isolation of *Histomonas meleagridis* in the Field. *Avian Dis* **2017**, *61* (2), 242-244.
184. Bilic, I.; Hess, M., Interplay between *Histomonas meleagridis* and Bacteria: Mutualistic or Predator-Prey? *Trends Parasitol* **2020**, *36* (3), 232-235.
185. Ganas, P.; Liebhart, D.; Glosmann, M.; Hess, C.; Hess, M., *Escherichia coli* strongly supports the growth of *Histomonas meleagridis*, in a monoxenic culture, without influence on its pathogenicity. *Int J Parasitol* **2012**, *42* (10), 893-901.
186. Mitra, T.; Kidane, F. A.; Hess, M.; Liebhart, D., Unravelling the immunity of poultry against the extracellular protozoan parasite *Histomonas meleagridis* is a cornerstone for vaccine development: a review. *Frontiers in Immunology* **2018**, *9*, 2518.
187. Rivlin, R. S.; PINTO, J. T. J. H. o. V., 4th ed.; Zemleni, J., Rucker, RB, McCormick, DB, Suttie, JW, Eds, Riboflavin (vitamin B2). **2007**.
188. Qi, B.; Kniazeva, M.; Han, M., A vitamin-B2-sensing mechanism that regulates gut protease activity to impact animal's food behavior and growth. *Elife* **2017**, *6*.
189. Thakur, K.; Tomar, S. K.; De, S., Lactic acid bacteria as a cell factory for riboflavin production. **2016**, *9* (4), 441-451.
190. García-Angulo, V. A. J. C. r. i. m., Overlapping riboflavin supply pathways in bacteria. **2017**, *43* (2), 196-209.
191. García-Angulo, V. A., Overlapping riboflavin supply pathways in bacteria. *Critical Reviews in Microbiology* **2017**, *43* (2), 196-209.
192. Sepúlveda Cisternas, I.; Salazar, J. C.; García-Angulo, V. A., Overview on the Bacterial Iron-Riboflavin Metabolic Axis. **2018**, *9* (1478).
193. Council, N. R., *Nutrient Requirements of Poultry: Ninth Revised Edition*, 1994. The National Academies Press: Washington, DC, 1994; p 176.
194. Forouzesh, A.; Forouzesh, F.; Samadi Foroushani, S.; Forouzesh, A., A new method for calculating riboflavin content and determining appropriate riboflavin levels in foods. *Available at SSRN 4133567* **2022**.

195. Hauck, R., Interactions Between Parasites and the Bacterial Microbiota of Chickens. *Avian Diseases* **2017**, *61* (4), 428-436.
196. McDougald, L. R., Blackhead disease (histomoniasis) in poultry: a critical review. *Avian Dis* **2005**, *49* (4), 462-76.
197. Hess, M.; Liebhart, D.; Bilic, I.; Ganas, P., Histomonas meleagridis--new insights into an old pathogen. *Vet Parasitol* **2015**, *208* (1-2), 67-76.
198. Couch, J.; German, H.; Knight, D.; Sparks, P.; Pearson, P. J. P. S., Importance of the cecum in intestinal synthesis in the mature domestic fowl. **1950**, *29* (1), 52-58.
199. Kamphorst, J. J.; Fan, J.; Lu, W.; White, E.; Rabinowitz, J. D., Liquid chromatography-high resolution mass spectrometry analysis of fatty acid metabolism. *Anal Chem* **2011**, *83* (23), 9114-22.
200. Chong, J.; Wishart, D. S.; Xia, J., Using MetaboAnalyst 4.0 for Comprehensive and Integrative Metabolomics Data Analysis. *Current Protocols in Bioinformatics* **2019**, *68* (1), e86.
201. Lo, H. S.; Reeves, R. E., Riboflavin requirement for the cultivation of axenic Entamoeba histolytica. *Am J Trop Med Hyg* **1979**, *28* (2), 194-7.

VITA

Courtney Christopher was born in Knoxville, TN in 1995. She attended Pigeon Forge High School where her chemistry teacher, Mr. Henegar, helped her uncover her love for science. Courtney went on to attend Lincoln Memorial University (LMU) in Harrogate, TN where she received her degree in chemistry in 2018. During her time at LMU, she was a Ledford scholar award recipient and was mentored by Dr. Ashleigh L.P. Thomas and Dr. Giancarlo Cuadra where she conducted research on synthesizing chalcone derivatives with antimicrobial properties. Thanks to her mentor and University of Tennessee, Knoxville (UTK) alumni, Dr. Thomas, Courtney decided to pursue a doctoral degree in analytical chemistry at UTK. Courtney joined Dr. Shawn Campagna's lab at UTK where she had the opportunity to work on a vast majority of projects using mass spectrometry-based metabolomics and lipidomics to answer complex biological questions. Through her experiences in the Campagna lab, Courtney has developed a specific interest in studying gut microbiome metabolism and mitochondrial-mediated cellular reprogramming.